Regulation of postnatal skeletal muscle growth and metabolism by peroxisome proliferator-activated receptorβ/δ

Chandrashekar, Preeti

2016

Chandrashekar, P. (2016). Regulation of postnatal skeletal muscle growth and metabolism by peroxisome proliferator-activated receptorβ/δ. Doctoral thesis, Nanyang Technological University, Singapore.

https://hdl.handle.net/10356/67320

https://doi.org/10.32657/10356/67320

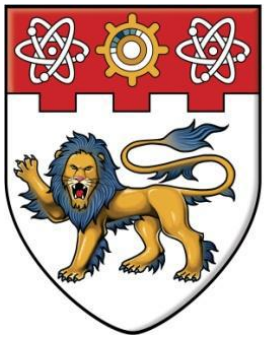

NANYANG TECHNOLOGICAL UNIVERSITY

REGULATION OF POSTNATAL SKELETAL MUSCLE GROWTH AND METABOLISM BY PEROXISOME PROLIFERATOR-ACTIVATED RECEPTORβ/δ

PREETI CHANDRASHEKAR

SCHOOL OF BIOLOGICAL SCIENCES

2016

REGULATION OF POSTNATAL SKELETAL MUSCLE GROWTH AND METABOLISM BY PEROXISOME PROLIFERATOR-ACTIVATED RECEPTORβ/δ

PREETI CHANDRASHEKAR

SCHOOL OF BIOLOGICAL SCIENCES

A thesis submitted to the Nanyang Technological University
in partial fulfillment of the requirement for the degree of
Doctor of Philosophy

2016

Acknowledgement

Wisdom must be intuitive reason combined with scientific knowledge

- Aristotle

First and foremost, I would like to convey my deep gratitude and respect for my research supervisor Professor Ravi Kambadur for his excellent guidance, patience and providing me with an excellent atmosphere for doing research. I would like to thank you for encouraging my research. I am also very grateful to Professor Walter Wahli for being my co-supervisor and for providing insightful discussions about research. I would also like to sincerely thank Assoc. Professor Mridula Sharma for offering me valuable comments towards improving my work and for correcting my thesis carefully.

I would also like to thank Assoc. Professors Koh Cheng Gee and Tan Nguan Soon for their time, and valuable feedback as members of my Thesis Advisory Committee. I also take this opportunity to sincerely thank Dr. Craig McFarlane for his scientific advice and suggestions and for critically reading and correcting my thesis and manuscripts that are doubtlessly time-consuming.

I am thankful to all the members of my lab who have helped me to carry out my work successfully. My special thanks to Dr. Ravikumar Manickam for mentoring me and teaching me various techniques during my initial days in the lab and also during my PhD. I wish to further extend my thanks to Gavian who as a batch-mate and a good friend, was always willing to help and give his best suggestions, Dr. Ge Xiaojia for teaching me and helping me with the muscle injury, Durga Sathiakumar for being a great friend and a lovely person to spend time with. I would also like to thank my labmate Nesibe Peker for helping me with some experiments. My thanks to Subha, Anantharaj and past members of my lab Dr. Bipasha Bose and Dr. Sudheer Shenoy for being good friends. I would also like to thank Dr. Piyush Khandelia, Dr. Ge Xiaojia and Isuru for giving their inputs for my thesis. I would also like to thank all the lab members

of SICS (A-Star) for having given a friendly environment to work. I would also like to acknowledge Animal house manager Ms. Lee Shok Li and staff of Animal house at NTU without whom it would have been a difficult task to perform animal studies for my research.

As the quote says: "An exemplary teacher will not just enlighten the student, but will also empower the student". My special thanks to Dr. A.G.Gopalakrishna (Chief Scientist and Head, CFTRI, Mysore) for inspiring me towards pursuing research. Finally, I would like to specially thank my father and mother, for having faith in me and for having been there for me during all the good and bad times during my PhD days. These past 3 years have not been an easy ride, both academically and personally. A special thanks to my husband Sriganesh, sister Shruti, brother-in-law Rajath and all family members for their unconditional love, moral support and encouragement, and Sriganesh for having been there with me whenever I needed you throughout the course of this endeavor. I would also like to convey my heartfelt thanks to my grandparents for their immense support and blessings throughout my PhD days. I would also like to thank my in-laws for having given me an opportunity to fulfill my wish of pursuing PhD. It would not have been possible to complete this thesis without all of your support and encouragement.

Preeti Chandrashekar

1st June 2015

TABLE OF CONTENTS

LIST OF FIGURES

Introduction

Results

LIST OF TABLES

Introduction

Materials and methods

ABBREVIATIONS

°C	Degree Celcius
3'	3 prime
5'	5 prime
%	Percentage
A band	Anistropic band
ActRIIB	Activin type II receptor
AF	Alexa Fluor
AF-1	Activation function-1
AIDS	Acquired Immuno Deficiency Syndrome
ATP	Adenosine triphosphate
BF	Biceps femoris muscle
BMP	Bone morphogenetic protein
BSA	Bovine serum albumin
Cdk2	Cyclin-dependent kinase 2
cDNA	Complementary DNA
CD68	Cluster of differentiation 68
CD163	Cluster of differentiation 163
CEE	Chick embryo extract
CHO	Chinese hamster ovary
C2C12	Murine myoblast cell line
CO_2	Carbon dioxide
DAPI	4', 6-diamidino-2-phenylindole
DB	Dialysis buffer
DEPC	Diethyl pyrocarbonate
DMEM	Dulbecco's Modified Eagle Medium
Drp-1	Dynamin related protein-1
ECM	Extra-cellular matrix
E.coli	*Escherichia coli*
EDTA	Ethylenediaminetetraacetic acid
EDL	Extensor digitorum longus muscle
FBS	Foetal bovine serum
FGF	Fibroblast growth factor

Fis 1	Fission 1
FoxO1	Forkhead box O1
FoxO3	Forkhead box O3
g	Gram
GAPDH	Glyceraldehyde 3-phosphate dehydrogenase
GAR	Goat anti-rabbit
Gas	Gastrocnemius muscle
Gasp-1	Growth and differentiation factor-associated serum protein-1
GDF-8	Growth and differentiation factor 8
G_0	Gap 0 phase of cell cycle
G_{Alert}	Alert phase of cell cycle
H & E	Hematoxylin and eosin
HCl	Hydrochloric acid
HDL	High density lipoprotein
HGF	Hepatocyte growth factor
hrs	Hours
HIV	Human Immunodeficiency Virus
H_2O	Water
HRP	Horse radish peroxidase
HS	Horse serum
IACUC	Institutional Animal Care and Use Committee
I band	Isotropic band
IGF-1	Insulin- like growth factor-1
IgG	Immunoglobulin G
IHC	Immunohistochemistry
IL-6	Interleukin 6
IL-10	Interleukin 10
IPTG	Isopropyl thio-β-galactoside
kDa	Kilo dalton
L	Litre
LB	Lennox LBroth
LBD	Ligand binding domain

LCFA	Long-chain fatty acids
μg	Microgram
μl	Microlitre
μm	Micrometer
μM	Micromolar
M	Molar
Mfn1	Mitofusin 1
Mfn2	Mitofusin 2
MHC	Myosin Heavy Chain
ml	Millilitre
MMI	Muscle mass index
MOPS	3-(N-morpholino) propanesulfonic acid
MRF4	Myogenic regulatory factor 4
mRNA	Messenger ribonucleic acid
Mstn	Myostatin
mtDNA	Mitochondrial deoxyribonucleic acid
mTORC1	mTOR Complex 1
MuRF-1	Muscle ring finger-1
Myf5	Myogenic factor 5
MyoD	Myogenic differentiation factor
NaCl	Sodium chloride
NaF	Sodium fluoride
NaOH	Sodium hydroxide
NF-κB	Nuclear factor- kappa B
NGS	Normal goat serum
NTU	Nanyang Technological University
NUS-CARE	National University of Singapore- Centre for Animal Resources
OCT	Optimal cutting temperature
Opa1	Optic atrophy 1
PAGE	Polyacrylamide gel electrophoresis
Park2	Parkin
Pax 3	Paired box gene 3

Pax 7	Paired box gene 7
PBS	Phosphate buffered saline
PBS-T	PBS-Tween 20
PFA	Paraformaldehyde
PMSF	Phenylmethanesulfonylfluoride
PPAR α	Peroxisome proliferator-activated receptor α
PPAR β/δ	Peroxisome proliferator-activated receptor β/δ
PPAR γ	Peroxisome proliferator-activated receptor γ
PPRE	Peroxisome proliferator Response elements
P/S	Penicillin/Streptomycin
Quad	Quadriceps muscle
qPCR	Quantitative Polymerase Chain Reaction
RNA	Ribonucleic acid
ROS	Reactive oxygen species
RXR	Retinoid X receptor
SC	Satellite cell
SDS	Sodium dodecyl sulphate
SEM	Standard Error of Mean
Sol	Soleus muscle
TA	Tibialis anterior muscle
TAE	Tris-acetate EDTA
TBS	Tris buffered saline
TBS-T	Tris buffered saline- Tween 20
TCA	Tricarboxylic acid
TG	Triglyceride
TGF- β	Transforming growth factor- β
TNF-α	Tumor necrosis factor- α
TZD	Thiazolidinedione
USA	United States of America
VO_2 max	Maximal oxygen consumption
WT	Wild-type

ABSTRACT

PPARβ/δ is ubiquitously expressed, however higher levels of *PPARβ/δ* are observed in skeletal muscle. Recently our laboratory showed that *PPARβ/δ* modulates Myostatin activity to induce myogenesis in skeletal muscle. Extending on from this previous work here we have investigated the role of *PPARβ/δ* in postnatal muscle growth and aging. Our results show that *PPARβ/δ*-null mice display reduced body weight, skeletal muscle weight and myofibre atrophy during postnatal development. In addition, a significant reduction in satellite cell number was observed in *PPARβ/δ*-null mice, suggesting a role for PPARβ/δ in muscle regeneration. Consistent with this hypothesis, immunohistochemical analysis on regenerating muscle revealed an increased inflammatory response and reduced myoblast proliferation. Histological analysis confirmed that the regenerated muscle fibres of *PPARβ/δ*-null mice maintained an atrophy phenotype with reduced numbers of centrally placed nuclei. Even though satellite cell numbers were reduced prior to injury, satellite cell self-renewal was found to be unaffected in *PPARβ/δ*-null mice after regeneration. Previously we showed that inactivation of *PPARβ/δ* increases myostatin signaling and inhibits myogenesis. Our results here confirm that inactivation of myostatin signaling rescues the atrophy phenotype and improves muscle fibre cross-sectional area in both uninjured and regenerated TA muscle from *PPARβ/δ*-null mice. Taken together, these data suggest that absence of *PPARβ/δ* leads to loss of satellite cells, impaired skeletal muscle regeneration and postnatal myogenesis. Furthermore, we also demonstrate that functional antagonism of myostatin has utility in rescuing these effects.

Since our study revealed that *PPARβ/δ* plays an important role in postnatal myogenesis, we next investigated whether or not deletion of *PPARβ/δ* affected aging related muscle wasting, termed Sarcopenia. Histological analysis revealed that there was enhanced myofibre atrophy at 3, 12 and 24- months of age and a significant reduction in myofibre number at 24-months of age in *PPARβ/δ*-null mice. In addition, we also observed reduced grip strength in *PPARβ/δ*-null mice at 18 months of age along with a significant reduction in

satellite cell number at 6 and 24 months. Since *PPARβ/δ* has been shown to influence oxidative muscle fibre number, we next investigated if deletion of *PPARβ/δ* influenced mitochondrial number and function in skeletal muscle. Our results show that *PPARβ/δ*-null muscle had remarkably reduced oxidative potential as assessed through SDH staining of TA muscle. Furthermore, a significant reduction in mitochondrial DNA content was also observed at 12 months of age in *PPARβ/δ*-null mice skeletal muscle. In addition, we observed reduced maximal respiration rate and spare respiratory capacity of mitochondria in differentiated myotubes cultured from aged *PPARβ/δ*-null mice. Molecular analysis further indicated that the reduced mitochondrial number in *PPARβ/δ*-null muscle could be due to enhanced mitophagy as *PPARβ/δ*-null mice displayed increased expression of the autophagy/mitophagy markers LC3, Parkin and Mul1 together with reduced expression of the Mul1 target Mfn2 in skeletal muscle at 12-months of age. Collectively, these data suggest that the premature muscle atrophy seen in young adult *PPARβ/δ*-null mice could be due to enhanced mitophagy.

In conclusion, we propose that PPARβ/δ expression is essential for proper postnatal development of skeletal muscle and that lack of *PPARβ/δ* results in reduced satellite cell number and poor regeneration. Furthermore, inactivation of PPARβ/δ could lead to enhanced mitophagy and premature wasting of skeletal muscle underscoring the benefits of *PPARβ/δ* agonists in alleviating aging-related muscle atrophy.

CHAPTER 1
INTRODUCTION

This thesis pertains to regulation of postnatal growth and metabolism by Peroxisome Proliferator-Activated Receptor β/δ (PPARβ/δ) in skeletal muscle. The functions of PPARβ/δ in various tissues have been well established. However, the role of PPARβ/δ in postnatal myogenesis of skeletal muscle and its role during aging has not been studied yet. Hence, this chapter will focus on PPARβ/δ and its role in skeletal muscle myogenesis and regeneration. It will also give an introduction to sarcopenia and the function of PPARβ/δ in mitophagy induced muscle wasting during aging.

1.1 Skeletal muscle

Skeletal muscles attach to bones and are involved in contraction to facilitate movement of skeleton. Skeletal muscles are one of the most abundant tissues in the human body. It comprises 40-50 % of body mass. Skeletal muscles aid in locomotion, heat production, energy storage and metabolism.

1.1.1 Skeletal muscle structure

Skeletal muscles are made up of fascicles composed of a series of multinucleated muscle fibres (*myofibres*). Skeletal muscle tissue is surrounded by connective tissue- endomysium, perimysium and epimysium (Jenkins *et al.*, 2006). Epimysium encompasses the entire muscle, whereas connective tissue fibres of perimysium groups together large number of myofibres into fascicles. Within a fascicle the individual skeletal muscle fibres are surrounded by endomysium.

The muscle fibres have multiple nuclei. Sarcolemma surrounds the muscle cell, and sarcoplasm appears beneath the sarcolemma, which encompasses the cellular proteins, organelles, myofibrils and large amounts of glycogen (Karagounis *et al.,* 2010). Sarcolemma invaginates into the cytoplasm of the

muscle cell, forming membranous transverse tubules (T-tubules) within the fibre. On either side of T-tubules are enlargements of smooth endoplasmic reticulum termed sarcoplasmic reticulum. Myofibrils are formed of bundles of protein filaments known as myofilaments. Myofilaments are composed mainly of actin and myosin filaments (Jenkins *et al.*, 2006). In skeletal muscles, the arrangement of actin and myosin protein filaments gives skeletal muscle its striated appearance and are mainly responsible for producing muscle contraction. The myofilaments consist of repeating functional units called sarcomeres (Figure 1.1).

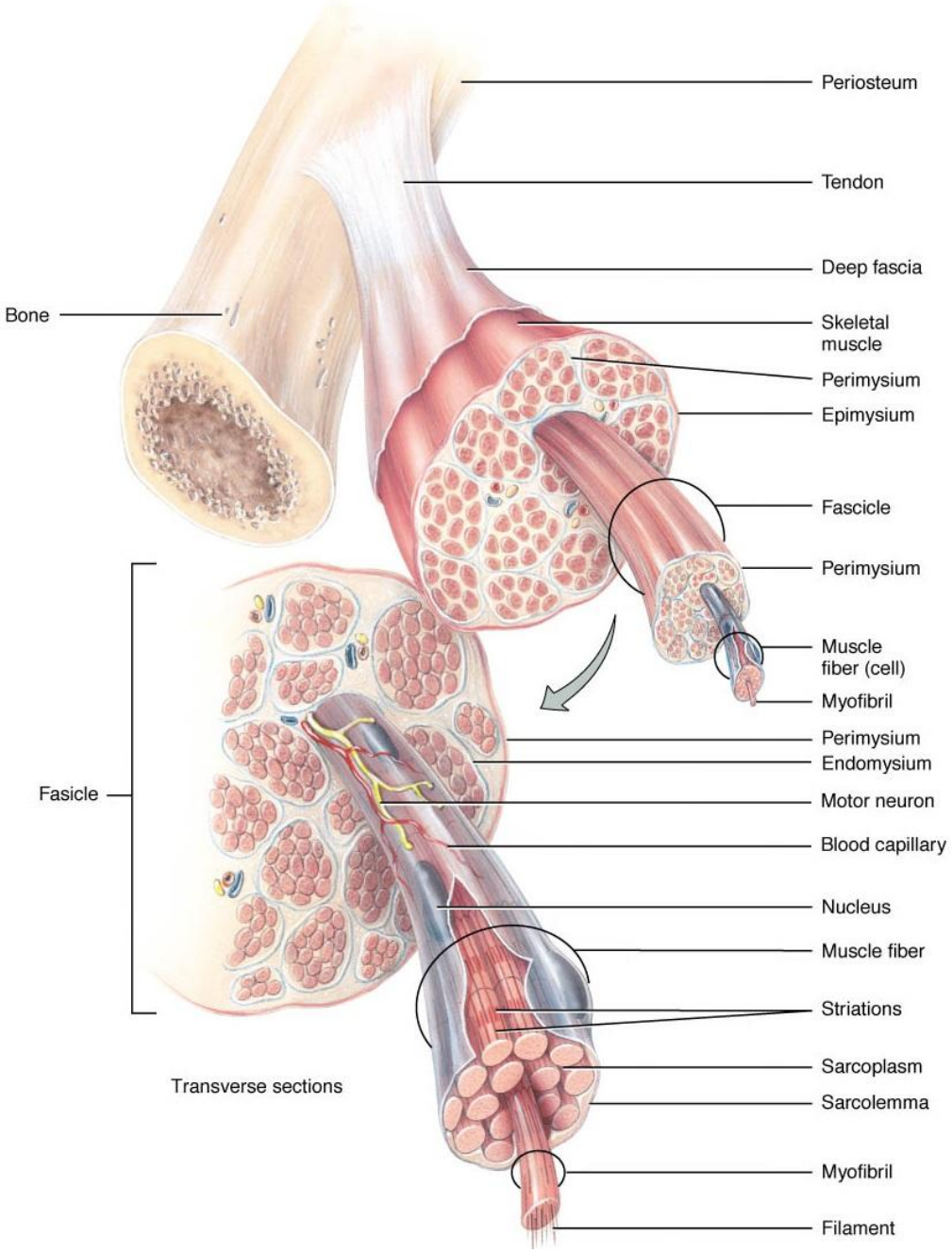

Figure 1.1 ***Skeletal muscle microstructure***

Skeletal muscle is composed of fascicles enclosed by the connective tissue epimysium. The bundles of muscle fibres are separated by connective tissue fibres of perimysium, and within each bundle the endomysium encompasses the muscle fibres. Each myofibre contains myofibrils, consisting of large number of sarcomeres along the myofibril length. Figure adapted from Anatomy and Physiology: From science to life, Jenkins *et al.*, (2006). This material is reproduced with permission from John Wiley and Sons, Ltd.

1.1.2 Sarcomere

Muscle fibres are striated, as are their constituent fibrils, resulting from an alignment of sarcomeres. Sarcomere being one of the smallest functional unit of muscle fibre has dark and light bands. The A band is a darker centrally localized region, and has the zone of overlap region, M line and H zone for the thick and thin filaments. The I band consists of mainly thin filaments. The centre of the H zone has M line that connects neighbouring thick filaments. Z line indicates the boundary of two adjacent sarcomeres and plays a role in binding the thin filaments of adjacent sarcomeres (Figure 1.2).

1.1.3 Muscle fibre types

Mammalian skeletal muscles are composed of heterogenous collection of muscle fibre types (Scott *et al.,* 2001). Since the first half of the 19th century skeletal muscles have been distinguished on the basis of their colour as red and white and their contractile properties as fast/glycolytic and slow/oxidative (Schiaffino *et al.,* 2011). The contractile ability of the muscle is determined by its composition of these fibre types. The different fibre types of mammalian skeletal muscle allows the muscle to perform various functions. The different types of skeletal muscle fibres are categorised into slow type I, fast type IIA, IIB, IID (X) based on the myosin heavy chain (MHC) isoform they express (Schiaffino *et al.,* 2011). Slow twitch muscles generate more fuel by consuming more oxygen. Consequently, the slow twitch muscles utilise the energy for continuous muscle contractions over a long period of time and fatigue slowly. In contrast, the fast twitch muscles have lesser capacity to produce energy and use it in a shorter duration contributing to rapid fatigue. Hence, among the various fibre types studied, the fastest contracting fibres are the type IIB fibres, followed by type IID, IIA and I (Galler *et al.,* 1994). These various fibre types play a very important role during postnatal skeletal muscle development. Table 1.1 represents characteristics of skeletal muscle fibre types.

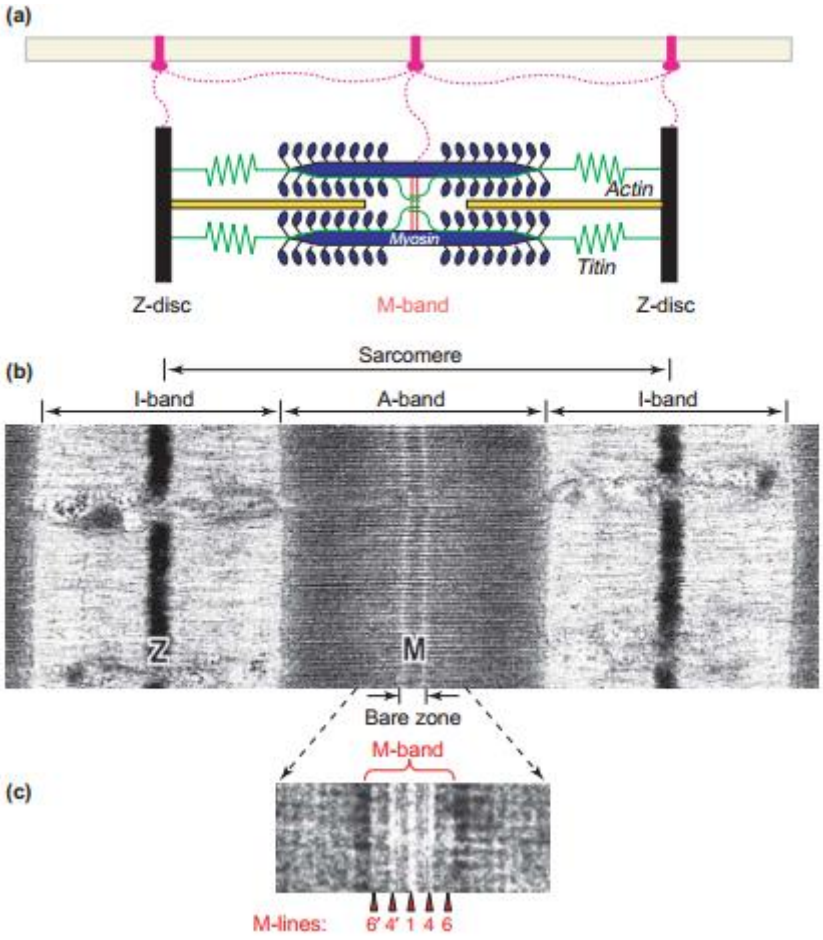

Figure 1.2 ***Structure of sarcomere in the skeletal muscle***

(A) Schematic representation of sarcomere strucutre. Myofibrils are composed of repeating sections of sarcomere. Color code: Actin filament- dark yellow, myosin filaments- blue, titin filaments- green, Z-disc- black, M-band- red. (B) Electron micrograph of a skeletal muscle sarcomere. Sarcomere is the segment between two neighbouring Z discs surrounded by thin (Actin/ I band) and thick (Myosin/ A band) filaments. The A band consists of a thin M-line formed of cross-connecting elements of cytoskeleton. (C) In negative-contrast picture of higher magnification view of human tibialis anterior muscle, the M band breaks up into a series of M lines (arrowheads). The five strongest M lines are indicated as M6', M4', M1, M4 and M6. Figure adapted from Trends in Cell Biology, Agarkova *et al.,* 2005, 477-485. This material is reproduced with permission from Elsevier provided by Copyright Clearance Centre.

Table 12.8 Fiber type Classification

	Motor unit type		
Property	**I (S) (SO)**	**IIA (FR) (FOG)**	**IIB (FF) (FG)**
Twitch speed	Slow	Fast	Fast
Twitch force	Small	Intermediate	Large
Fatigability	Low	Low	High
Red color	Dark	Dark	Pale
Myoglobin	High	High	Low
Capillary supply	Rich	Rich	Poor
Mitochondria	Many	Many	Few
Z-line	Intermediate	Wide	Narrow
Glycogen	Low	High	High
Alkaline ATPase	Low	High	High
Acid ATPase	High	Low	Moderate
Oxidative enzymes	High	Medium-high	Low

Table 1.1 Skeletal muscle fibre type characteristics

Table adapted from Skeletal muscle: Form and function, 2nd ed., MacIntosh BR *et al.*, 2006, 191. This material is reproduced with permission from Human Kinetics.

1.2 Myogenesis

Myogenesis is defined as the formation and development of skeletal muscle. The initial formation of skeletal muscle during embryogenesis is termed prenatal myogenesis whereas postnatal myogenesis occurs during adulthood wherein skeletal muscle undergoes repair and regeneration.

1.2.1 Embryonic myogenesis

The formation of the skeletal muscle begins from paraxial (presomitic) mesoderm in the embryo. Somites arise from the paraxial mesoderm present in between the neural tube and notochord (Buckingham *et al.,* 2003). Somite is further patterned into dermomyotome region and cells from dermomyotome gives rise to skeletal muscle and the dermis. Somites consist of epaxial and hypaxial dermomyotome. The back muscles are formed from the epaxial dermomyotome and the hypaxial dermomyotome gives rise to limbs (Figure 1.3A) (Buckingham *et al.,* 2003). Sclerotome, the ventral part of somite forms the cartilage and bone.

Myoblasts originating in the embryo from hypaxial region of the somite are categorised into embryonic myoblasts, foetal myoblasts and satellite cells (SCs) (Messina *et al.,* 2009). The embryonic myoblasts after migrating to the limb bud, undergoes fusion to form primary muscle fibres at around embryonic day 11 (E11). The embryonic phase is replaced by foetal phase, and finally postnatal growth involving adult myoblasts (Sambasivan *et al.,* 2007). These adult myoblasts also known as SCs, subsequently differentiate into multinucleated primary myotubes (Harris *et al.,* 1989) (Figure 1.3B). Following this period of primary myogenesis, secondary myogenesis involves fusion of primary fibres to adult myoblasts resulting in secondary fibres responsible for formation of the skeletal muscle (Messina *et al.,* 2009).

Myogenic regulatory factors (MRFs) are a family of basic Helix-Loop-Helix (bHLH) transcription factors. These transcription factors play a pivotal role in myogenesis. While Hepatocyte growth factor (HGF) and c-met, are involved in the delamination and migration of muscle progenitor cells. Pax3 (paired box gene 3) regulates the transcription of c-met during development of limb muscles (Epstein *et al.,* 1996). Mutation of either of the two external

growth factors leads to absence of skeletal muscle from the limb (Bladt *et al.*, 1995). During development, the paired box (Pax) genes are involved in cell specification and organogenesis. Pax3 and Pax7 are one of the important regulators of skeletal muscle myogenesis as they regulate the expression of MRFs. Absence of Pax3 results in the absence of limb muscle formation (Tajbakhsh *et al.*, 1997). In addition, $Pax3^{+}/Pax7^{+}$ cells are maintained through till the late foetal stages of growth and give rise to satellite cell pool in adult muscle (Kassar-Duchossoy *et al.*, 2004, Relaix *et al.*, 2005). In vertebrates, the MRF family of transcription factors includes MyoD, Myogenin, Myf5 and Mrf4. These transcription factors are known to be activated sequentially during embryonic myogenesis. Myf5 expression is detected as early as embryonic day (E8) in the developing somite (Ott *et al.*, 1991) and is known to function together with Mrf4 (Kassar-Duchossoy *et al.*, 2004). MyoD expression is detected throughout development after appearing around E10.5. Mutation of MyoD gene results in delayed myogenesis but with normal muscle formation, similarly mutation of Myf5 gene results in normal musculature but with reduced muscle fibre size and muscle mass (Kablar *et al.*, 1997). However, mice with mutations in MyoD and Myf5 show complete absence of skeletal muscle (Rudnicki *et al.*, 1993). Myogenin is critical for myogenic differentiation of committed precursors. Mrf4 identifies the embryonic myoblasts, and promotes the differentiation of myoblasts by activating Myogenin. Furthermore, Myf5-, MyoD- and Mrf4- deficient mice also show complete absence of skeletal muscle and myoblasts (Kassar-Duchossoy *et al.*, 2004, Rudnicki *et al.*, 1993).

Figure 1.3 ***Prenatal myogenesis***

(A) During the early stages of skeletal muscle formation presomitic (paraxial) mesoderm (PSM) segments into epithelial somites. Dorsal portion of somites-dermomyotome (DM) harbours muscle stem/progenitor cells. The progenitors in the dorsomedial lip of the DM undergo an epithelial to mesenchymal transition, migrate underneath the dermomyotome to form the myotome where they differentiate into mononucleated myocytes that are attached to the anterior (rostral) and posterior (caudal) edges of the somite. Pax3/Pax7 expressing stem/progenitors from hypaxial portion of the DM delaminate and migrate to the limb buds. The stem cells from epaxial portion of DM contributes to muscle formation elsewhere. Skeletal muscle precursor cells give rise to myoblasts which differentiate into multinucleated primary myotubes. (B) Illustration of multiple stages of developmental myogenesis. The expression patterns indicated at the bottom represent primarily the onset during the embryonic wave. Pax3 expression declines in the foetus. Mrf4 is not expressed in head and foetal progenitors. MyoD expression is also detected early in the somite. Around E16.5, proliferating, $Pax7^{+}$ cells appear in a satellite cell position. A subset of these cells will become the future adult quiescent satellite cells. Desmin is an intermediate filament protein expressed in muscle and Myosin is a component of the contractile apparatus. Figure adapted from Seminars in Cell and Developmental biology, Sambasivan *et al*., 2007, 870-882. This material is reproduced with permission from Elsevier provided by Copyright Clearance Centre.

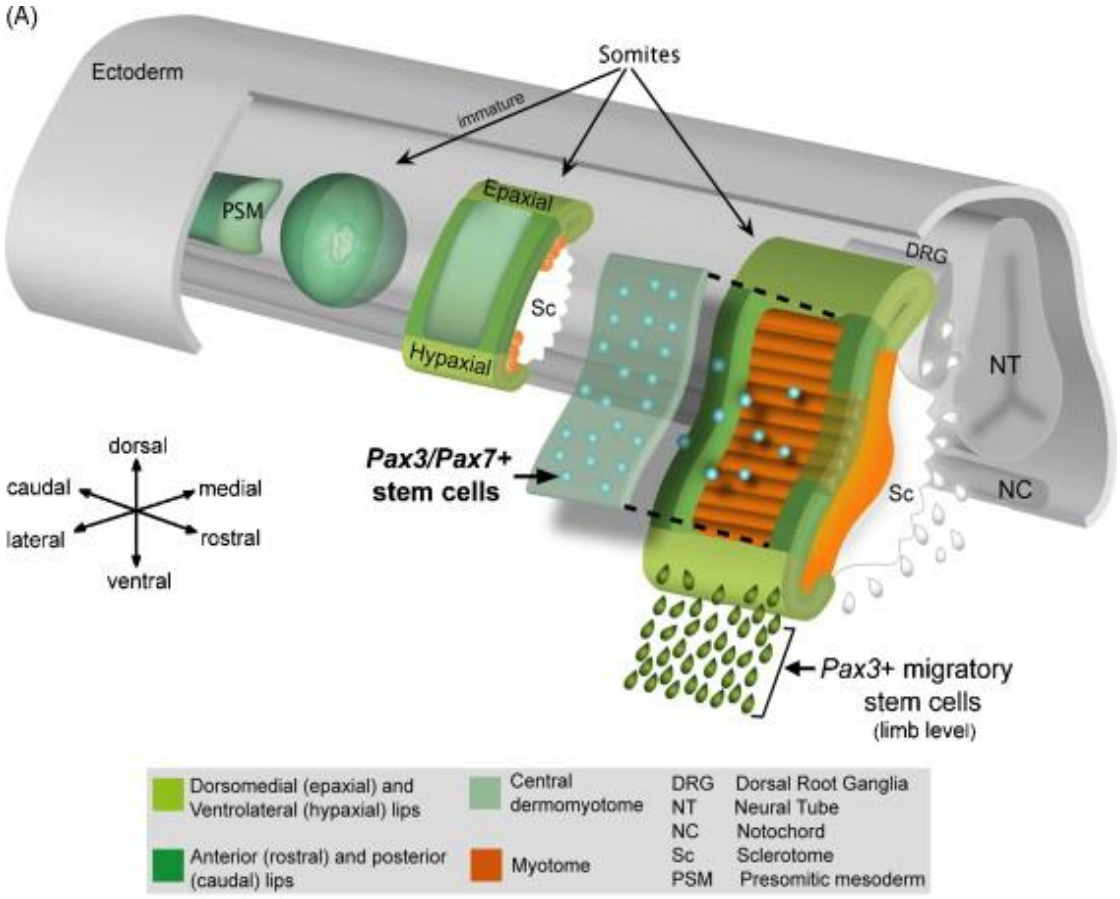
(A)
Ectoderm
Somites
immature
PSM
Epaxial
Hypaxial
Sc
DRG
NT
NC
dorsal
caudal
medial
lateral
rostral
ventral
Pax3/Pax7+
stem cells
Pax3+ migratory
stem cells
(limb level)
Dorsomedial (epaxial) and Ventrolateral (hypaxial) lips
Anterior (rostral) and posterior (caudal) lips
Central dermomyotome
Myotome
DRG Dorsal Root Ganglia
NT Neural Tube
NC Notochord
Sc Sclerotome
PSM Presomitic mesoderm

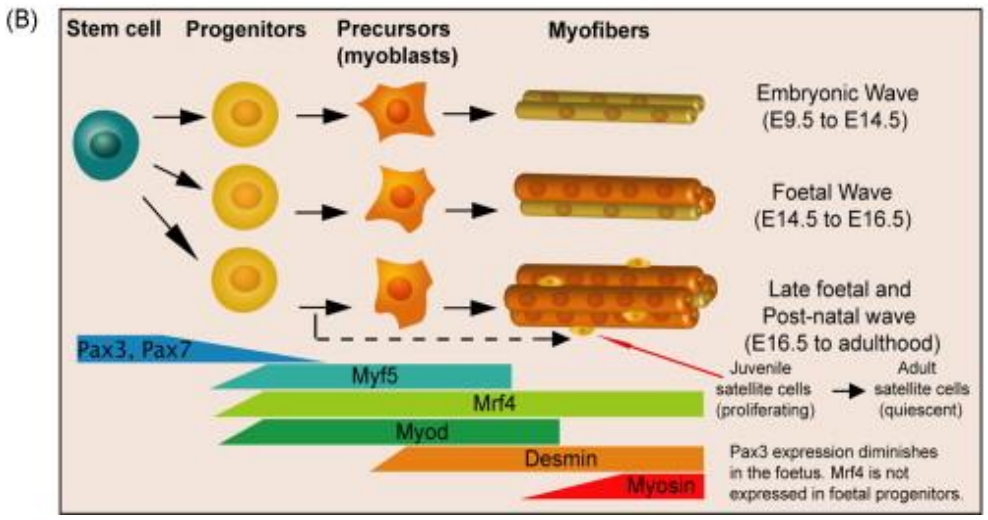
(B)
Stem cell
Progenitors
Precursors
(myoblasts)
Myofibers
Embryonic Wave
(E9.5 to E14.5)
Foetal Wave
(E14.5 to E16.5)
Late foetal and
Post-natal wave
(E16.5 to adulthood)
Pax3, Pax7
Myf5
Mrf4
Myod
Desmin
Myosin
Juvenile
satellite cells
(proliferating)
Adult
satellite cells
(quiescent)
Pax3 expression diminishes
in the foetus. Mrf4 is not
expressed in foetal progenitors.

1.2.2 Postnatal myogenesis

During postnatal stages, skeletal muscle is prone to injury as a result of daily wear and tear or acute trauma. If injured muscle is left unrepaired, the muscle could/can undergo atrophy, resulting in impaired locomotion and in some cases death. However, skeletal muscle has a unique property of regeneration. This repair process has been attributed to the satellite cell (SC) population present within the skeletal muscle. SCs play a major role in postnatal growth and regeneration of muscle fibre (Hawke *et al.*, 2001, Messina *et al.*, 2009).

SCs, also referred to as muscle stem cells, are derived from the somites (Schienda *et al.*, 2006). The SC niche consists of basal lamina and sarcolemma of muscle fibres. In resting muscle SCs reside in a quiescent state. SCs get activated and proliferate to form myoblasts in response to stimuli such as exercise, injury and stress, and fuse to form muscle fibres (Karagounis *et al.*, 2010).

In mice, SCs comprise 30 % of the sublaminal nuclei at birth, and thereafter declines to 5 % (Bischoff 1994) due to the contribution of SCs to postnatal muscle development. Accurate identification of SCs is made possible through several molecular markers. Quiescent SCs have been shown to express CD34 and Pax7 (Beauchamp *et al.*, 2000, Seale *et al.*, 2000). Upon activation, SCs begin expressing MyoD along with Pax7 and Myf5. The terminal phase of differentiation is characterised by up-regulation of Myogenin and a decline in Pax7 and MyoD (Yablonka- Reuveni *et al.*, 1994). Upon repeated cycles of skeletal muscle injury and regeneration, replenishment of satellite cell pool is required, enabling the maintenance of constant satellite cell number (Schultz *et al.*, 1994). The satellite cell self-renewal model suggested an asymmetrical mechanism where upon cell division one of the daughter cell gets committed to differentiation and the other cell proliferates and returns to quiescence (Dhawan and Rando, 2005). The self-renewal and myogenic differentiation of SCs occurs through the regulation of Pax7 and MyoD expression in SCs. During self-renewal, a small number of myoblasts maintain Pax7 expression while decreasing MyoD expression (Figure 1.4). These observations suggest that most SCs may determine their cell fate after cell proliferation and that the down-

regulation of MyoD expression could be an important factor contributing to the self-renewal of SCs (Motohashi *et al.*, 2012).

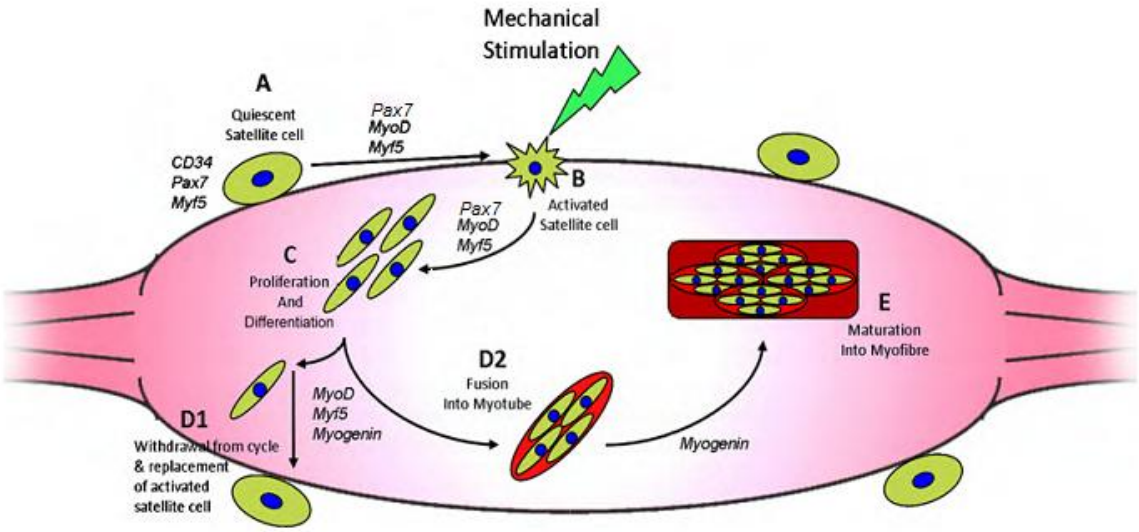

Figure 1.4 ***Schematic representation of satellite cell myogenesis and markers***

External stimuli such as mechanical stimulation activate quiescent SCs in normal adult muscle. Upon activation, SCs divide to form satellite cell derived myoblasts which further proliferate and differentiate to form myotubes, which then mature to form myofibres. In the process of self-renewal, some of the committed satellite cells withdraw from cell cycle and therefore replenish the pool of quiescent satellite cells. CD34, Pax7 and Myf5 are expressed in quiescent SCs. Satellite cell activation is marked by the expression of MyoD whereas Myogenin is associated with the differentiation and formation of myofibres. Figure adapted from The International Journal of Biochemistry and Cell biology, Karagounis *et al.*, 2010, 1376-1379. This material is reproduced with permission from Elsevier provided by Copyright Clearance Centre.

1.2.2.1 Factors contributing to postnatal myogenesis

Extracellular signaling molecules such as cytokines and growth factors play an important role during prenatal and postnatal myogenesis (Hawke 2001, Charge *et al.,* 2004). The various phases of adult satellite cell myogenesis have been shown to be regulated by growth factors including recruitment from quiescent state (Wozniak 2005) to proliferation, withdrawal of SCs from the cell cycle, differentiation of myoblasts (Bischoff 1997) and fusion of myoblasts to form growing myofibres. The influence of growth factors and a sequence of cellular events are involved in the skeletal muscle repair and regeneration, (Hawke *et al.,* 2001). For example Insulin like Growth Factor-1 (IGF-1), the pro-inflammatory cytokines interleukin-6 (IL-6) and tumor necrosis factor-α (TNF-α), neural-derived factors, Fibroblast like Growth Factor (FGF) and transforming growth factor-β (TGF-β) superfamily members are critical for the proliferation and subsequent myogenic differentiation of SCs to maintain postnatal muscle mass (Charge *et al.,* 2004). Recent reports also show that quiescent SCs exist in two different phases G_0 and G_{Alert} phase: G_0 phase indicates the resting phase of cell cycle and G_{Alert} phase indicates proliferative phase of cell cycle. mTORC1 is known to be involved in the transition of these SCs from G_0 to G_{Alert} phase through factors such as active HGF (Rodgers *et al.,* 2014). In addition to the positive regulators of myogenesis several negative regulators also play a crucial role in skeletal muscle development. For instance, Myostatin belonging to the TGF-β superfamily is one such negative regulator of skeletal muscle growth and development. It has been well established that inactivation of myostatin gene contributes to double-muscling phenotype (Kambadur *et al.,* 1997, McPherron *et al.,* 1997).

Interestingly, nuclear hormone receptors also play a major role in postnatal myogenesis, which include PPAR (Peroxisome proliferator-activated receptor) family members. PPARs are heterogeneous in nature and regulate transcription during various stages of embryonic development, cell differentiation and homeostasis (Mangelsdorf *et al.,* 1995). In particular, there are three PPAR isoforms of which PPARβ/δ has been shown to regulate both myoblast proliferation and differentiation and to positively regulate postnatal skeletal muscle growth (Bonala *et al.,* 2012) (discussed further in Section 1.4).

1.2.2.2 Skeletal muscle regeneration

Skeletal muscle can regenerate effectively after tissue damage, in three phases: degeneration, regeneration and remodeling. In the degenerative phase, the ruptured myofibres become necrotized and release chemotactic factors. The disruption of myofibre results in increased calcium dependent protein degradation, causing tissue degeneration via the action of calpains (Spencer *et al.,* 1995, Williams *et al.,* 1999). The initial phase of regeneration is characterised by influx of mononucleated cells, which recruit inflammatory cells to the damaged area to promote phagocytosis of necrotized tissue by blood derived monocytes. Macrophages form the other inflammatory cell type, which migrates towards the damaged area. The neutrophils and macrophages secrete cytokine proteins that increase the inflammatory response and attracts muscle SCs to the injury site (Turner *et al.,* 2012). The damaged muscle undergoes a process of repair and regeneration after the degenerative phase (Karalaki *et al.,* 2009). In the regeneration phase, the SCs begin to proliferate to form myoblasts and thereby self-renew to maintain tissue homeostasis (Rantanen *et al.,* 1995, Kuang *et al.,* 2007). The myoblasts then either proliferate and terminally differentiate to replace the damaged myofibres or fuse to form nascent skeletal muscle fibres. In the remodelling phase, the regenerating myofibres undergo maturation and increase in size. The newly formed myofibres are characterised by centrally located myonuclei (Whalen *et al.,* 1990). These nuclei are usually located along the entire length of regenerating myofibre or in discrete portions of myofibre (Blaveri *et al.,* 1999). Thus, the newly formed myofibres resemble the undamaged muscle fibre after the complete regeneration (Figure 1.5). Each phase of skeletal muscle regeneration is characterised by expression of specific markers. Molecular marker such as MyoD is induced within a short duration after injury (Megeney *et al.,* 1996) and is expressed mainly by activated SCs. Myf5 and Myogenin show delayed expression (Goetsch *et al.,* 2003). Following an injury, often the tendon-myofibre-tendon unit gets disrupted. Hence, a balance between the regeneration of muscle fibres and formation of connective tissue helps in the successful repair of damaged muscle. This causes fibrosis characterised by accumulation of extracellular matrix (ECM) leading to the formation of scar tissue (Menetrey *et al.,* 1999). The ECM also contains the

growth factors IGF-1, FGF, TGF-β and TNF-α, which can activate the SCs (Baoge *et al.*, 2012).

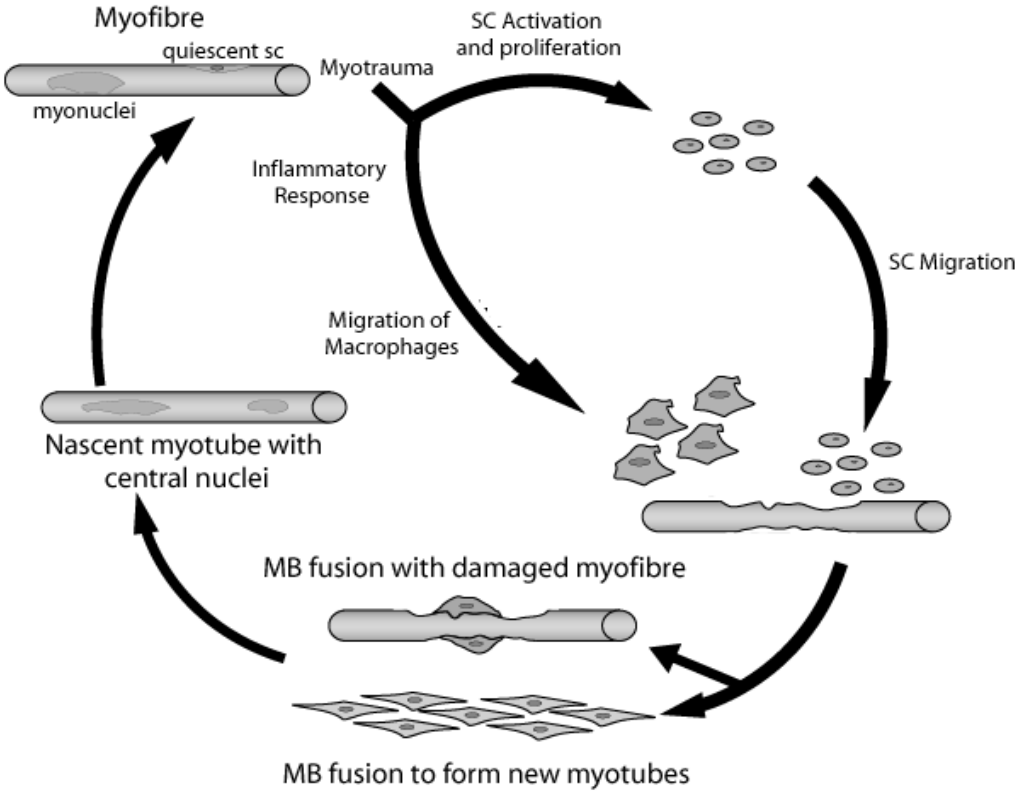

Figure 1.5 ***Model for skeletal muscle regeneration***

Representation of regenerative stages after injury showing satellite cell activation, proliferation, differentiation and maturation on injury. Macrophages and SCs migrate to the site of injury; the activated satellite cells proliferate at the site of injury and further the myoblasts either fuse with damaged myofibre or form new myotube by fusion. Figure modified from Journal of Cell Science, McCroskery *et al.*, 2005, 3531-3541. Open access publishing.

1.2.2.3 Inflammatory response in skeletal muscle regeneration

Muscle injury induced through acute myotrauma is characterized by rapid invasion of muscle with inflammatory cells that can persist for days to weeks followed by muscle repair, regeneration and growth. As shown in Figure 1.5 the muscle regeneration begins with infiltration of monocytes and neutrophils alongwith the macrophages. The regeneration process is characterised by an initial proinflammatory phase which involves release of chemokines and cytokines contributing to the removal of cellular debris from the site of injury (Paulsen *et al.,* 2010). The first inflammatory cell population dominating the injured tissue are the neutrophils. They appear within 1 hr of muscle damage and their concentrations can remain elevated for longer duration (Tidball 2005). Neutrophils release proteases, oxygen-derived reactive species and cytokines that can degrade the cellular debris.

Following neutrophil infiltration, macrophages derived from blood monocytes dominate the injured tissue. Macrophages are the scavengers of cellular debris and apoptotic cells. In addition, macrophages play a significant role in satellite cell activation and matrix remodelling (Qian *et al.,* 2010).

Macrophages are classified as M1 (or classically activated) and M2 (or alternatively activated) macrophages (Figure 1.6). Recent reports portray an important role for cytokines and pathogens involvement in the development and maturation of macrophages (Martinez and Gordon, 2014). M1 macrophages ($CD68^{+}$) are important for acute inflammatory response. Immediately after skeletal muscle damage monocytes are recruited, which participate in the removal of necrotic material through phagocytosis. These also produce proinflammatory cytokines such as IL-12 and TNF-α (Mann *et al.,* 2011). M2 macrophages ($CD163^{+}$) are divided into distinct subtypes: M2a macrophages (alternatively activated macrophages) are mostly associated with skeletal muscle repair, regeneration and fibrosis and M2c macrophages deactivate M1 macrophages and release anti-inflammatory cytokines, such as IL4 and IL-10 (Mann *et al.,* 2011). Thus, appropriate activation and resolution of inflammatory response is crucial for muscle regeneration.

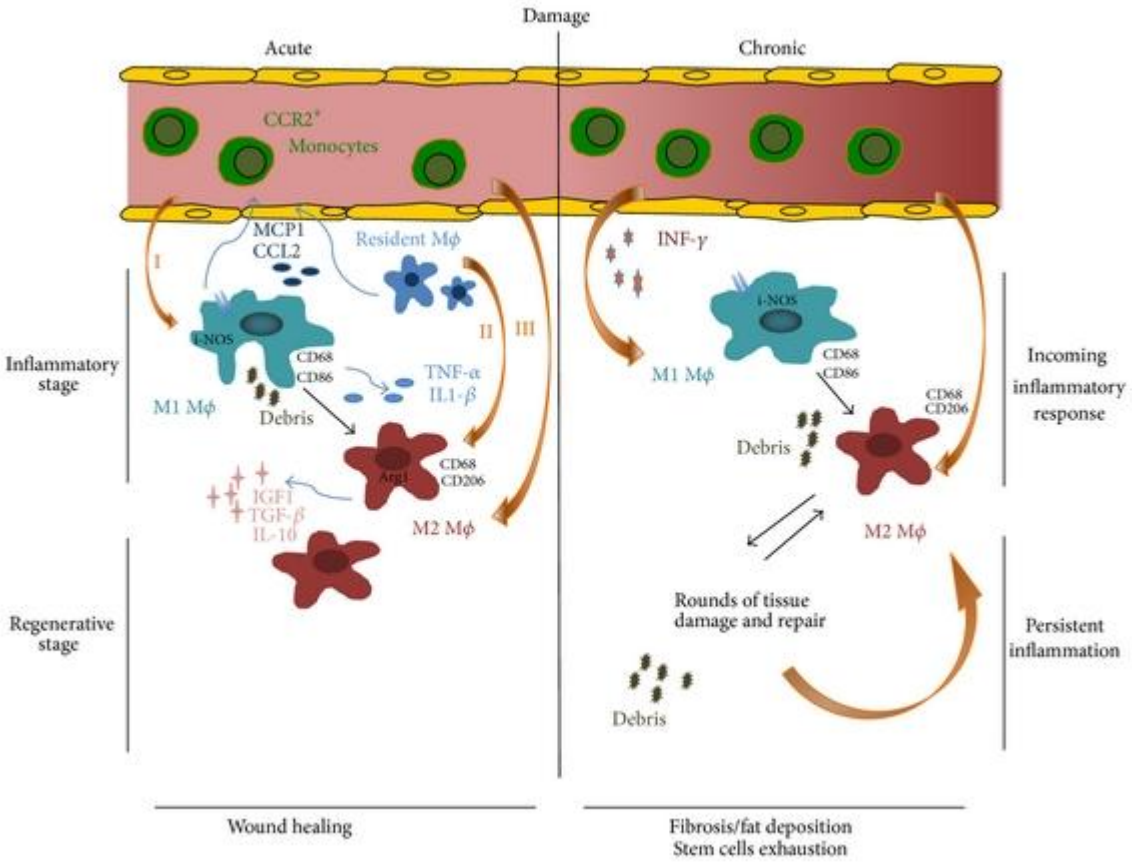

Figure 1.6 ***Macrophages in skeletal muscle regeneration***

The M1 macrophages activate an inflammatory response and the secreted cytokines promote the clearance of tissue debris and activation of stem cells. Phagocytosis of necrotic cells causes transition of M1 to M2 macrophages. The CD68+ macrophages release pro-inflammatory cytokines to promote inflammatory reactions and are responsible for clearance of tissue debris. The CD68+ macrophages undergo a phenotype switch to CD163+ macrophages after the necrotic tissue is cleared. During the regenerative stage stem cells differentiate and improve the regeneration. In chronic diseases both M1 and M2 macrophages persist in the tissue leading to fibrosis and fat deposition. Figure adapted from Biomed Research International, Rigamonti *et al.*, 2014, 1-9. Open access publishing under Creative Commons Attribution License.

1.3 Skeletal muscle metabolism

The main function of skeletal muscle is to provide movement by contraction at the expense of chemical energy. In addition, as a metabolic organ it is involved in energy homeostasis and also plays an important role in thermogenesis. During contraction of skeletal muscle fibre, each thick filament breaks down around 2500 ATP molecules per second. Muscles cannot completely depend on intracellular ATP store, and hence require other metabolic pathways for ATP generation. These metabolic pathways can be divided into aerobic and anaerobic pathways (Westerblad, Bruton and Katz, 2010). The anaerobic pathway of ATP generation involves the breakdown of phosphocreatine (PCr) and the formation of lactate and hydrogen ions upon breakdown of muscle glycogen. However, aerobic metabolism of carbohydrates and lipids produce larger amounts of ATP during prolonged periods of exercise. Glycogen acts as one of the major carbohydrate substrates for aerobic metabolism. Glycogen breaks down to form glucose molecules which contributes to increased ATP production during periods of excessive exercise. During aerobic metabolism, mitochondria consume ADP, oxygen and phosphate ions from cytoplasm, thereby entering the TCA cycle. Thereafter, organic molecules are broken down to produce carbon dioxide, hydrogen and water molecules. Resting skeletal muscle fibres depend on fatty acid metabolism to generate ATP. On the other hand, during contraction of muscles, mitochondria breaks down pyruvic acid instead of fatty acids. The glycolytic pathway provides two molecules of pyruvic acid, by break down of glucose. When pyruvic acid is produced at a faster rate than it can be used in the mitochondria, levels of pyruvic acid increase. The higher amounts of pyruvic acid further gets converted to lactic acid. The lactic acid produced by the anaerobic pathway diffuses out of the muscle cell and is absorbed by the liver, but the excessive lactic acid left over in the muscle fibres contributes to weakness in muscles. Metabolic activities in skeletal muscle fibres and the performance capability of any skeletal muscle is determined by the skeletal muscle fibre types.

The classification system of skeletal muscle fibres is primarily based on isoforms of myosin heavy chain (MHC). Muscles from rodents have been shown to express all four types of MHC, whereas human muscles do not

express type IIB MHC (Scott *et al.*, 2001; Choi *et al.*, 2014). As stated above in Table 1.1 the various types of skeletal muscle fibres mainly include fast fibres/white muscle fibres, slow fibres/red muscle fibres (Figure 1.7) and intermediate fibres. Based on the perspective of energy metabolism the fast MHC isoforms consume ATP faster than slower ones, allowing the skeletal muscles to be formed of muscle fibres with different metabolic profiles (Martini, Frederic *et al.*, 2007).

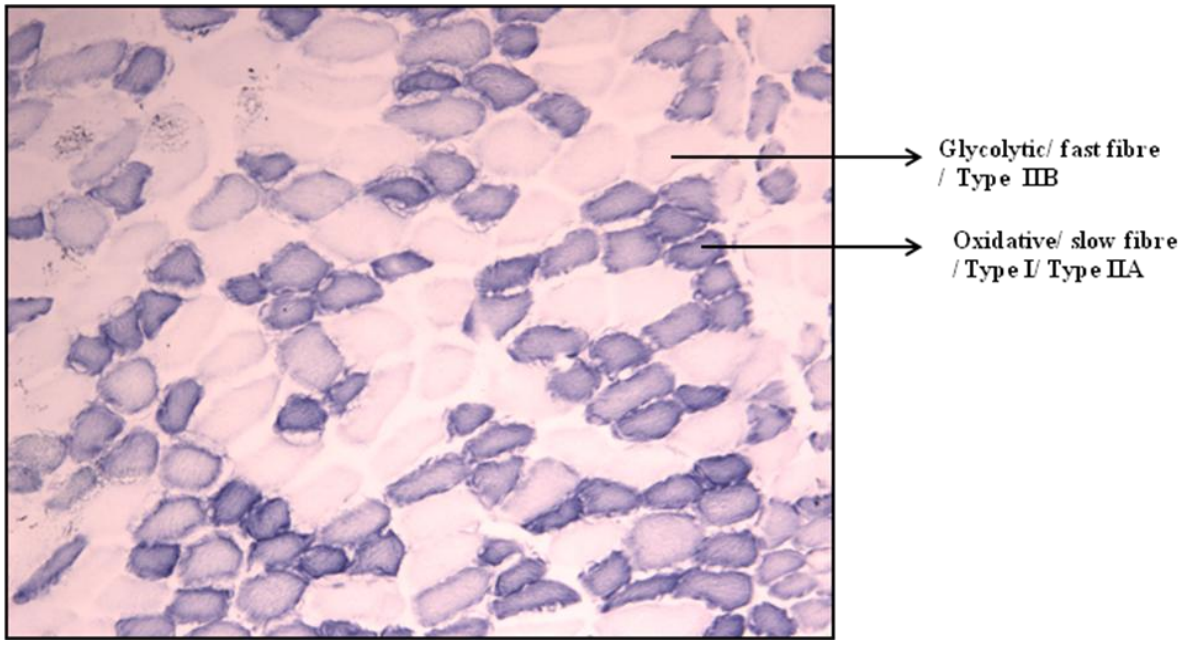

Figure 1.7 ***Skeletal muscle fibre types***

Histochemical representation of different skeletal muscle fibre types. The unstained fibres are the glycolytic fibres and darkly stained fibres represent oxidative fibres, stained for succinate dehydrogenase. The representative image has been taken from studies carried out in Chapter 4 of this thesis.

1.4 Regulators of metabolism: Orphan nuclear receptors

The discovery of nuclear receptors and their respective ligands have their roots in endocrinology (Evans, 1988). Nuclear receptors belong to a large superfamily of transcription factors and play a major role in embryonic development, cell differentiation and homeostasis (Novac *et al.*, 2004; Mohan *et al.*, 2003). Forty-eight nuclear receptors have been identified so far in human. These include steroid, thyroid and retinoid receptors. The cloning of initial set of nuclear receptors in 1985 led to the discovery of the first *orphan nuclear receptors* in 1988 (Giguere *et al.*, 1988) (see Figure 1.8). These orphan receptors were found to be conserved throughout the metazoa. The retinoid X receptor (RXR) was isolated in 1990, and the first Peroxisome Proliferator-Activated Receptor (PPAR) was isolated around 1991. Although different orphan nuclear receptors seemed to be related to one another, no activators or ligands were known for these receptors till now. The first orphan-receptor ligands were discovered by using orphan receptors as screening targets in a cotransfection assay, and this led to the identification of ligand 9-cis-retinoid acid for RXR. This high-throughput screening process, referred to as 'reverse endocrinology', began the linking of specific ligands to the different orphan receptors (Blumberg & Evans, 1998; Evans *et al.*, 2014) including ligands for PPARs, FXRs (farnesoid X receptors), and LXRs (liver X receptors). PPARs were so termed when these assays identified interactions between them and the ligands that promote peroxisome proliferation (*e.g.* fibrates and nafenopin). Three isoforms of PPARs - PPARα, PPARβ/δ and PPARγ - have since been discovered. PPARs were found to heterodimerize with RXRs to initiate transcription of target genes. PPARs now constitute important members of the nuclear orphan receptor superfamily.

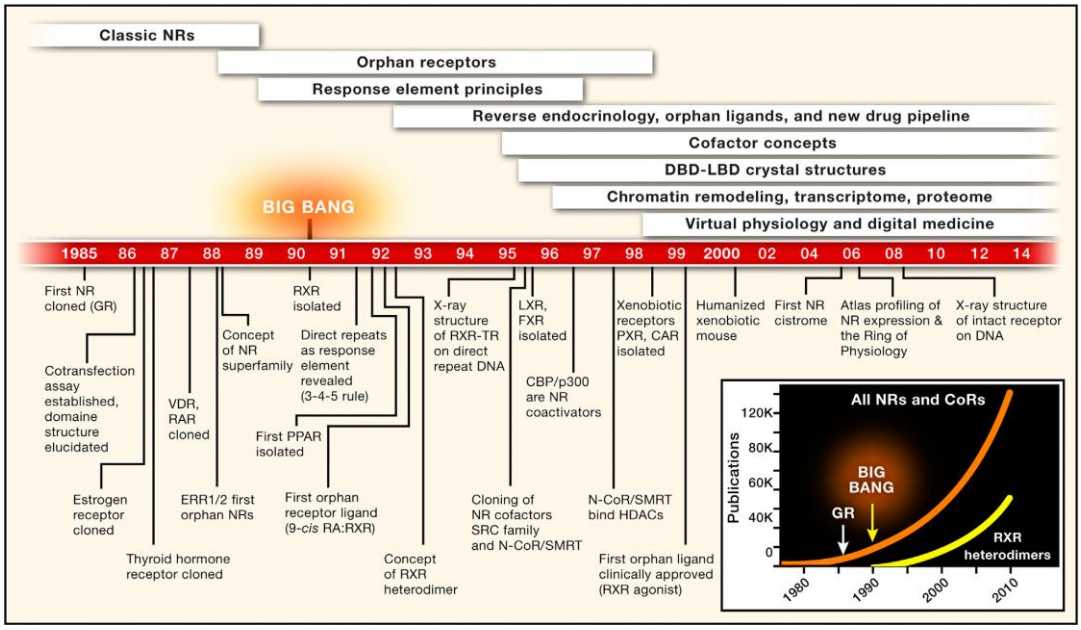

Figure 1.8 ***Nuclear receptor discovery timeline***

Schematic representation of landmark discoveries in the area of nuclear receptors. The timeline starts from the cloning of first steroid hormone receptor cDNA to most recent "omic" findings. Figure adapted from Cell, Evans *et al.*, 2014, 255-266. This material is reproduced with permission from Elsevier provided by Copyright Clearance Centre.

1.4.1 Peroxisome Proliferator-Activated Receptors (PPARs)

PPARs were first discovered in 1990s as receptors activated by chemicals (ligands) causing the proliferation of peroxisomes in cells (Issemann and Green, 1990), and hence their name. Among the well known forty-eight human nuclear receptors, four subfamilies have been defined - Subfamily 1: Thyroid hormone receptor-like, Subfamily 2: Retinoid X Receptor-like, Subfamily 3: Estrogen receptor-like, Subfamily 4: Nerve growth factor 1B-like. The Subfamily 1 is further categorised into group A- group I, of which PPARs constitute group C and hence they are referred to as NR1C.. Three isotypes of PPARs were discovered in *Xenopus* (Dreyer, Krey *et al.*, 1992): PPARα, PPARβ (PPARδ) and PPARγ (Laudet *et al.*, 1999).

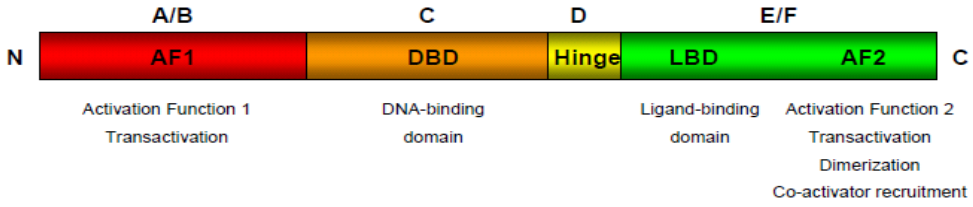

Figure 1.9 ***Schematic illustration of domain structure of PPARs***

The region most conserved amongst nuclear receptors is the C region that is the DNA binding domain of nuclear receptors. The E/F domain represents the ligand binding domain which contains the AF2 ligand dependent activation domain. The N terminal A/B domain contains the AF1 ligand independent activation domain. The D domain consists of a highly flexible hinge region. Figure adapted from Comparative Hepatology, Boitier *et al.*, 2003, 1-15. Open access publishing. Copyright 2003 licensee Biomed Central.

PPARs are organized into the following structural and functional domains (Figure 1.9). The AF-1 or activation function-1 domain is ligand-independent, and is encoded by the amino terminal A/B region. This domain is active only in some cell types, and is among the least conserved domains between the three isotypes.

Next is the ligand binding or E/F domain. This domain caters for the transcription-factor role of PPARs by enabling the binding of PPARs to regions of the DNA called peroxisome proliferator response elements (PPREs). Ligands bind to this domain, thereby bring conformational changes to the PPAR protein structure, thus allowing recruitment of other cofactors including steroid receptor coactivator-1, the PPAR binding protein and PGC-1, during the regulation of gene transcription (Krey *et al.,* 1997, Zhu *et al.,* 1997, DiRenzo *et al.,* 1997). Specifically, this E-domain is composed of thirteen α-helices and a four-stranded β-sheet forms a large Y-shaped cavity capable of holding the binding ligands. PPARs first form a heterodimer complex with 9-*cis* retinoid X receptor (RXR), which enables their binding to PPREs *via* the C domain.

The C domain consists of two zinc finger-like binding structure and an α-helical DNA binding motif which enable binding of PPARs to PPREs on the DNA (Osada *et al.,* 1997, Tugwood *et al.,* 1992, IJpenberg *et al.,* 1997). These PPREs are composed of a direct repeat (DR-1) element that consists of two AGGTCA hexanucleotide sequences with a single nucleotide space in between, *i.e.* AGGTCA_AGGTCA. These PPREs are found in enhancer/promoter regions of several genes involved in lipid and glucose homeostasis, and cell cycle regulation.

Finally is an adaptable or flexible hinge domain encoded by the D region. This enables flexible movement of the ligand binding domain relative to the DNA binding domain (Boitier *et al.,* 2003).

1.4.1.1 Mechanism of transcriptional regulation by PPARs

PPARs form a heterodimeric complex with retinoid X receptor (RXR). The binding of PPAR-RXR complex to specific endogenous ligands induces conformational changes, which causes them to bind to specific elements in promoter regions of target genes known as PPREs, thus resulting in the

transcription of these genes (Figure 1.10) (Fiege *et al.*, 2005; Gearing *et al.*, 1993; Keller *et al.*, 1993, Kim and Ahn, 2004). These ligands include free fatty acids, prostaglandins, and leukotrienes.

The heterodimers can activate transcription in response to only one of the ligands *i.e.* either 9-*cis*-retinoic acid binding to RXR or a PPAR ligand (fibrates, fatty acids) binding. PPAR while activated by both ligands contributes to enhanced gene expression (Kliewer *et al.*, 1992; Desvergne *et al.*, 1999; Palmer *et al.*, 1995).

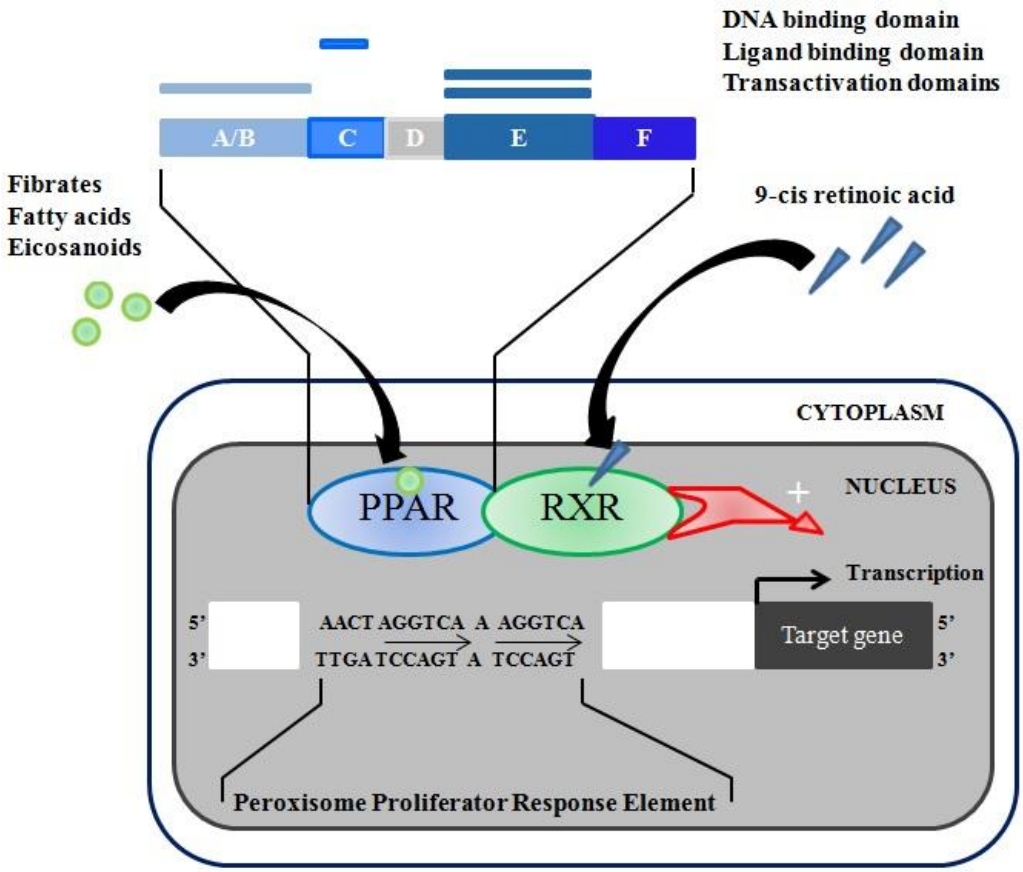

Figure 1.10 ***Transcriptional activation of target genes by PPAR***

PPAR forms a heterodimer with RXR. Ligand binding to PPAR activates the expression of target genes containing PPREs in their promoter. A number of possible ligands are depicted, including fibrates, fatty acids and eicosanoids. Figure adapted from The International Journal of Developmental Biology, Michalik *et al.*, 2002, 105-114. Open access publishing.

1.4.1.2 Expression pattern of PPARs during vertebrate development

The pattern of expression of a protein is usually the first step in understanding the physiological function of the protein. The three different PPAR isotypes are expressed in different cells having specific, yet overlapping expression patterns. PPAR is known to have variable expression patterns in *Xenopus*, rodents and humans. In *Xenopus laevis*, PPAR α, β and γ were first isolated from cDNA libraries using the DNA sequence of estrogen receptor (ER) binding domain as hybridization probe (Dreyer *et al.,* 1992; Dreyer *et al.,* 1993). Earlier reports have shown that mRNAs and proteins for PPARα and β were present in *Xenopus* oocytes throughout oogenesis and also in the early embryo, whereas PPARγ mRNA had been detected only during later stages (Dreyer *et al.,* 1993). During foetal development in rodents PPARα and γ transcripts appear at E13.5 whereas, PPARβ transcript appears as early as E8.5 of gestation (Braissant *et al.,* 1998). Furthermore, in humans the three PPAR isotypes are expressed as early as seven weeks of gestation in cell types of endodermal and mesodermal origin (Huin *et al.,* 2000).

1.4.1.3 Distribution and function of PPARs

PPAR isotypes are expressed in a tissue-specific manner. Apart from organs including heart and liver, PPARα is primarily expressed in tissues that are metabolically active and use energy from fat metabolism, such as skeletal muscle and brown adipose tissue (Figure 1.12) (Beck *et al.,* 1992). Consequently, this underlines the roles of PPARα in fat or lipid metabolism (Figure 1.11), namely in the transportation of fatty acids *via* intracellular binding with fatty-acid binding proteins, the uptake of these fatty acids by hepatocytes, and catabolism by β-oxidation in the peroxisomes and mitochondria. Moreover, PPARα aids in amino acid metabolism which is crucial to maintain energy homeostasis.

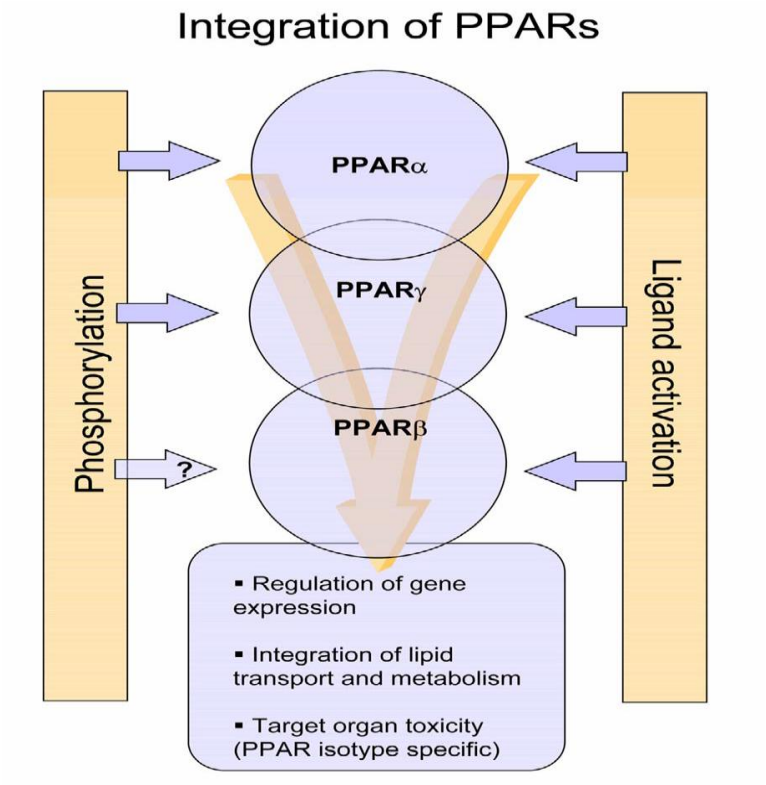

Figure 1.11 ***PPAR isotype functions and activation profiles***

PPAR isotypes having different functions and activation profiles share the ability to be activated by natural or synthetic ligands. The activity of PPARα and γ is modulated by phosphorylation enabling various functions such as regulation of gene expression, and integration of lipid transport and metabolism and also by sumoylation. Figure adapted from Comparative Hepatology, Boitier *et al.*, 2003, 1-15. Open access publishing. Copyright 2003 licensee Biomed Central.

PPARγ is expressed primarily in white and brown adipose tissues, large intestine and spleen, thereby underlining the role of PPARγ in adipocyte differentiation, lipid storage and enhancing insulin sensitivity (Figure 1.12) (Rosen *et al.*, 1999).

PPARβ/δ expression is ubiquitous, however the levels are different between tissues (Braissant *et al.*, 1996, Tyagi *et al.*, 2011), and consequently is expected to have multiple roles depending on the tissue in which it functions. Till date, PPARβ/δ has been studied for its roles in lipid metabolism, energy homeostasis and wound healing, in particular in the epidermal maturation and repair process (Wahli 2002). PPARβ/δ has also been studied for its regulatory roles in hepatic gene expression, which is critical for glucose homeostasis (Lee *et al.*, 2006). Furthermore, a role PPARβ/δ in tumorigenesis has also been reported although whether it is pro- or anti-tumorigenic is still unclear (Michalik *et al.*, 2004, Peters *et al.*, 2012).

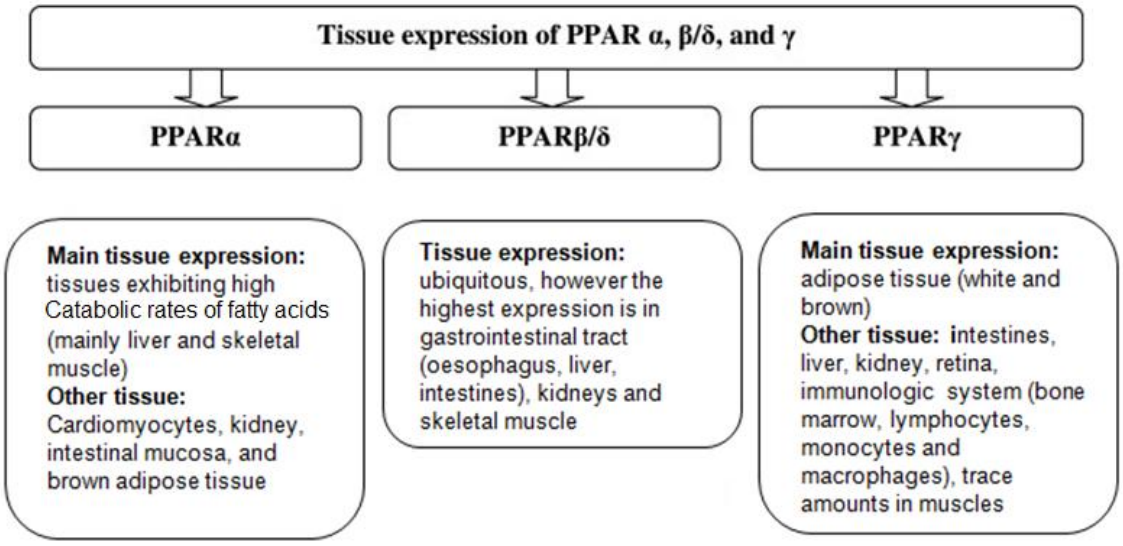

Figure 1.12 ***Expression of PPARs in specific tissues***

PPAR isotypes exhibit specific tissue related functions. PPARα plays an important role in the transport of fatty acids, PPARβ/δ is known to be involved in lipid metabolism, PPARγ is known to be involved in adipocyte differentiation. Figure modified from Nutrition Journal, Grygiel-Gorniak, 2014, 1-10. Open access publishing under Creative Commons Attribution License.

1.4.1.4 Ligands of PPARs

Peroxisome proliferators were intially shown to activate PPARs in rodents (Issemann and Green, 1990). In addition, various endogenous and exogenous PPAR ligands specific for each PPAR isotype have been identified. The three different isotypes of PPARs have natural and synthetic ligands performing various functions as shown below in Table 1.2.

PPAR Isotypes	Natural ligands	Functions	Synthetic ligands	Functions
PPAR α	Fatty acids, Prostaglandins, Eicosanoids (Ferre 2004)	Catabolism of fatty acids (Ferre 2004)	Fibrates (Ferre 2004)	Treatment of hyperlipidemia, Decreases plasma TG, increase of plasma HDL-cholesterol level (Ferre 2004)
PPAR β/δ	Long chain fatty acid, Retinoic acid, Prostaglandin (Borland *et al.*, 2008)	Control by LCFA of preadipocyte proliferation & differentiation, Differentiation and proliferation of keratinocytes (Borland *et al.*, 2008)	GW 501516, L165041 (Borland *et al.*, 2008)	Normalizes plasma TG, insulinemia & HDL cholesterol (Borland *et al.*, 2008)
PPAR γ	Prostaglandins, Isoflavones, n-3 & n-6 fatty acids, Polyunsaturated fatty acids, 15d-PGJ2 (Ferre 2004)	Adipocyte differentiation, Inflammatory response (Ferre 2004)	Thiazolidinedione (TZD) (Ferre 2004)	Antidiabetic, Hypoglycemic properties, inhibition and proliferation of smooth muscle cells, secretion of proatherogenic cytokines (Ferre 2004)

Table 1.2 ***Natural and synthetic ligands of PPARs***

The three PPAR isotypes have specific synthetic and natural ligands contributing to various functions.

1.4.1.5 PPARβ/δ and its role in skeletal muscle

To date a plethora of evidence indicates a role of PPARβ/δ in skeletal muscle. Interestingly, in *Xenopus* development, PPARβ/δ has been shown to be essential for muscle differentiation as early as gastrulation when PPARβ/δ governs a massive wave of transcriptional modifications affecting the later differentiation of muscle and brain (Rotman *et al.,* 2013). Earlier reports have also shown that mRNA for the PPARβ/δ isotype was found to be higher in the soleus compared to the glycolytic extensor digitorum longus (EDL) muscle upon overexpression of PPARβ/δ. Lunde *et al.,* have also demostrated that the most oxidative fibres display the highest levels of PPARβ/δ protein (Lunde *et al.,* 2007). The higher expression of PPARβ/δ is likely due to the distribution of different fibre types in these muscles: soleus muscles contain more oxidative fibre types compared to EDL muscles. Such differences in fibre types has also been observed previously in rats (Soukup *et al*., 2002). PPARβ/δ overexpression also promotes hyperplasia, and increase in the myonuclear density (Giordano *et al.,* 2009). In addition, PPARβ/δ plays a pivotal role in the acclimatization of skeletal muscle to environmental changes such as long-term fasting, by increasing the number of oxidative fibres (Gaudel, and Grimaldi, 2007). As increase in fibres with oxidative capability has been associated with overexpression of PPARβ/δ, transgenic mice overexpressing PPARβ/δ have also shown enhanced running capacity (Wang *et al.,* 2004). Furthermore, overexpression of PPARβ/δ in skeletal muscle of mouse was found to induce the differentiation of oxidative type I muscle fibres rich in mitochondria (Wang *et al.,* 2004). In line with these observations, muscle-specific ablation of PPARβ/δ causes a functional switch of the skeletal muscle fibre type toward lower oxidative capacity, which is followed by the appearance of age-dependent obesity and type 2 diabetes (Schuler *et al.,* 2006). Activation of PPARβ/δ is also associated with calcineurin dependent signaling pathway which enhances the oxidative phenotype of muscle (Gaudel *et al.,* 2008, Lahiri and Wahli 2010). A recent report suggests that activation of PPARβ/δ through addition of specific agonist enhances myogenesis in C2C12 myoblasts via an increase in both myoblast proliferation and differentiation (Bonala *et al.,* 2012). Also, loss of PPARβ/δ resulted in reduced proliferation of primary myoblasts

and defective differentiation. It has been shown that PPARβ/δ positively regulates postnatal myogenesis of skeletal muscle through a mechanism involving transcriptional activation of Gasp-1 and reduced activity of its downstream target myostatin (Bonala *et al.,* 2012). Furthermore, a recent study reported that skeletal muscle-specific knock out of PPARδ in mice (*PPAR δ*-cKO) leads to reduced satellite cell number and impaired skeletal muscle regeneration upon cardiotoxin-mediated injury (Angione *et al.,* 2011). Recently it has also been established that PPARβ$^{-/-}$ diabetic mice showed impaired musculoskeletal response to age and exercise parallel to reduced muscle and bone strength (Fu *et al.,* 2014).

1.5 Myostatin

Myostatin (Mstn) is a secreted growth factor that belongs to TGF-β superfamily (McPherron *et al.,* 1997).

1.5.1 Myostatin and its role in myogenesis

The biological function of myostatin have been based upon various experimental approaches, by knocking out the myostatin gene or by ablation of myostatin protein. The skeletal muscle development and homeostasis also depends on the specific expression pattern of the myostatin transcript (Carnac *et al.,* 2007). The function of myostatin was discovered in 1997 through studies on transgenic mice lacking the myostatin gene (Figure 1.13A) (McPherron *et al.,* 1997). Specifically these mice have a dramatic increase in skeletal muscle mass, which is due to both hyperplasia (increase in myofibre number) and hypertrophy (increase in myofibre size) (McPherron and Lee 1997). Naturally occuring mutations in *myostatin* contribute to double muscling phenotype in cattle breeds such as Belgian blue and Piedmontese (Figure 1.13B) (Kambadur *et al.,* 1997), whippet dogs and humans (Figure 1.13C) (Schuelke *et al.,* 2004). Consistent with this, overexpression of myostatin causes atrophy of skeletal muscles by reducing the muscle mass (Durieux *et al.,* 2007). Taken together these data solidify myostatin as an inhibitor of skeletal muscle growth.

Myostatin signaling operates through a serine/threonine kinase receptor complex. The canonical signaling pathway, involves various activin type II

receptors of which activin type IIB (ActRIIB) receptor binds to myostatin peptide to a greater extent than activin type IIA (ActRIIA) receptor. The myostatin and activin type II receptor complex further undergoes phosphorylation to activate the type I receptor (ALK-4/5) leading to activation of downstream canonical Smad signaling (Lee *et al.*, 2001, Rebbapragada *et al.*, 2003). Myostatin also inhibits muscle differentiation and growth by interacting with Wnt/β-catenin signaling pathway (Maltzhan *et al.*, 2012). Furthermore, Myostatin has also been shown to up-regulate p21 by activating p38 MAPK through TGF-β activated kinase 1 (TAK1) non-canonical signaling pathway (Philip *et al.*, 2005). Myostatin also inhibits proliferation and differentiation of C2C12 myoblasts by activating JNK pathway (Huang *et al.*, 2007). Thus, myostatin is highly conserved during mammalian evolution, and functions through various signaling pathways suggesting an essential role for this gene.

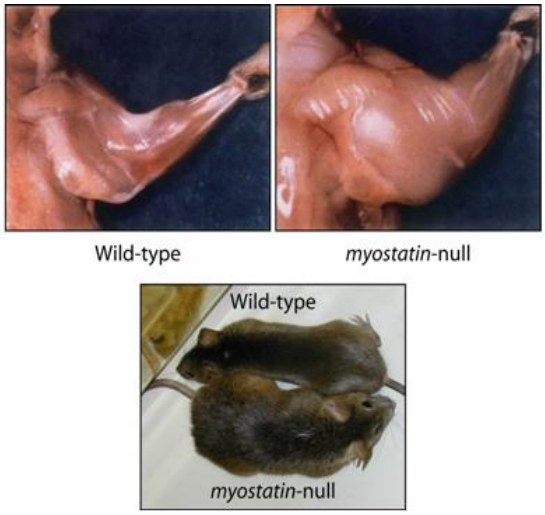

(A)

(B)

(C)

Figure 1.13 ***Mutations of myostatin characterized by double-muscling***

(A) Increased skeletal muscle is observed in myostatin-null mice in comparison to wild type mice. Adapted from Nature, McPherron and Lee, 1997, 83-90. This material is reproduced with permission from Nature publishing group. (B) Double muscling phenotype in Belgian blue bull. Adapted from Proceedings of the National Academy of Sciences USA, McPherron and Lee, 1997, 12457-12461. This material is reproduced with permission from The National Academy of Sciences, USA. (C) Heavy muscling phenotype in whippet dog and a human child at 7 months of age. Figure adapted from New England Journal of Medicine from Schuelke *et al.*, 2004, 2682-2688. This material is reproduced with permission from scientific research citation, Copyright Massachusetts Medical Society.

Myostatin also plays a role in the cell cycle regulation of several muscle cell lines. Myostatin regulates muscle growth by inhibiting myoblast proliferation (Thomas *et al.,* 2000, Taylor *et al.,* 2001, Joulia *et al.,* 2003), differentiation (Ríos *et al.,* 2001, Langley *et al.,* 2002), as well as negatively regulating activation of SCs and their self-renewal by signaling through Pax7 (McCroskery *et al.,* 2003, McFarlane *et al.,* 2008). The inhibition of myoblast proliferation by myostatin involves various mechanisms. Myostatin inhibits the proliferation by reducing the levels of both Cdk2 (cyclin-dependent kinase 2) and phosphorylated Rb (retinoblastoma protein) along with the upregulation of p21 resulting in inhibition of cell cycle (Thomas *et al.,* 2000, Ríos *et al.,* 2001). In addition, myostatin inhibits the differentiation of myoblasts through repression of MyoD activity (Langley *et al.,* 2002, Joulia *et al.,* 2003). Recently, it has also been established that, myostatin has the potential to negatively regulate the differentiation of human myoblasts by reducing MyoD and Myogenin expression (McFarlane *et al.,* 2011). In addition to SC activity, myostatin also regulates the synthesis and degradation of proteins in skeletal muscle (McFarlane *et al.,* 2006). Recently, Bonala *et al.,* established that PPARβ/δ positively regulates myogenesis, by negatively modulating myostatin activity via Gasp-1 (growth and differentiation factor-associated serum protein-1) (Bonala *et al.,* 2012).

In addition, myostatin appears to be involved in postnatal growth and repair of skeletal muscles. It has been suggested that through satellite cell activation, myostatin also regulates the postnatal myogenesis of skeletal muscle. Regeneration studies have shown that myostatin-null mice display improved healing and reduced scar tissue formation following injury. Myostatin-null mice injury models also displayed an accelerated movement and enhanced accumulation of myogenic cells and macrophages at the site of regeneration after 2 days of notexin induced injury (Figure 1.14) (McCroskery *et al.,* 2005). These results indicate that myostatin negatively regulates muscle regeneration by inhibiting the SC activation, proliferation and subsequent myogenic differentiation. Furthermore, myostatin plays a role in glucose metabolism and insulin signaling (Chen *et al.,* 2010; Zhang *et al.,* 2011). Apart from the role of myostatin in skeletal muscle, considerable amount of evidence shows the association of myostatin with obesity and diabetes. A study by Allen *et al.,*

supports the hypothesis that increased *myostatin* mRNA levels were observed in adipose tissue and skeletal muscle from leptin deficient obese mice (ob/ob) mice and WT mice fed high fat diet (Allen *et al.*, 2008). Reports have also shown an increase in epididymal fat pad mass with a decrease in muscle mass upon over-expression of myostatin (Reisz-Porszasz *et al.*, 2003).

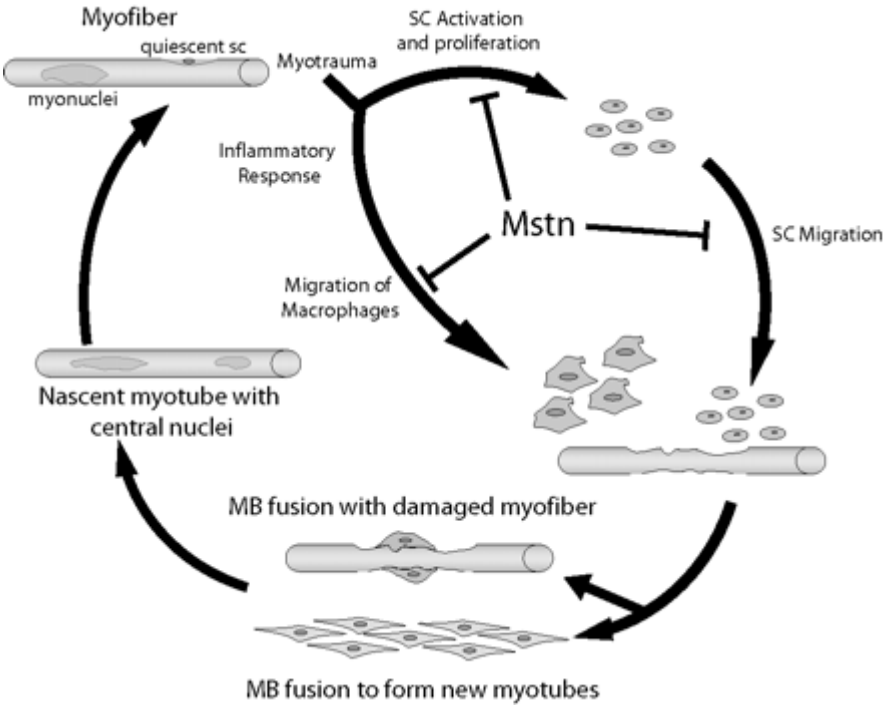

Figure 1.14 ***Role of myostatin in skeletal muscle regeneration***

Myotrauma of skeletal muscle contributes to activation of SCs and migration of macrophages to the site of injury. Myostatin also inhibits SC activation and macrophage migration. The activated SCs proliferate at the site of injury and resulting myoblasts either fuse with the damaged myofibre or form new myotubes by fusion. Figure adapted from Journal of Cell Science, McCroskery *et al.*, 2005, 3531-3541. Open access publishing.

1.5.2 Myostatin and skeletal muscle wasting

Myostatin is a cytokine which apart from controlling myogenesis, is also known to play a potential role in promoting skeletal muscle wasting. Several studies have associated myostatin with muscle wasting observed during AIDS, diabetes, cancer and aging. Myostatin levels have been shown to be higher in both serum and muscles from HIV-infected men (Gonzalez-Cadavid *et al.*, 1998). The upregulation of myostatin has been observed in the pathogenesis of muscle wasting during cachexia, and heart failure (Yarasheski *et al.*, 2002; Zimmers *et al.*, 2002; Costelli *et al.*, 2008; Lenk *et al.*, 2009; Breitbart *et al.*, 2011). Zimmers *et al.*, have also reported severe atrophy in mouse skeletal muscle injected with Chinese hamster ovary (CHO) cells to express myostatin (Zimmers *et al.*, 2002) by secreting cachectic factors. In addition, myostatin expression in adult muscle induces atrophy comparable to that of transgenic mice (Durieux *et al.*, 2007). Furthermore, loss of *myostatin* prevents dexamethasone-induced muscle atrophy (Gilson *et al.*, 2007). Increased myostatin expression also contributes to sarcopenia (Schulte *et al.*, 2001) and inhibition of myostatin is known to enhance muscle regeneration during sarcopenia (Siriett *et al.*, 2007). Antagonism of myostatin has also been shown to improve the muscle wasting associated with muscular dystrophy (Wagner *et al.*, 2002; Bogdanovich *et al.*, 2002). Increased myostatin levels contributing to muscle wasting have also been reported in patients with liver disease (Garcia *et al.*, 2010). Myostatin has been implicated as a pro-cachectic factor which induces cachexia through a Fox-O dependent mechanism (McFarlane *et al.*, 2006). It has also been established earlier that myostatin treatment causes the degradation of sarcomeric proteins through Atrogin-1 and MuRF-1 (McFarlane *et al.*, 2006). Recently our laboratory established that myostatin promotes the wasting of human myoblast cultures along with reduced expression of both myosin heavy chain and myosin light chain through the Ubiquitin-proteasome mediated pathway (Lokireddy *et al.*, 2011). Myotube atrophy induced through myostatin resulted in lesser p-AKT levels with accumulation of FOXO1 and FOXO3 and increased activation of Atrogin-1 and MuRF-1 (Figure 1.15) (Sandri *et al.*, 2004; Lokireddy *et al.*, 2011a; Lokireddy *et al.*, 2011). Our laboratory also established myostatin as a novel tumoral factor that induces

cancer cachexia by increased activity of Atrogin-1, MuRF-1, Smad and NF-κB signaling and reduced activity of IGF-1/PI(3)K/Akt pathway (Lokireddy *et al.*, 2012a, Argiles *et al.*, 2014). Our laboratory recently also demonstrated that skeletal muscle of streptozotocin-induced type-1 diabetic mice are more susceptible to myostatin induced DNA damage (Sriram *et al.*, 2014).

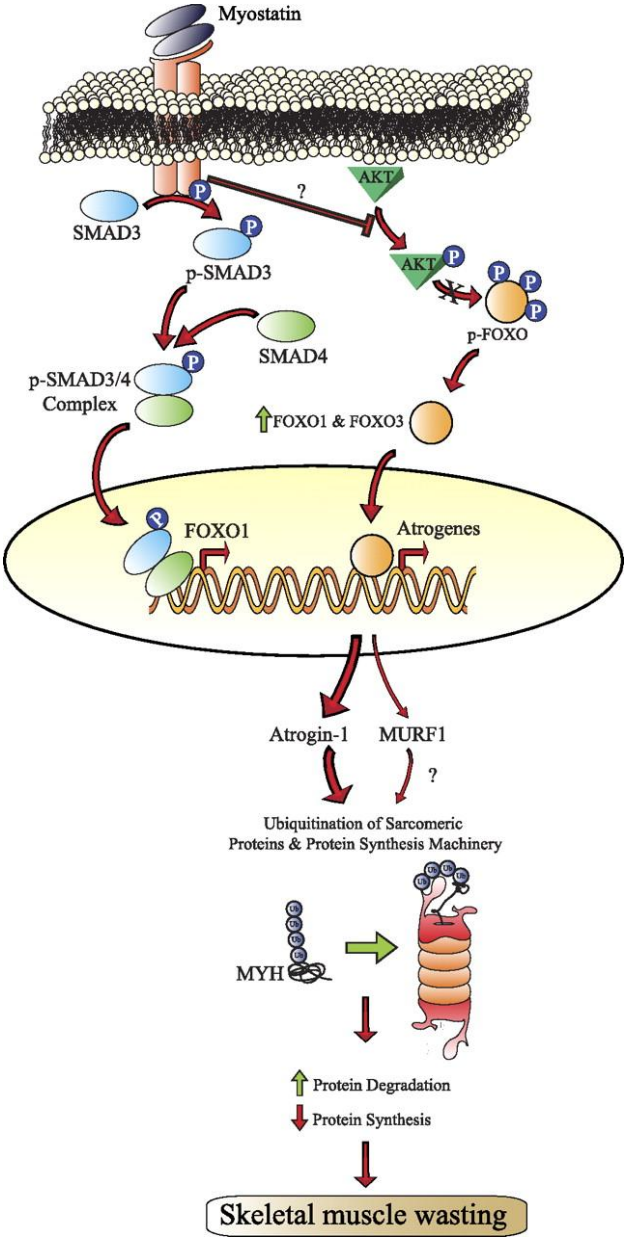

Figure 1.15 ***Myostatin- induced skeletal muscle wasting***

Myostatin increases FOXO1 expression via Smad3 signaling. Myostatin treatment results in the accumulation of FOXO transcription factors through inhibition of Akt, with the activation of Atrogin-1 and MuRF-1, leading to increased protein degradation and through ubiquitination of sarcomeric proteins. Figure adapted from American Journal of Physiology Cell Physiology, Lokireddy *et al.*, 2011, C1316-C1324. This material is reproduced with permission from The American Physiological Society, Copyright © 2011.

1.6 Sarcopenia

Over the last two decades, aging population is emerging as one of the major demographic trend worldwide, thereby posing a major health concern. Decline of muscles due to aging is associated with sarcopenia (Baumgartner *et al.,* 1998; Janssen *et al.,* 2002). Irwin Rosenberg in 1988 proposed sarcopenia as loss of skeletal muscle mass and function during aging. (Rosenberg *et al.,* 1997).

1.6.1 Phenotype of the aged muscle

Sarcopenia is considered as a dynamic process characterised by progressive reduction in skeletal muscle mass, function and strength with a risk of physical disability. In humans the lower limbs show a prominent decline in muscle mass during aging as revealed by imaging techniques used for measuring specific muscle mass (Janssen *et al.,* 2000). A progressive loss of skeletal muscle mass occurs from approximately 50 years of age, with 8 % of muscle loss occuring until 70 years, and after which a faster loss, ranging from 25 % to 40 % by decade occurs (Grimby *et al.,* 1983, Hughes *et al.,* 2001; Goodpaster *et al.,* 2006). Aging is also associated with decreased hormonal secretion, metabolism, lean body mass and increased fat accumulation in turn contributing to inflammatory diseases, obesity and type 2 diabetes with age. Sarcopenia is characterised by a muscle mass index (MMI) two standard deviations lower than MMI of younger population (Baumgartner *et al.,* 1998).

Several studies have indicated that loss of muscle strength is greater than decline in muscle mass during aging (Goodpaster *et al.,* 2006; Metter *et al.,* 1999; Faulkner *et al.,* 1995; Gonzalez and Delbono, 2001). Till date, the molecular mechanisms underlying sarcopenia have not been clearly explained. A large number of intrinsic and extrinsic factors play a major role in age related decreases in muscle mass and function. Intrinsic factors include: increase in apoptosis (Degens and Alway, 2006; Buford *et al.,* 2010; Marzetti *et al.,* 2012), and reactive oxidative species causing oxidative stress (Johnston *et al.,* 2008), decrease in autophagy (Wohlgemuth *et al.,* 2010), DNA damage (Aiken *et al.,* 2002*;* Szczesny *et al.,* 2010), mitochondrial dysfunction and mitophagy (Herbst *et al.,* 2007; Drew *et al.,* 2003; Bua *et al.,* 2002; Mansouri *et al.,* 2006; Chu *et*

al., 2010; Scheibye-Knudsen *et al.,* 2014) and reduced protein synthesis (Yarasheski *et al.,* 1999; Hasten *et al.,* 2000). Extrinsic factors such as lower nutrient intake, reduced physical activity, denervation of muscle fibre (Degens and Alway, 2006) and reduced satellite cell content (Conboy & Rando, 2005; Snijders *et al.,* 2009; Barberi *et al.,* 2013; Buford *et al.,* 2010) also contribute extensively in aging.

Loss of muscle mass and strength with age result in atrophy of muscle fibres, reduction in muscle fibre number, loss of motor innervation, fibre type changes and reduced grip strength described below.

1.6.2 Factors contributing to Sarcopenia

Frailty in the elderly population has become a widespread problem. Intrinsic factors such as increase in apoptosis results from fragmentation of DNA, subsequently resulting in cell death. Apoptosis is mainly characterised by cell shrinkage, condensation of chromatin and formation of apoptotic bodies (Alway and Siu, 2009). Apoptotic signaling is initiated by regulators such as hydrogen peroxide (H_2O_2), TNF-α and calcium (Leeuwenburgh 2003). In addition, mitochondrial dysfunction associated with increased oxidative damage (Cadenas *et al.,* 2000; Sohal *et al.,* 1994) may trigger the earlier phase of mitochondrial mediated apoptosis (Green and Reed, 1998). Increased oxidative damage can be initiated by production of reactive oxygen species (ROS). ROS are formed mainly in the mitochondrial respiratory chain of skeletal muscle fibres, which get accumulated over time. The ROS products play a major role in contributing to oxidative stress which further damages cellular components, such as DNA, proteins and lipids (Fulle *et al.,* 2004). The increase in ROS production with age contributes to age-related decrease in muscle performance. DNA damage due to oxidative stress might also contribute to telomere shortening (von Zglinicki *et al.,* 2005). Another potent factor responsible for loss of muscle mass is autophagy. Autophagy is an important cellular process involving the degradation of intracellular components within the lysosomes (Meijer and Codogno, 2004; Xie and Klionsky, 2007). Studies also report a decrease in autophagy during aging of the invertebrates and higher organisms (Cuervo and Dice, 2000; Cuervo *et al.,* 2005). Apart from the above

described factors, mitochondrial dysfunction contributes mainly to the skeletal muscle atrophy during aging. The dysfunctional mitochondria are removed by mitophagy wherein the autophagosome fuses with lysosome for degradation (Levine 2004). With increasing age, the impaired removal of damaged mitochondria could result in complete loss of mitochondrial function, in turn contributing to loss of muscle mass (Dirks *et al.,* 2006). Furthermore, reduced muscle mass and strength are accompanied by decline in the synthesis of muscle protein (Morley *et al.,* 2001).

Apart from the intrinsic factors, extrinsic factors such as lower nutrient intake also contribute significantly towards aging (Bartali *et al.,* 2006). The loss in muscle mass and strength also occurs due to lower nutrient intake, which along with reduced endurance, causes reduced physical activity. The loss of muscle mass and physical activity contributes to reduced expenditure of energy in elderly people, further contributing to increased fat accumulation. These factors play a vital role in contributing to various metabolic disorders with age (Nair 2005). Although a large number of factors contribute towards the atrophy of muscle fibres, denervation of muscle fibres also plays a potent role along with the co-expression of myosin heavy chain (Edström *et al.,* 2007; Rowan *et al.,* 2012). In addition, reduced satellite cell function also contributes significantly to sarcopenia (Carlson *et al.,* 2009; Beccafico *et al.,* 2007; Alway *et al.,* 2014).

1.6.3 Physiological characteristics associated with Sarcopenia

During aging, the strength of skeletal muscles is reduced which in turn causes difficulty in performing daily activities (Rogers and Evan 1993, Frontera *et al.,* 2000). Large number of reports indicate that loss of strength in older people is due to the result of atrophy of muscle fibres and loss of fibre number (Nilwik *et al.,* 2013).

1.6.3.1 Loss of fibre number

The loss of fibre number with age is mostly species-specific and depends mainly on the fibre types (Hooper 1981; Alnaqeeb and Goldspink 1987; Larsson *et al.,* 1978; Lexell *et al.,* 1983; Klitgaard *et al.,* 1990; Brown 1987;

Lexell *et al.,* 1988; Williams *et al.,* 2002; Narici *et al.,* 2010; Nilwik *et al.,* 2013). However, it is also noteworthy to mention that different fibre types influence the fibre size and number (Narici *et al.,* 2010; Nilwik *et al.,* 2013), though some reports have shown no change in fibre number (Sato *et al.,* 1984; Lexell *et al.,* 1988). The change in fibre numbers could also be due to splitting of fibres which can occur due to mitochondrial deletions, increased levels of oxidative damage and incomplete fusion of regenerating fibres (Blaivas and Carlson 1991, Wanagat *et al.,* 2001). Furthermore, one of the vital factors responsible for fibre loss during aging is through denervation of muscle fibres (Deschenes 2004).

1.6.3.2 Atrophy of muscle fibres

The aging skeletal muscle is characterized by atrophy of muscle fibres which contributes to weakness and increased risk of frailty and mobility impairment (Hepple 2014). Muscle atrophy can develop due to disuse of muscles, or due to aging, and can occur through different mechanisms in different fibre types. It has been reported that both slow-twitch and fast-twitch fibres undergo acute atrophy and degeneration during aging (Tomanek and Lund 1974; Larrson 1983).

A combination of factors contribute to aging-related muscle atrophy. The increased induction of apoptosis results in loss of myonuclear number (Chabi B *et al.,* 2008; Tamilselvan *et al.,* 2007; Dirks *et al.,* 2004). Muscle atrophy models have indicated that changes in myonuclei number are synchronized/ correlated with fibre cross-sectional area, and these consistently decrease with age (Kasper and Xun 1996a; Kasper and Xun 1996; Teixeira *et al.,* 2011). Mitochondria, which play a vital role in the regulation of myonuclear domain (Marzetti *et al.,* 2010; Min *et al.,* 2011) could be influencing this loss of myonuclear number (Chabi B *et al.,* 2008; Tamilselvan *et al.,* 2007; Dirks *et al.,* 2004).

In contrast, it has also been shown that denervation induced skeletal muscle atrophy also occurs independent of loss of myonuclei number (Wada *et al.,* 2003). Interestingly, the atrophy phenotype is mostly associated with aging type II muscle fibres rather than type I fibres (Larrson *et al.,* 1978; Lexell *et al.,*

1983; Lexell *et al.*, 1988; Matsakas *et al.*, 2009; Nilwik *et al.*, 2013). The reduction in fibre size during aging could also be due to a decrease in the satellite cell number and function (Figure 1.16) (Brack *et al.*, 2005).

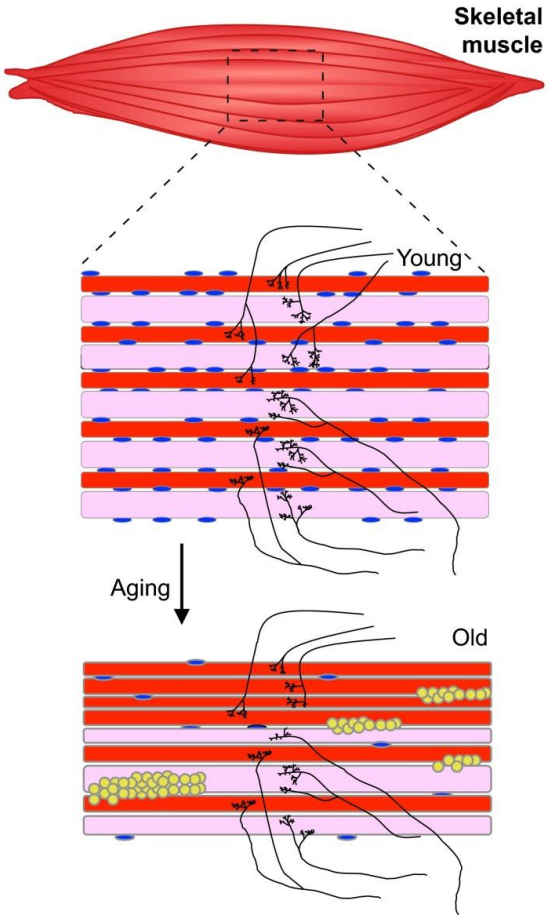

Figure 1.16 ***Physiological changes in skeletal muscle during aging***

Skeletal muscle aging in mammals is caused by a reduction in the number of satellite cells (shown in blue), decrease in strength, number and size of type IIb fibres (pink) and type I fibres (red) to a lesser extent. Aging is also characterized by defects in neuromuscular junctions and innervation (black). Aging of muscle leads to fibre type changes with an increase in type I fibres (red) along with accumulation of adipocytes (yellow). Figure adapted from Disease Models and Mechanisms, Demontis *et al.*, 2013, 1339-52. Open access publishing.

1.6.3.3 Fibre type changes associated with aging

As discussed above, muscle fibre atrophy depends on the specific fibre types. Large number of studies indicate fibre type shifts from type II muscle fibres to type I fibres during aging (Alnaqeeb and Goldspink, 1987; Larrson *et al.,* 1993; Musaro *et al.,* 1995; Yarovaya *et al.,* 2002; Narici *et al.,* 2010). In addition, during aging a large number of fibres are neither type I nor type II as they co-express both *MHC* isoforms- MHC-I and MHC-II (Andersen, 2003; Klitgaard *et al.,* 1990a). This shift in fibre types from fast MHC expressing isoform to slow MHC expressing isoform could also be due to motor unit denervation (Campbell *et al.,* 1973; Lexell 1995). Muscle disuse favours the expression of fast MHC isoform, whereas, exercising causes a shift towards fast fibres expressing slow MHC isoform *viz.* MHC- IIa (Figure 1.17) (Fluck and Hoppeler, 2003; Liu *et al.,* 2003). Hence, there is no gold standard for the MHC distribution during aging, since various factors influence the distribution of different fibre types.

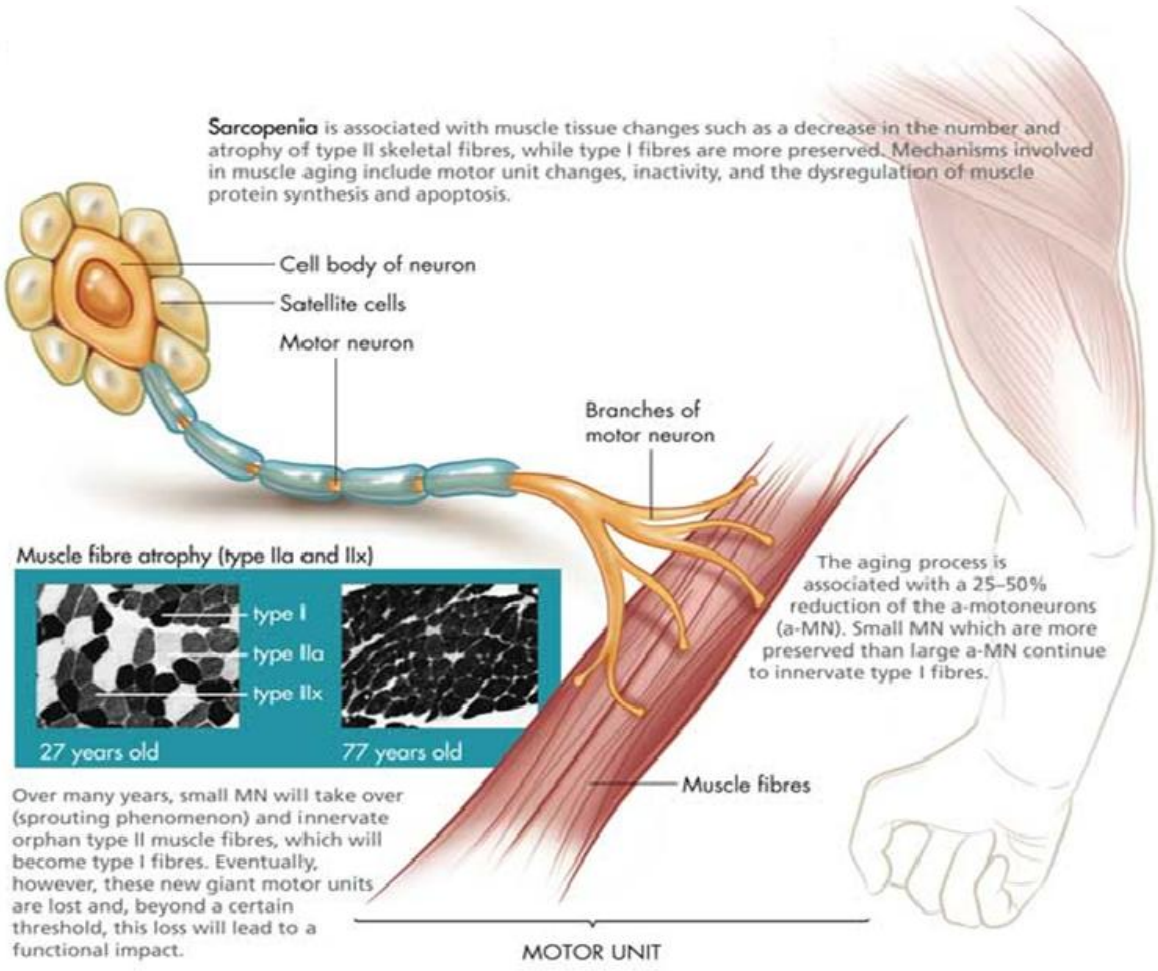

Figure 1.17 ***Age related mechanisms in muscle tissue***

Sarcopenia is characterized by decrease in the number and atrophy of type II skeletal muscle fibres, whereas type I fibres are more preserved. Aging also shows decreased expression of MHC type IIA and type IIX isoforms, while expression of type I isoform remains unchanged. Figure adapted from Clinical Orthopaedics and related research, Lee *et al.*, 2006, 231-237. This material is reproduced with permission from Wolters Kluwer Health, Inc.

1.7 Skeletal muscle wasting mechanisms

Skeletal muscle wasting is characterized mainly by increased protein degradation and reduced protein synthesis. Several proteolytic systems such as the ubiquitin-proteasome, autophagy lysosomal, the calcium-dependent calpain pathway, and the caspase system are responsible for muscle wasting (Ventadour and Attaix 2006).

The calcium dependent protein degradation system is formed of cysteine proteases known as calpains. The calpain family comprises of two isoforms: calpain-1 (μ-calpain) and calpain-2 (m-calpain) (Croall and Ersfeld, 2007). The calpain activity is mainly controlled by calpstatin in addition to its regulation by calcium. In skeletal muscle, apart from calpain-1 and calpain-2, calpain-3 isoform also gets expressed (Bartoli and Richard 2005; Murphy 2009). Calpains 1 and 2 function mainly in apoptosis and myogenesis and calpain-3 plays an important role in sarcomeric remodelling. Calpain activation regulates muscle mass by disrupting the sarcomere and releases actin, myosin, desmin, titin and nebulin (Hasselgren *et al.,* 2001; Huang *et al.,* 1998; Solomon *et al.,* 1996; Williams *et al.,* 1999). Studies have also shown that defects in the expression of calpain-3 lead to skeletal muscle dystrophy (Pandurangan and Hwang 2012). Calpains may also regulate protein degradation during cancer and various substrates such as IκB, focal adhesion proteins and proto-oncogenes have been implicated in tumor pathogenesis (Storr *et al.,* 2011).

Autophagy is an evolutionarily conserved lysosomal process that degrades cytoplasmic material and organelles (Kundu and Thompson 2008; Eskelinen 2008). During the process of autophagy, targeted cytoplasmic organelles get encompassed by double membraned vesicles known as autophagosome. The autophagosome further fuses with a lysosome and its cargo gets degraded and recycled (Patel *et al.,* 2012). Earlier studies have indicated autophagy-lysosome system to be activated in muscle cells (Bechet 2005; Deval *et al.,* 2001). The autophagy-lysosomal system has been known to be modulated in various situations such as cancer, aging, calorie restriction, sepsis, disuse and denervation (Penna *et al.,* 2013; Wenz *et al.,* 2009; Wohlgemuth *et al.,* 2010; Grumati *et al.,* 2010; Mofarrahi *et al.,* 2012; Brocca

et al., 2012; O'leary *et al.,* 2012; Zhao *et al.,* 2007). During autophagy, when autophagosomes fuse with the lysosomes several proteins undergo degradation and genes such as LC3 and Gabarap promote the degradation of proteins. (Mammucari *et al.,* 2007; Mammucari *et al.,* 2008; Zhao *et al.,* 2007). These indicate that during atrophy the autophagic flux increases and it requires transcriptional regulation for replenishment of components that are lost (Sandri 2010). Autophagy might also contribute to sarcopenia in the elderly (Wohlgemuth *et al.,* 2010). Primarily, three types of autophagy have been characterized namely, microautophagy, macroautophagy and chaperone-mediated autophagy (Mizushima, 2007). Microautophagy involves the engulfment of cytoplasmic material by the lysosomes, macroautophagy involves eradication of damaged organelles or unused proteins, and chaperone-mediated autophagy involves removal of proteins with the assistance of the hsc70 chaperone. Autophagy can remove specific organelles. The selective removal of mitochondria occurs by macroautophagy, whereas non-selective removal of mitochondria is termed *mitophagy* (Jin *et al.,* 2012).

Ubiquitin-mediated protein degradation is another proteolytic pathway which is active during skeletal muscle wasting. The ubiquitin proteasome pathway causes degradation of proteins in 26S proteasome through action of enzymes that link chains of polypeptide ubiquitin onto proteins (Glickman *et al.,* 2002; Baumeister *et al.,* 1998; Pickart, 2004). The ubiquitination of proteins requires three enzymatic components- the E1 ubiquitin- activating enzyme, E2 ubiquitin conjugating protein and the key enzyme E3 ubiquitin-protein ligase, responsible for recognizing a specific protein substrate and transferring activated ubiquitin to it (Nandi *et al.,* 2006). Two of the most important markers of skeletal muscle wasting are Atrogin-1 and MuRF-1 which are muscle-specific E3 ubiquitin ligases (Bodine *et al.,* 2001, Gomes *et al.,* 2001). Expression of Atrogin-1 and MuRF-1 is elevated in muscle wasting associated with denervation, hindlimb suspension, diabetes, renal failure and cancer (Bodine *et al.,* 2001, Gomes *et al.,* 2001). Thus, Atrogin-1 and MuRF-1 are the vital markers for detecting skeletal muscle wasting.

1.8 Skeletal muscle wasting and its association with mitochondria

1.8.1 Mitochondrial diseases

Aging is mainly characterised by loss of muscle strength and mass.This loss is due to reduced skeletal muscle mitochondria. Mitochondria are small cytoplasmic organelles ranging from 0.5-1 μm in diameter, which perform various cellular metabolic functions and hence termed as "cellular power plants". Mitochondria produce larger amounts of ATP used as chemical energy. In addition, mitochondria also perform other functions such as cellular differentiation, cell death and maintaining the process of cell cycle and cell growth (McBride *et al.,* 2006). Mitochondria can be found in between the myofibrils of muscles and also in liver cells. Mitochondrial biogenesis and degradation play a major role in maintaining the mitochondrial population. Mitochondrial biogenesis is regulated by factors such as transcriptional co-activator PGC-1α, which activates nuclear respiratory factor 1 and nuclear respiratory factor 2, which further activates mitochondrial transcription factor A (Jornayvaz *et al.,* 2010). On the other hand, mitochondrial degradation is acheived through a form of autophagy known as *mitophagy* (Kim *et al.,* 2007). Over the past years, large amount of research has been done on the dysfunctional mitochondria and its role in mitochondrial diseases and during aging. Mitochondrial diseases are caused mainly due to mutations in the mitochondrial DNA and also nuclear DNA. The mitochondrial diseases showing neuromuscular disease symptoms are known as mitochondrial myopathy. Most of the mitochondrial disorders are inherited. People having mitochondrial disorders demonstrate symptoms such as poor muscle growth, muscle weakness, visual problem, hearing problems, liver and kidney diseases, heart failure and dementia (Chinnery and Turnbull, 1999; Chinnery and Turnbull, 2000; Chinnery and Schon, 2003; Chinnery *et al.,* 2004; Chinnery 2014). Aging also seems to affect mitochondria significantly. During aging, damage to mitochondria often causes activation of mitophagy and also mitochondrial apoptosis in the same cell. In order to prevent cell death, the damaged mitochondria are engulfed by autophagosomes and degraded. Mitophagy involves selective removal of only dysfunctional mitochondria by autophagosomes. The PINK1/Parkin pathway plays a major role in regulating

mitophagy in cells (Kubli DA *et al.,* 2012). Furthermore, it has also been well established that PPARδ plays a major role in regulating mitochondrial biogenesis, oxidative capacity in skeletal muscle and also protects against fatty acid-induced dysfunction (Wang *et al.,* 2004, Ravnskjaer *et al.,* 2010).

1.8.2 Loss of mitochondria and atrophy of muscle fibres

It has been well established over the past 40 years that increased mitochondrial production of ROS and mitochondrial dysfunction contributes to disuse muscle atrophy. Mitochondria are known to form a complex inter-connected network in living organisms. The complex process of mitochondrial fission and fusion mainly play a role in forming this network (Dimmer *et al.,* 2006). While, Drp1 (Dynamin- related protein-1) and Fis 1 (Fission 1) promote mitochondrial fission, Opa 1 (Optic atrophy 1) and Mfn1/2 (Mitofusin 1 and 2) regulate mitochondrial fusion (Figure 1.18) (Dimmer *et al.,* 2006; Youle *et al.,* 2005). Increased mitochondrial fission leads to increased apoptosis and increased atrophy in skeletal muscle fibres (Youle *et al.,* 2005). It has also been shown that mice lacking Mfn1/2 exhibit mitochondrial dysfunction and enhanced muscle atrophy (Chen *et al.,* 2010). Mitochondrial fusion provides stability to mtDNA in skeletal muscle and prevents mtDNA mutations (Chen *et al.,* 2010).

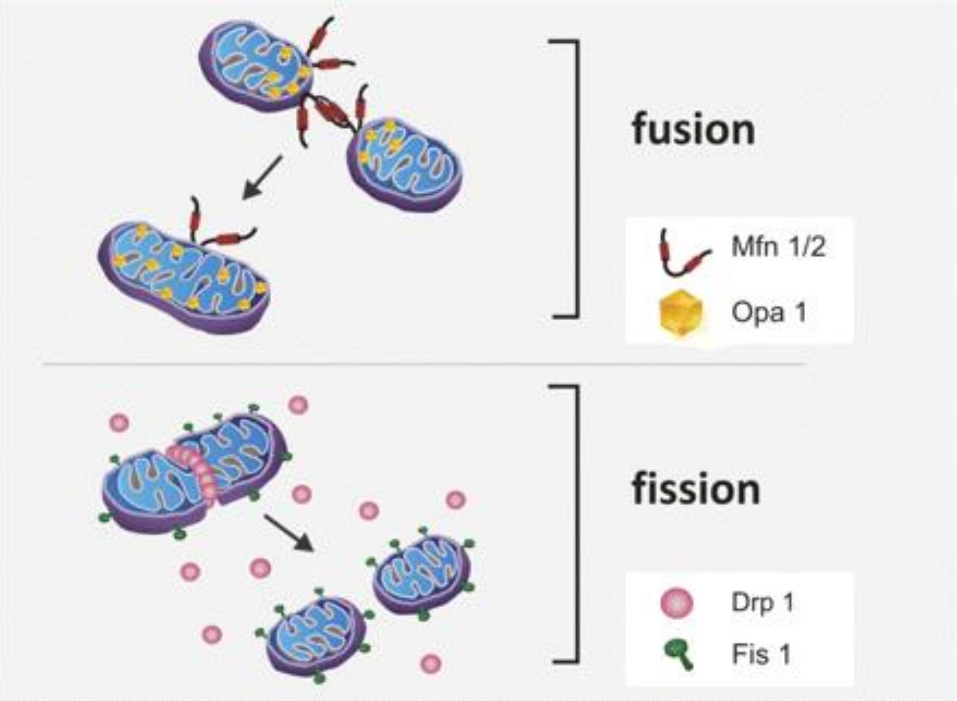

Figure 1.18 ***Mitochondrial fission and fusion***

Mitochondrial fission and fusion determine the shape and size of mitochondria. Opa1 and Mfn1/2 are involved in mitochondrial fusion, and Drp1 and Fis1 are involved in fission. Figure adapted from American Journal of Physiology, Endocrinology and Metabolism, Powers *et al.*, 2012, E31-9.

Furthermore, mitochondrial damage occurs due to enhanced mitochondrial ROS production (Brookes *et al.,* 2004; Kowaltowski *et al.,* 2009). Our laboratory has recently established that Mul1 ubiquitin ligase induces mitophagy in skeletal muscle during muscle wasting conditions (Lokireddy *et al.,* 2012). In mammals, mitophagy and mitochondrial abnormalities are regulated by PINK1, Parkin, Bnip3 and Bnip3L (Bothe *et al.,* 2000; Hara *et al.,* 2006). Parkin an E3 ubiquitin ligase being cytosolic ubiquitinates mitochondrial proteins, upon loss of mitochondrial membrane potential contributing to mitophagy. It has also been reported that recruitment of Parkin to impaired mitochondria requires PINK1 expression. Upon translocation to the mitochondrial surface, Parkin ubiquitylates the outer mitochondrial membrane proteins, which further recruits other proteins such as p62 on mitochondria to initiate mitophagy (Jin *et al.,* 2012). Earlier studies have shown that a large number of pathways negatively regulate the activity of autophagy-lysosomal pathway such as Raptor and mTORC1 (Grumati 2012). The age related mutations and deletions occuring in mitochondria contribute to the loss of mitochondrial DNA (Barazzoni *et al.,* 2000). In addition, the decline in protein synthesis has also been correlated with reduction in oxidative enzymes produced in mitochondria and VO_2 max that occurs with age (Rooyackers *et al.,* 1996).

1.9 Aims and Objectives

As discussed before PPARβ/δ has been implicated in the *in vitro* regulation of postnatal myogenesis through a mechanism involving transcriptional activation of *Gasp-1* and reduced activity of its down-stream target myostatin. It has also been established that absence of PPARβ/δ shows increased activity of myostatin. The role of PPAR in lipid metabolism and epidermal maturation and repair process has been well established. However, the role of PPARβ/δ in *in vivo* postnatal myogenesis and skeletal muscle regeneration has not been studied yet. Studies have also addressed skeletal muscle wasting in association with diseases such as cancer, AIDS, muscular dystrophy and aging. Despite, the current level of understanding of muscle wasting in relation to various diseases, the role of PPARβ/δ in muscle wasting during aging has not been studied. Therefore, the overall aim of my thesis was to investigate PPARβ/δ function during muscle wasting, and whether absence of PPARβ/δ impairs skeletal muscle regeneration and promotes pre-mature aging of muscles. The following aims were investigated using *in vitro* and *in vivo* experiments.

1. To establish the role of PPARβ/δ in postnatal myogenesis and skeletal muscle regeneration.

2. To investigate if lack of PPARβ/δ influences muscle aging.

CHAPTER 2
MATERIALS AND METHODS

This chapter outlines materials and methods used in this thesis including reagents, oligonucleotides, antibodies, chemicals and solutions.

2.1 Materials

2.1.1 Oligonucleotides

All oligonucleotides used in this study were synthesized by Sigma-Aldrich, Singapore. The stock solutions (100 µM) were stored in -20°C and working concentrations of primers used were 2.5 µM for quantitative Polymerase Chain Reaction (qPCR). The oligonucleotides used are listed in Table 2.1.

Table 2.1 ***qPCR primer sequences***

Gene	Forward (5'➔3')	Reverse (5'➔3')
Gapdh	GTGGCAAAGTGGAGATTGTTGCC	GATGATGACCCGTTTGGCTCC
mtDNA	CCTATCACCCTTGCCATCAT	GAGGCTGTTGCTTGTGTGAC
nuDNA	ATGGAAAGCCTGCCATCATG	TCCTTGTTGTTCAGCATCAC
Park2	TCTTCCAGTGTAACCACCGTC	GGCAGGGAGTAGCCAAGTT

2.1.2 Antibodies

Details of the primary, secondary and tertiary antibodies used in this thesis are listed in Table 2.2, Table 2.3 and Table 2.4. The final working dilutions of each antibody used in this thesis are also given in each table.

Table 2.2 ***Primary antibodies used for Western blot***

Antibody	*Company name*	*Catalog no.*	*Dilution*
GAPDH	Santa Cruz	SC-32233	1:10,000
LC3	Novus Biological	NB100-2220	1:500

Mul1	Abcam	Ab84067	1:2000
Pink1	Abcam	Ab23707	1:1000
Parkin	Abcam	Ab15954	1:1000
p62	Abcam	Ab109012	1:5000
Mfn2	Santa Cruz	SC-100560	1:500

Table 2.3 ***Primary antibodies used for Immunohistochemistry (IHC)***

Antibody	*Company name*	*Catalog no.*	*Dilution*
Pax7	DSHB	Pax7-b	1:1000
MyoD	Santa Cruz	SC-304	1:40
MyoD	BD Pharmingen	554130	1:25
Mac-1	BD Pharmingen	550282	1:100
Laminin	Sigma-Aldrich	L9393	1:1000

Table 2.4 ***Secondary and tertiary antibodies for Western blot and Immunohistochemistry (IHC)***

Antibody	*Company name*	*Catalog no.*	*Dilution*
Streptavidin, Alexa Fluor 488 conjugate	Invitrogen	S11223	1:1000
Goat anti-rabbit IgG (H+L) Alexa Fluor 594 conjugate	Invitrogen	A-11012	1:1000
Goat anti-mouse IgG HRP conjugate	Bio-Rad	170-6516	1:5000
Goat anti-rabbit IgG HRP conjugate	Bio-Rad	170-6515	1:5000
Rat IgG, biotinylated whole antibody (from goat)	GE Healthcare	RPN1005	1:400
M.O.M biotinylated anti-mouse IgG	Vector Labs	FMK-2201	1:500

2.1.3 Reagents and chemicals

Table 2.5 ***List of reagents and chemicals used in this thesis***

Chemical Name	*Company name*
β-mercaptoethanol	Sigma-Aldrich
Bovine serum albumin	Sigma-Aldrich
Bradford protein assay dye reagent concentrate	Bio-Rad
X-ray film	Kodak
IGEPAL CA-630 (NP40)	Fluka
NuPAGE LDS Sample Buffer (4x)	Life Technologies
MES-SDS (20x)	Life Technologies
NaF	Sigma-Aldrich
Nitrocellulose membrane	Bio-Rad
Ponceau S	Sigma-Aldrich
PMSF	Sigma-Aldrich
Sodium dodecyl sulphate	Sigma-Aldrich
Sodium Vanadate	Sigma-Aldrich
Tris base	1st BASE
SeeBlue Plus Pre-Stained protein standard	Life Technologies
Tris glycine SDS (2X)	Life Technologies
Skim milk powder	Fluka
EDTA	1st BASE
Chloroform	Merck Chemicals
DEPC treated water	Life Technologies
Formaldehyde	Sigma-Aldrich
MOPS	Fluka
TAE	1st BASE
Trizol reagent	Life Technologies
ProLong Gold Antifade reagent	Life Technologies
DPX mounting medium	Merck Chemicals

Eosin	Merck Chemicals
Hematoxylin	Merck Chemicals
Normal goat serum	Sigma-Aldrich
Triton X-100	Promega
Tween20	Promega
M.O.M kit	Vector labs
Xylene	Sigma-Aldrich
DAPI	Invitrogen Molecular Probes
Sodium tetraborate decahydrate	Sigma-Aldrich
Nitroblue tetrazolium	Sigma-Aldrich
Sodium succinate dibasic hexahydrate	Sigma-Aldrich
Ferric chloride	Sigma-Aldrich
Acid Fuchsin	Sigma-Aldrich
PBS (Dulbecco A)	Oxoid
DMEM	GE Healthcare
HI FBS	Gibco
Chick embryo extract	US Biologicals
Horse serum	Gibco
XF Calibrant (pH 7.4)	Seahorse Bioscience
XF Assay medium modified DMEM	Seahorse Bioscience
Matrigel	Corning
Penicillin-Streptomycin	Gibco
Glycine	Bio-Rad
Hydrochloric acid	Merck Chemicals
IPTG	Fermentas
2-propanol	Merck Chemicals
Sodium hydroxide	Merck Chemicals
Methylene blue	Sigma-Aldrich
Picric acid	Sigma-Aldrich
Ethanol	Merck Chemicals
Methanol	Merck Chemicals

2-methyl butane	Sigma-Aldrich
Magnesium sulphate heptahydrate	Sigma-Aldrich
Guanidine hydrochloride	Sigma-Aldrich
Sodium bicarbonate	Sigma-Aldrich
Bromophenol blue	GE Healthcare
Sodium acetate	Sigma-Aldrich
Collagenase Type IA	Sigma-Aldrich
Reverse transcriptase	Bio-Rad (iScript™cDNA synthesis kit)
Trypsin-EDTA	Life Technologies

2.1.4 Solutions

Table 2.6 ***Formal saline fixative***

10 % formaldehyde	250 ml
NaCl	8.7 g
MilliQ water	750 ml

Table 2.7 ***Borate buffer***

Sodium tetraborate	7.63 g
MilliQ water	2 L, adjust pH to 8.5 with concentrated HCl

Table 2.8 ***Methylene blue stain***

Methylene blue	1 g
0.01 M borate buffer (pH 8.5)	100 ml

Table 2.9 ***HCl (1M)***

Concentrated HCl	8.33 ml
MilliQ water	100 ml

Table 2.10 ***1:1 0.1M HCl : Ethanol***

Absolute ethanol	500 ml
Concentrated HCl	50 ml
MilliQ water	450 ml

Table 2.11 ***Scott's tap water***

Sodium bicarbonate	3.5 g
$MgSO_4$. $7H_2O$	20 g
MilliQ water	1 L

Table 2.12 ***10 % matrigel***

Matrigel	0.4 ml
DMEM (4^oC)	3.6 ml

Table 2.13 ***0.2 % Collagenase 1A solution***

Collagenase 1A (490U)	0.04 g
DMEM	20 ml
Freshly prepared and filter sterilized.	

Table 2.14 ***RIPA buffer***

1M Tris (pH 7.5)	2.5 ml
5 M NaCl	1.5 ml
0.5 M EDTA	0.1 ml
Igepal CA-630 (NP40)	5 ml
10 % SDS	5 ml
Sodium deoxycholate	10 ml
50 X protease inhibitor cocktail	1 ml
500 mM NaF	52.5 mg
100 mM PMSF	0.5 ml
700 mM Na_3VO_4	71.43 µl
Make up to 50 ml with MilliQ water. Store at 4°C.	

Table 2.15 ***MES-SDS running buffer (1X)***

20 X MES-SDS	50 ml
MilliQ water	950 ml

Table 2.16 ***Western blot transfer buffer***

Tris	3.03 g
Glycine	14.4 g
Methanol	200 ml
Make up to 1000 ml with MilliQ water. Store at 4°C	

Table 2.17 ***TBS (Tris buffered saline) (1X)***

1 M Tris-HCl (pH 7.5)	50 ml
5 M NaCl	30 ml
Make up to 1000 ml with MilliQ water. Store at 4°C	

Table 2.18 ***TBS-T (1X)***

1 M Tris-HCl (pH 7.5)	50 ml
5 M NaCl	30 ml
Tween-20	1 ml
Make up to 1000 ml with MilliQ water. Store at 4°C	

Table 2.19 ***5 % Western blot milk blocking solution***

Non fat milk powder	5 g
1X TBS-T	100 ml

Table 2.20 ***TAE buffer (1X)***

10 X TAE	100 ml
Make up to 1000 ml with MilliQ water	

Table 2.21 ***4 % Paraformaldehyde***

Paraformaldehyde	4 g
1 X PBS	100 ml
Stir slowly at 60°C inside fume hood. 1 N NaOH added to make clear solution. Remove from heat, and adjust pH to 7.2 with concentrated HCl. Filter with a 0.22 µm filter unit (Millipore)	

Table 2.22 ***2 % Paraformaldehyde***

Paraformaldehyde	2 g
1 X PBS	100 ml
Stir slowly at 60°C inside fume hood. 1 N NaOH added to make clear solution. Remove from heat, and adjust pH to 7.2 with concentrated HCl. Filter with a 0.22 µm filter unit (Millipore)	

Table 2.23 ***PBS (1X)***

PBS tablets	10
MilliQ water	1000 ml

Table 2.24 ***PBS-T (1X)***

1 X PBS	10 ml
10 % Tween-20 in water	20 µl

Table 2.25 ***MOPS buffer (10X)***

MOPS	41.9 g
1 M Sodium acetate	50 ml
0.5 M EDTA	10 ml
MilliQ water	500 ml
Filter sterilize and store at 4°C, protected from light	

Table 2.26 ***RNA loading dye***

10 X MOPS	1 ml
20 % deionized formaldehyde	2 ml
50 % deionized formamide	5 ml
0.02 % bromophenol blue	2 mg
Glycerol	0.5 ml
EDTA	3.7 mg
10 mg/ml ethidium bromide	40 µl
Make up to 10 ml with MilliQ water.	

Table 2.27 ***Van Gieson solutions***

Van Gieson solution

1 % acid Fuchsin	10 ml
Saturated picric acid	90 ml
Concentrated HCl	0.25 ml

Solution A

1% hematoxylin in absolute ethanol

Solution B

30 % Ferric chloride	4 ml
Concentrated HCl	1 ml
MilliQ water	100 ml

Table 2.28 ***DNA extraction buffer***

5M NaCl	100 µl
1 M Tris-HCl (pH 8.0)	50 µl
1 mM EDTA (pH 8.0)	10 µl
10 % SDS	500 µl
Proteinase K (0.2 µg/ µl)	100 µl
Make up to 5 ml with MilliQ water. Store at 4°C.	

2.2 Methods

2.2.1 Mice breeding

PPARβ/δ-null mice (mixed genetic background of Sv129/C57BL6) were gifted from Prof. Walter Wahli (University of Lausanne, Lausanne, Switzerland). Animals were maintained on standard chow diet at a constant temperature (20°C) with a 12 hr light-dark cycle with *ad libitum* access to water at the Nanyang Technological University animal facility. Wild type (WT) mice (C57BL/6) were purchased from the Center for Animal Resources, National University of Singapore (NUS-CARE), Singapore. All animal procedures were reviewed and approved by the Institute Animal Ethics Committee, Singapore.

2.2.2 RNA extraction

Total RNA from skeletal muscle tissue was isolated using TRIZOL (Invitrogen) as per the manufacturer's protocol. For RNA isolation from muscles, 50 mg of muscle tissue was homogenized in 1 ml of TRIZOL. Following 5 minutes incubation at room temperature, 200 µl of chloroform was added and the tubes were shaken vigorously for 15 seconds. After 3 minutes incubation at room temperature, the samples were centrifuged at 12,000 rpm for 15 minutes at 4°C. The upper clear aqueous phase was then transferred to a new tube and the RNA was precipitated with 500 µl of 2-propanol. Following 10 minutes incubation at room temperature, the samples were centrifuged at 12,000 rpm for 10 minutes at 4°C. The total RNA was then washed with 1 ml of 75 % ethanol (made in DEPC water) and finally pelleted at 5,000 rpm for 5 minutes and resuspended in an appropriate volume of DEPC-treated MilliQ water. RNA isolated from muscle was quantified using the Nanodrop spectrophotometer (ND-1000; Nanodrop Technologies Inc., DE, USA) to measure concentration and purity. In addition the RNA quality was checked by RNA electrophoresis. All RNA samples were stored at -80°C.

2.2.3 RNA gel electrophoresis

Formaldehyde-agarose denaturing gels used for electrophoresis contained between 1-2 % agarose, 1 X MOPS and 0.66 M Formaldehyde. Total RNA (1 µg) was mixed with an equal volume of RNA loading dye and incubated at

65°C for 5 minutes prior to loading. Electrophoresis of RNA was done between 40-80 V until the desired separation was achieved. The RNA loading dye contained ethidium bromide for visualisation of the RNA by UV trans illumination. A Gel Doc system (Bio-Rad Molecular Imager) was used to photograph the gels. The quality of the RNA was monitored by observing the integrity of 28S and 18S ribosomal RNA bands.

2.2.4 cDNA synthesis

cDNA was synthesized using iScript^{TM} cDNA synthesis kit (Bio-Rad), according to the manufacturer's instructions. For each cDNA reaction, 1 µg of RNA, 1 µl of iScript Reverse transcriptase, 4 µl of 5 X iScript reaction mix and 10 µl of nuclease-free water was added. The reaction mixture was incubated at 25°C for 5 minutes, followed by incubation at 42°C for 30 minutes and 85°C for 5 minutes and finally maintained at 4°C. After the completion of reactions, the synthesized cDNA was stored at -20°C prior to use.

2.2.5 Quantitative Polymerase Chain Reaction (qPCR)

RNA was isolated from muscles using TRIZOL (Invitrogen) and cDNA was synthesized using iScript^{TM} cDNA synthesis kit (Bio-Rad), as described above. Gene expression analysis by qPCR was carried out using the CFX96 system (Bio-Rad Laboratories, Inc., Hercules, CA, USA). Each 10 µl qPCR reaction contained 2 µl of cDNA, 5 µl of SsoFast Evagreen (Bio-Rad Laboratories, Inc., Hercules, CA, USA) and forward and reverse primers as stated in Table 2.1 at a final concentration of 2.5 µM. The thermal cycler conditions used for all the reactions are as follows: 98°C for 3 minutes, followed by 45 cycles of a three-step reaction, denaturation at 98°C for 3 seconds, annealing at 55°C (*mtDNA* and *nuDNA*) or 63°C (*Park2* and *Gapdh*) for 10 seconds and extension at 72°C for 10 seconds, with a final extension at 95°C. Gene expression levels were expressed as fold change and calculated using the ΔΔCt method.

2.2.6 Recombinant soluble ActRIIB purification

An overnight *E.coli* (BL21 strain) culture harboring the recombinant sActRIIB expression vector (Zhang Chen *et al.*, 2011) was diluted (1:50) and grown to an OD of 0.8 (600 nm) at 37°C in 1 L of LB Broth, Lennox (LB) medium containing 50 mg/ml ampicillin. Expression of the sActRIIB fusion protein was induced by adding 0.5 mmol/L isopropyl thio-β-galactoside (IPTG) to the culture for 2 hrs. Bacteria was then harvested by centrifugation, resuspended in 40 ml of lysis buffer (6 mol/L guanidine hydrochloride, 20 mmol/L Tris (pH 8.1), 5mmol/L 2-mercaptoethanol), sonicated and centrifuged at 10,000 g for 30 minutes. sActRIIB was purified from the supernatant fraction by Ni-Sepharose agarose affinity chromatography (Qiagen, Valencia, CA, USA) according to manufacturer's instructions. sActRIIB fractions obtained from the column were pooled and dialysed with two changes of 50 mmol/L Tris-HCl (pH 8.0) containing 150 mmol/L NaCl for 6 hrs. The purity of the recombinant sActRIIB protein was verified by SDS-PAGE.

2.2.7 Protein estimation

The protein concentration of the primary myotube and muscle homogenates was determined by Bradford's assay (Bradford 1976) using Bradford Protein Assay Dye Reagent Concentrate (Bio-Rad Laboratories, Inc., Hercules, CA, USA), as per the manufacturer's instructions.

2.2.8 Muscle injury model

Six-week-old male WT and *PPARβ/δ*-null mice were anesthetized by intraperitonial injection of a mixture of 10 mg/ml ketamine and 1 mg/ml xylazine at 0.1 ml/10 g body weight. Fifteen microlitres of notexin (10 μg/ml in 0.9 % saline; Latoxan, Rosans, France) was injected into the left *M. Tibialis anterior* (TA) muscle of mice using a 28-gauge needle (Hamilton Co., Whittier, California, USA). The TA muscle from the contralateral limb was used as the uninjured control. TA muscles were harvested on days 3, 5, 7 and 28 after notexin-induced injury. For the sActRIIB myostatin antagonist trial, mice were anesthetized with ketamine and xylazine as stated above. Fifteen microlitres of notexin (10 μg/ml) was injected into the left TA muscle with a 28-gauge needle

and the contralateral limb was used as an uninjured control. The mice were subsequently injected intraperitonially with sActRIIB (4 μg/g body weight) 3 times per week for a period of 4 weeks. TA muscles were harvested on day 28 after notexin-induced injury for further histological and molecular analysis.

2.2.9 Histological assessment of muscle regeneration

Muscle tissues were embedded in OCT (Optimal Cutting Temperature, Tissue-Tek, Sakura Fine TEK, Torrance, CA, USA) compound and then frozen in liquid nitrogen cooled isopentane. Serial cross sections (10 μm) were cut from the mid-belly of the muscle and mounted on cryoslides for histological, immunochemical and metabolic staining. Hematoxylin and Eosin (H&E) and Van Gieson's staining were performed according to the manufacturer's instructions [Catalog No. 115973-1 (Solution A), 115973-2 (Solution B) Merck Millipore, Singapore]. For H&E staining, the cryosections were stained with Hematoxylin for 1 minute and rinsed with tap water. Following a further 2 x 1 minute wash in Scott's tap water the sections were stained with Eosin for 2 minute, rinsed 3 times in 50 % ethanol and then in 70 % ethanol. Sections were further rinsed for 2 minutes in 95 % ethanol, washed 2 x 2 minutes each in 100 % ethanol, followed by 2 x 5 minutes in xylene. The stained sections were mounted with DPX mounting reagent and allowed to dry overnight. Images were captured using the Leica CTR 6500 microscope equipped with the Leica DFC 310 FX camera (Leica, Singapore). ImagePro Plus software (Media Cybernetics, Bethesda, MD, USA) and ImageJ software (National Institute of Health, USA) were used for image analysis. H&E stained images were used for Cross Sectional Area (CSA) measurement and fibrotic tissue was assessed through Van Gieson's stain. The area of interstitial fibrosis was quantitatively assessed using Van Gieson's stained images and was measured according to Luz *et al.* (2002). 5 images (magnification, 10X) around the lesion area from each sample were used for quantification, according to Ge *et al*. (2012) and calculated as the ratio of fibrotic area to total muscle cross sectional area (CSA) (%) of the images. For the contralateral uninjured control, the CSA from 1000 myofibres from randomly selected fields were counted. For regenerated myofibres, the CSA of centrally nucleated myofibres within the field were measured.

2.2.10 Immunohistochemical staining for Mac-1

Frozen muscle sections (10 μm) were stained for macrophages according to the previously established protocol. Briefly, sections were fixed in 2 % paraformaldehyde (PFA) for 5 minutes and then permeabilized with 0.3 % Triton X-100 in PBS for 5-10 minutes. The sections were then blocked with 10 % normal goat serum (NGS) in TBS (1X) for 1 hr at room temperature and then incubated with primary rat anti-mouse Mac-1 antibody (BD Pharmingen, San Diego, CA, USA; 1:100) in TBS overnight at 4°C. Following incubation with goat anti rat IgG biotinylated (1:400) secondary antibody, in 5 % NGS/TBS for 1 hr at room temperature, the sections were then incubated with streptavidin conjugated Alexa Fluor 488 (Invitrogen; 1:400) tertiary antibody in 5 % NGS/TBS for 30 minutes. Nuclei were counterstained with 4',6-diamidino-2-phenylindole (DAPI) (1:1000; Invitrogen Molecular Probes, Singapore) and mounted with ProLong Gold Antifade mounting reagent (Invitrogen, Singapore). Mac-1 positive cells were counted and expressed as a percentage of DAPI positive nuclei.

2.2.11 Immunohistochemical staining for Pax7 and MyoD

To detect Pax7 and MyoD co-immunostaining on TA muscle sections (10 μm), muscle sections were fixed in 4 % PFA for 5 minutes and then permeabilised with 0.2 % PBS-Tween 20. The sections were blocked with a solution containing 6 % mouse IgG blocking reagent (M.O.M Immunodetection kit; Vector laboratories, Inc, CA, USA) and 3 % bovine serum albumin (BSA) in PBS for 1 hr, followed by blocking again with M.O.M protein diluent with 1.5 % BSA/PBS, as per the manufacturer's instruction. Muscle sections were then incubated with mouse monoclonal Pax7 primary antibody (Developmental Studies Hybridoma Bank; DSHB, Iowa city, IA, USA; 1:1000) in 1.5 % BSA/PBS overnight at 4°C. Following incubation with M.O.M biotinylated anti-mouse IgG (Vector laboratories, Inc., CA, USA; 1:500), rabbit polyclonal anti- Laminin (Sigma Aldrich, Singapore, 1:1000) and rabbit polyclonal MyoD (Santa Cruz, USA; 1:40) antibodies in M.O.M protein diluent and 1.5 % BSA/PBS for 3 hrs. The sections were washed and incubated with Streptavidin conjugated Alexa Fluor 488 (Invitrogen; 1:1000) and Goat anti-rabbit Alexa

Fluor 594 (Invitrogen; 1:1000) in M.O.M protein diluent and 1.5 % BSA/PBS for 30 minutes- 1 hr. Nuclei were counterstained with DAPI for 5 minutes (Invitrogen Molecular Probes, Singapore; 1:5000) and mounted with ProLong Gold Antifade mounting medium (Invitrogen, Singapore). $Pax7^{+}/MyoD^{-}$ cells were quantified in the stained sections and expressed as a percentage of the total fibre number per section.

For MyoD immunostaining TA muscle sections (10 μm) were fixed in 4 % PFA for 5 minutes and permeabilised with 0.2 % PBS-Tween 20. The sections were blocked with a solution containing 6 % mouse IgG blocking reagent (M.O.M Immunodetection kit; Vector laboratories, Inc, CA, USA) and 3 % bovine serum albumin (BSA) in PBS for 1 hr, followed by blocking again with M.O.M protein diluent with 1.5 % BSA/PBS, as per the manufacturer's instruction. Muscle sections were incubated with MyoD (1:25; BD Pharmingen, San Diego, CA, USA) primary antibody in 1.5 % BSA/PBS overnight at 4°C. Following incubation with M.O.M biotinylated anti-mouse IgG in M.O.M protein diluent and 1.5 % BSA/PBS for 1 hr. The sections were washed and incubated with Streptavidin conjugated Alexa Fluor 488 (Invitrogen; 1:1000) in M.O.M protein diluent and 1.5 % BSA/PBS for 1 hr. Nuclei were counterstained with DAPI for 5 minutes (Invitrogen Molecular Probes, Singapore; 1:5000) and mounted with ProLong Gold Antifade mounting medium (Invitrogen, Singapore). MyoD positive cells were counted and expressed as a percentage of DAPI positive nuclei.

2.2.12 Succinate dehydrogenase (SDH) staining

SDH activity indicative of overall oxidative capacity of skeletal muscles was measured using a colorimetric assay, as described by Masuda *et al.* (2009). Muscle sections were air-dried for 30 minutes and incubated in pre-warmed PBS buffer containing 50 mM sodium succinate and 0.6 mM Nitro Blue Tetrazolium (NBT) (Sigma-Aldrich, Singapore) for 25 minutes at 37°C. The reaction was terminated by rinsing the sections thoroughly with distilled water. After dehydration and clearance by xylene, the sections were mounted using DPX (Sigma-Aldrich, Singapore). Images were captured using the Leica CTR 6500 microscope, equipped with the Leica DFC 310 FX camera and ImagePro Plus software (Media Cybernetics, Bethesda, USA).

2.2.13 DNA extraction

Total DNA was isolated from skeletal muscle by phenol chloroform extraction method. Fifty mg of skeletal muscle was digested with 500 µl of DNA extraction buffer overnight at 50°C. Following addition of 500 µl of phenol: chloroform: isoamyl alcohol (25:24:1) the digested sample in the tubes were shaken vigorously for 10 seconds. The samples were centrifuged at 12,000 g for 5 minutes. The upper aqueous phase was transferred to a new tube and 500 µl of chloroform was added to the samples. The tubes were shaken vigorously for 10 minutes, and samples were centrifuged at 12,000 g for 5 minutes. The aqueous phase was further transferred to a new tube and 1/10 volume of 3 M sodium acetate (pH 5.0) and 1 ml of 100 % ethanol was added to precipitate DNA. The tubes were centrifuged further at 12,000 g for 5 minutes to pellet the DNA. The pellet was washed with 1 ml of 70 % ethanol and centrifuged at 12,000 g for 2 minutes. The supernatant was discarded and the pellet was air dried for 5- 10 minutes and resuspended in MilliQ water. DNA isolated from muscle was quantified using the Nanodrop spectrophotometer (ND-1000; Nanodrop Technologies Inc., DE, USA) to measure concentration and purity. In addition the DNA quality was checked by DNA electrophoresis.

Agarose gels for DNA electrophoresis was prepared using 0.8 % agarose. The gels were made up in 1 X TAE, with ethidium bromide added for visualization of DNA bands. DNA samples were mixed with 10 X DNA loading dye before loading. DNA molecular marker of 1 kB molecular weight was run beside the DNA samples. Following electrophoresis, the DNA bands were then visualized by UV trans illumination. A Gel Doc system (Bio-Rad Molecular Imager) was used to photograph the gels.

2.2.14 Assessment of mitochondrial DNA (mtDNA) copy number vs. nuclear DNA (nuDNA) copy number by qPCR

The relative copy number of mitochondrial DNA (mtDNA) *vs* nuclear DNA (nuDNA) was measured as per the previously published protocol described by Lokireddy *et al.,* 2012. Primers used for mtDNA and nuDNA qPCR are listed in Table 2.1. mtDNA *vs* nuDNA levels were analyzed as relative gene expression and calculated using the ΔΔCt method.

2.2.15 Cell culture

2.2.15.1 Myoblast proliferation assay

The C2C12 mouse myoblast cell line obtained from ATCC was used for myoblast proliferation assay. The cell stocks were passaged in C2C12 proliferation medium: Dulbecco's Modified Eagle Medium (High glucose DMEM), 10 % Foetal bovine serum (HI FBS), 1 % Pencillin/Streptomycin (P/S) and allowed to proliferate. Proliferating C2C12 cells treated with/without sActRIIB were fixed at 0, 24, 48 and 72 hr intervals in 96-well plates with 100 µl of formal saline fixative. C2C12 myoblast proliferation was assessed using the methylene blue photometric end-point assay (Oliver *et al*., 1989). After removal of fixative, 100 µl of methylene blue stain was added to each well and incubated for 30 minutes at room temperature. The stain solution was then removed and washed 4 times with 200 µl of 0.01M sodium borate buffer. Following this, 200 µl of 0.1 M HCl: Ethanol (1:1) was added to each well. Absorbance at 655 nm was determined using a microplate reader, which is directly proportional to cell number.

2.2.15.2 Isolation of primary myoblasts (satellite cells)

To isolate primary myoblasts hind limb skeletal muscles from mice were dissected, minced in PBS and then centrifuged at 3000 rpm for 10 minutes at 37°C. Following removal of PBS the minced muscle was digested in 0.2 % collagenase type 1A in warmed DMEM (3 ml per mouse for WT mice and *PPARβ/δ*-null mice) for 90 minutes at 37°C with shaking (70 rpm). Once the digestion was complete, the tube was topped up with PBS and centrifuged at 3000 rpm for 10 minutes to remove the collagenase. The digested muscle was gently triturated for 5 minutes in 10 ml of PBS and this was filtered through a 100 µm filter. The filtered suspension was centrifuged at 3000 rpm for 10 minutes and the pellet was resuspended in Satellite cell (SC) medium: DMEM, 20 % FBS, 10 % HS, 1 % P/S and 1 % Chick embryo extract (CEE). The supernatant was plated onto an uncoated 10 cm dish and incubated at 37°C and 5 % CO_2 for 3 hrs to let fibroblasts settle down, this is Pre-plate 1 (PP1). After 3 hrs, the cell suspension from PP1 was transferred to 10 % matrigel DMEM coated 10 cm dish, this is PP2, and was incubated overnight at 37°C and 5 % CO_2. After overnight attachment of cells onto the matrigel coated plate, the cell

suspension from PP2 was transferred to another matrigel coated 10 cm dish, this was PP3. Isolated satellite cells were later washed with SC medium and PBS and trypsinized and seeded for differentiation assay.

2.2.16 Assessment of Cellular Oxygen Consumption Rate (OCR) using the XF^{e}24 extracellular flux analyzer

The oxygen consumption rate (OCR) of cells was analyzed using XF Cell Mito Stress Test kit and the XF^{e}24 extracellular flux analyzer. Prior to commencing the assay XF^{e}24 cell culture microplates were incubated at 37°C in a non-CO_2 incubator for 1 day to ensure the plates were hydrated. Primary myoblasts were seeded onto matrigel coated XF^{e}24 cell culture microplates at a density of 30,000 cells (primary myoblasts) per well in satellite cell medium. After an overnight period of attachment at 37°C and 5 % CO_2, the primary myoblasts were washed with Assay medium containing 1 mM sodium pyruvate and 25 mM glucose of pH 7.4 and incubated in a non-CO_2 incubator for at least 30 minutes. During the incubation, 1 μM Oligomycin, 1 μM of carbonyl cyanide-p-trifluoromethoxyphenylhydrazone (FCCP) and 0.5 μM Antimycin + Rotenone was prepared to be loaded into injection ports. Assessment of OCR using the XF^{e}24 extracellular flux analyzer was performed at 37°C. OCR due to proton leak and ATP turnover was measured in the presence of oligomycin, maximal mitochondrial respiratory capacity was measured by adding FCCP and non-mitochondrial respiration was determined through addition of Rotenone and Antimycin. OCR graphs and respective error bars were generated by the XF^{e}24 extracellular flux analyzer during the course of the analysis. All OCR values were normalized against total protein content.

2.2.17 Measurement of Grip strength

Grip strength of both the fore and hind limbs was assessed in mice of different age groups using a grip strength apparatus (MK380S, Muromachi) (Angelis *et al.*, 2006). The mice were pulled backwards by their tail and the maximal force generated by the mice was digitally recorded. The grip strength of each mouse was measured three times with a pause of 30 seconds between each reading.

The mean maximal force of the three grip strength tests was calculated and expressed in Newtons.

2.2.18 Statistical analysis

Statistical differences between groups were determined using unpaired two-tailed Student's *t*-test and the results were considered significant at $P<0.05$ (*), $P<0.01$ (**), or $P<0.001$ (***). Data are expressed as mean ± S.E.M (standard error of the mean).

CHAPTER 3
INACTIVATION OF PPARβ/δ ADVERSELY AFFECTS SATELLITE CELLS AND REDUCES POSTNATAL MYOGENESIS

All of the data in this chapter has been published with several co-authors in *Am J Physiol Endocrinol Metab.* In conjunction with my Supervisor, I have bred and maintained *PPARβ/δ*-null mice and Wild-type mice. I have performed all experiments on my own entirely. I have also interpreted the results and discussion with my Supervisor and Co-Supervisor. Also, I have written the research work and all the figures were prepared by me.

3.1 Results

3.1.1 PPARβ/δ-null mice exhibit pronounced skeletal muscle atrophy

PPARβ/δ-null mice had reduced body weight and a significant reduction in *M. tibialis anterior* (TA), *M. gastrocnemius* muscle (Gas), *M. extensor digitorum longus* (EDL) and *M. soleus* (Sol) muscle weights when compared to Wild-type (WT) at post-natal age of 10 weeks (Figure 3.1A, B, C). Although, no significant difference in *M. quadriceps* (Quad) muscle weights was noted, there was a trend towards reduced muscle weight in *PPARβ/δ*-null mice (Figure 3.1B). Consistent with the reduced muscle weights, *PPARβ/δ*-null mice also showed significantly reducted TA muscle fibre Cross Sectional Area (CSA) when compared to WT mice (Figure 3.1D), although no change was observed in myofibre number (*data not shown*). Satellite cells being muscle precursor cells play essential roles in postnatal muscle growth and maintenance (Pannerec *et al.*, 2012). As such, immunohistochemical analysis was performed to quantify the number of $Pax7^{+}/MyoD^{-}$ satellite cells in muscle fibre sections. Results showed a significant reduction in the number of $Pax7^{+}/MyoD^{-}$ satellite cells in resting muscle fibres of *PPARβ/δ*-null mice, compared to WT controls (Figure 3.1E).

Figure 3.1 Enhanced skeletal muscle atrophy in *PPARβ/δ*-null mice.
(A) Body weight (g) of Wild type (WT) and *PPARβ/δ*-null mice at 10 weeks of age. Error bars represent mean ± s.e.m, n=3 for *PPARβ/δ*-null mice and n=4 for WT mice. (B) Graph showing combined average weight of left and right TA, Gas and Quad muscles, normalized to total body weight, of WT and *PPARβ/δ*-null mice at 10 weeks of age. Error bars represent mean ± s.e.m, n=3 for *PPARβ/δ*-null mice and n=4 for WT mice. (C) Graph showing combined average weight of left and right EDL and Sol muscles, normalized to total body weight of WT and *PPARβ/δ*-null mice at 10 weeks of age. Error bars represent mean ± s.e.m, n=3 for *PPARβ/δ*-null mice and n=4 for WT mice. (D) Frequency distribution of TA muscle fibre cross sectional area (CSA; μm^2) in resting muscle from WT and *PPARβ/δ*-null mice at 10weeks of age. (E) Number of quiescent SCs ($Pax7^+/MyoD^-$) per 100 myofibre, in resting TA muscle from 10-week-old WT and *PPARβ/δ*-null mice. Error bars represent mean ± s.e.m, n=3 per group. Statistical differences are indicated in relevant panels, $P<0.05$ (*), $P<0.01$ (**) $P<0.001$ (***).

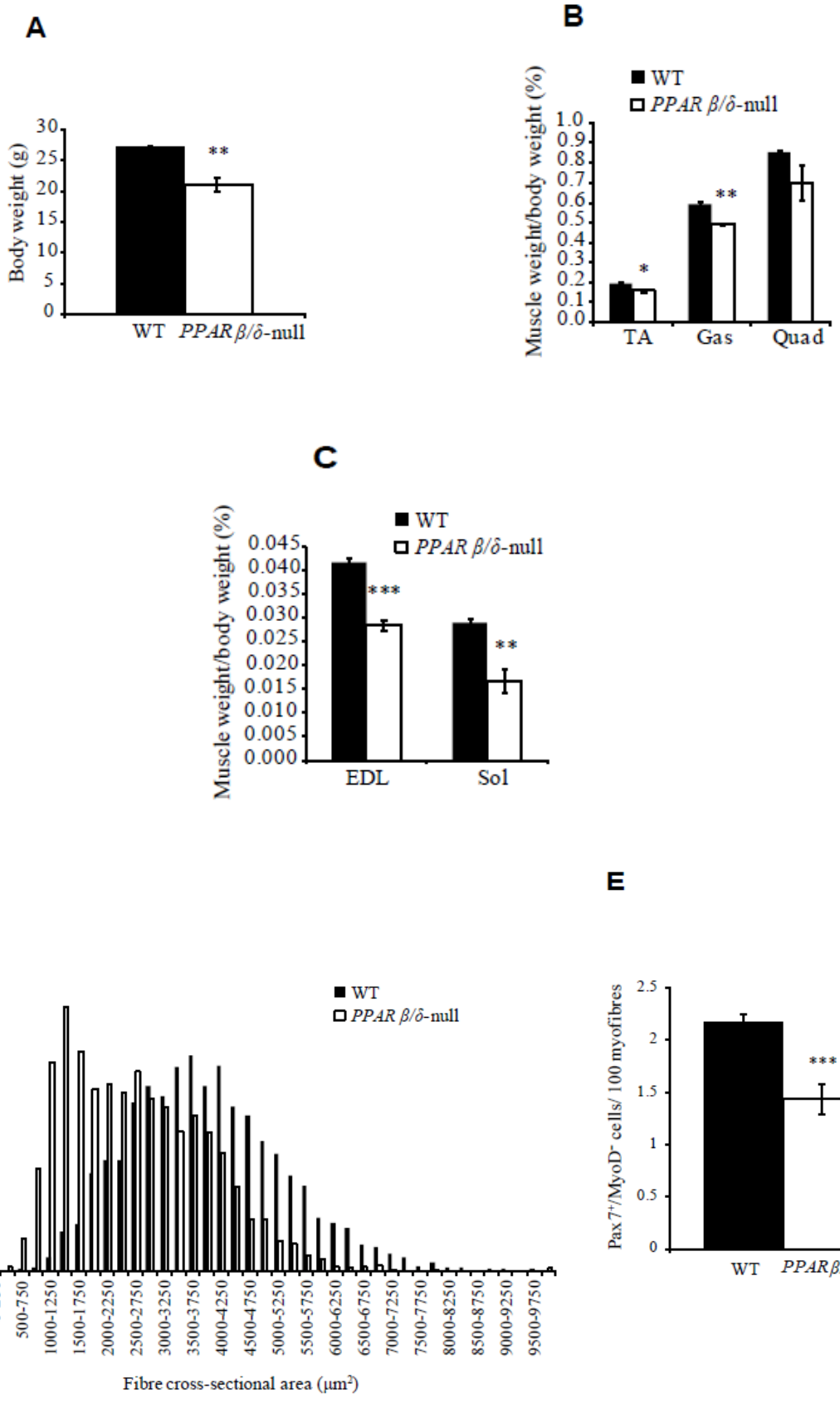
A
Body weight (g)
30
25
20
15
10
5
0
**
WT
PPARβ/δ-null
B
WT
PPAR β/δ-null
Muscle weight/body weight (%)
1.0
0.9
0.8
0.7
0.6
0.5
0.4
0.3
0.2
0.1
0.0
*
**
TA
Gas
Quad
C
WT
PPAR β/δ-null
Muscle weight/body weight (%)
0.045
0.040
0.035
0.030
0.025
0.020
0.015
0.010
0.005
0.000
***
**
EDL
Sol
D
WT
PPAR β/δ-null
Fibre number
120
100
80
60
40
20
0
0-250
500-750
1000-1250
1500-1750
2000-2250
2500-2750
3000-3250
3500-3750
4000-4250
4500-4750
5000-5250
5500-5750
6000-6250
6500-6750
7000-7250
7500-7750
8000-8250
8500-8750
9000-9250
9500-9750
Fibre cross-sectional area (μm²)
E
Pax7⁺/MyoD⁻ cells/ 100 myofibres
2.5
2
1.5
1
0.5
0
***
WT
PPARβ/δ-null

3.1.2 Histological analysis of skeletal muscle during early regeneration

To further study the effect of loss of *PPARβ/δ* on postnatal myogenesis, skeletal muscle regeneration was assessed in WT and *PPARβ/δ*-null mice injected with notexin. The uninjured TA muscles from both *PPARβ/δ*-null and WT mice are shown in Figure 3.2A, and upon injury both the genotypes showed complete and extensive muscle degeneration 3 days post notexin-induced injury with decreased intact muscle fibres (Figure 3.2A). However, more extensive necrosis was seen on day 3-post notexin injection in *PPARβ/δ*-null mice, compared to WT mice (Figure 3.2A). A mixed population of hyperstained necrotic myofibres and newly developing myofibres were observed in TA muscle from both *PPARβ/*δ-null mice and WT controls at day 5-post injury (Figure 3.2A). Nascent myofibres characterized by centrally located nuclei and small fibre size, were abundant at 7 days post-injury in TA muscle from both *PPARβ/δ*-null mice and WT controls; however, *PPARβ/δ*-null mice had visibly smaller myofibres when compared to WT controls (Figure 3.2A). At day 3 post-notexin injection, immunohistochemical analysis with Mac-1 antibodies revealed increased infiltration of macrophages in *PPARβ/δ*-null mice when compared to WT controls (Figure 3.2B). However, after 28 days of regeneration no significant difference in the percentage of Mac-1 positive cells was noted between *PPARβ/*δ-null mice and WT controls (Figure 3.2C). Collectively these data suggest that loss of *PPARβ/*δ affects the early stages of muscle regeneration.

3.1.3 Reduced numbers of proliferating myoblasts in PPARβ/δ-null regenerating muscle

To assess whether or not loss of *PPARβ/δ* affects satellite cell (SC) activation, we performed MyoD immunohistochemical analysis on notexin-injured TA muscle sections. A significant reduction in MyoD-positive myoblasts was observed from 3 days post-notexin injection; with greater than 50% reduction in MyoD-positive cells noted at day 3, ~38 % reduction at day 7 and ~50% reduction at day 28 post injury in *PPARβ/δ*-null TA muscle, compared to respective WT controls (Figure 3.2D). These data indicate that absence of

PPARβ/δ significantly reduces the pool of proliferating myoblasts present in injured and regenerating skeletal muscle.

SC self-renewal was further assessed in *PPARβ/δ*-null muscle through MyoD and Pax7 immunohistochemical analysis on regenerated (day 28-post notexin injection) TA muscle sections. After injury and regeneration *PPARβ/δ*-null mice revealed a significant reduction in SC number in comparison to WT mice (Figure 3.2E). However, we did not observe any significant difference in SC number between uninjured and regenerated TA muscle in both the genotypes (comparison not shown). These data suggest that the self-renewal capacity of SCs remains unaffected in *PPARβ/δ*-null mice.

Figure 3.2 *PPARβ/δ* deficiency leads to increased inflammatory response and reduced myoblast activation following notexin-induced injury.
(A) Representative images of H&E stained uninjured TA muscle cross sections and TA muscle sections at day 3-, 5-, and 7-post notexin injection. Infiltration of inflammatory cells (I), necrotic fibres (N) and newly formed myofibres (←) are marked on the images. Scale bars represent 100 μm. (B) Quantification of Mac-1 positive cells, as assessed through immunohistochemistry, in TA muscle cross sections from WT and *PPARβ/δ*-null mice at day 3- post notexin injection. Mac-1 positive cells were expressed as a percentage of the total nuclei (DAPI positive). (C) Quantification of Mac-1 positive cells, as assessed through immunohistochemistry, in TA muscle cross sections from WT and *PPARβ/δ*-null mice at day 28- post notexin injection. Mac-1 positive cells were expressed as a percentage of the total nuclei (DAPI positive). (D) Quantification of MyoD positive cells, as assessed through immunohistochemistry, in TA muscle cross sections from WT and *PPARβ/δ*-null mice at day 3-, 7- and 28-post notexin injection. MyoD positive cells were expressed as a percentage of total nuclei (DAPI positive). (E) Quantification of $Pax7^{+}/MyoD^{-}$ cells, as assessed through immunohistochemistry, in regenerated (day 28-post notexin-induced injury) TA muscles cross sections harvested from WT and *PPARβ/δ*-null mice. $Pax7^{+}/MyoD^{-}$ cells were expressed as number of $Pax7^{+}/MyoD^{-}$ cells per 100 myofibre. Error bars represent mean ± s.e.m, n=3 per group. Statistical differences are indicated in relevant panels, $P<0.05$ (*), $P<0.01$ (**) and $P<0.001$ (***).

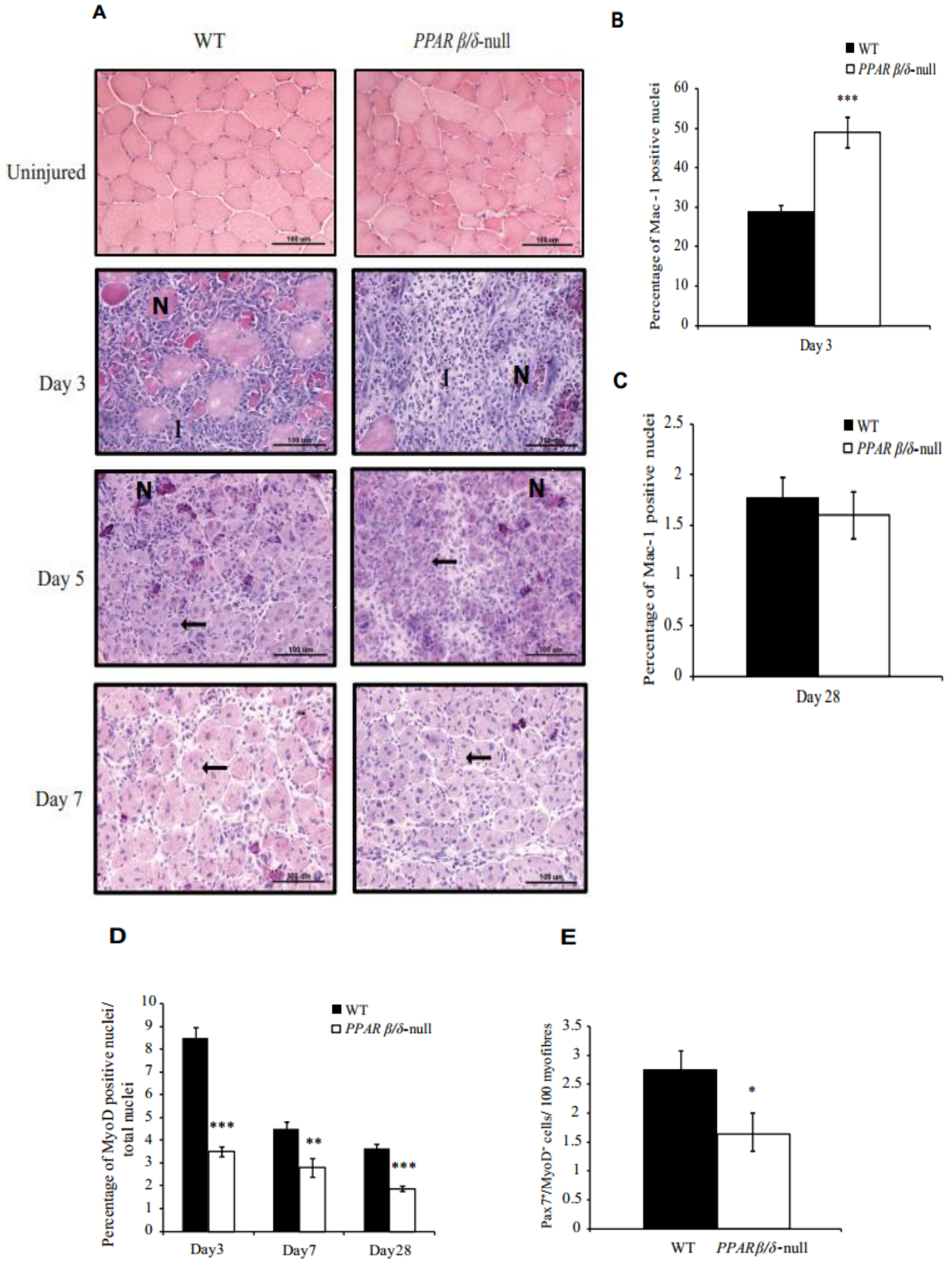
A
WT
PPAR β/δ-null
Uninjured
Day 3
Day 5
Day 7
N
I
B
WT
PPAR β/δ-null
Percentage of Mac-1 positive nuclei
***
Day 3
C
WT
PPAR β/δ-null
Percentage of Mac-1 positive nuclei
Day 28
D
WT
PPAR β/δ-null
Percentage of MyoD positive nuclei/ total nuclei
***
**
***
Day3
Day7
Day28
E
Pax7+/MyoD+ cells/ 100 myofibres
*
WT
PPARβ/δ-null

Figure 3.3 Impaired muscle regeneration in *PPARβ/δ*-null mice.

(A) Representative images of H&E stained TA muscle cross sections at day 28-post notexin injection. Newly formed myofibres (←) are marked on the images. Scale bars represent 100 μm. (B) Frequency distribution of WT and *PPARβ/δ*-null mice TA muscle fibre cross-sectional area (CSA; μm^2) at day 28-post notexin injection. (C) TA muscle weights, normalized to total body weight, of WT and *PPARβ/δ*-null mice at day 28-post notexin injection. (D) Quantification of centrally formed myonuclei within regenerated (day 28-post notexin-induced injury) TA myofibres from WT and *PPARβ/δ*-null mice. Graph displays the percentage of myofibres with 1, 2 or ≥3 centrally formed myonuclei. Error bars represent mean ± s.e.m, n=3 in each group. Statistical differences are indicated in relevant panels, $P<0.05$ (*), $P<0.01$ (**) and $P<0.001$ (***).

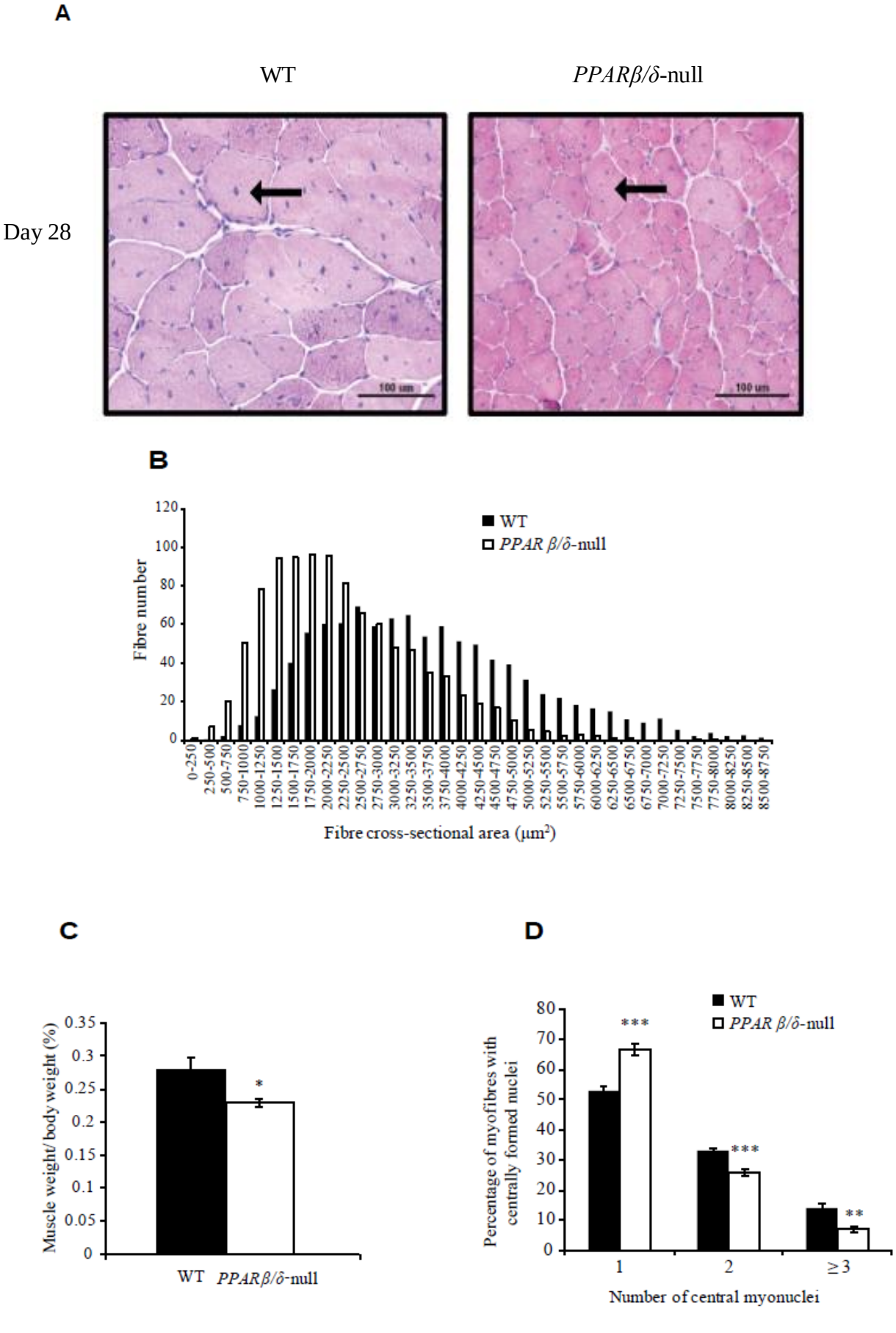
A
WT
PPARβ/δ-null
Day 28
100 um
100 um
B
WT
PPAR β/δ-null
Fibre number
120
100
80
60
40
20
0
0-250
250-500
500-750
750-1000
1000-1250
1250-1500
1500-1750
1750-2000
2000-2250
2250-2500
2500-2750
2750-3000
3000-3250
3250-3500
3500-3750
3750-4000
4000-4250
4250-4500
4500-4750
4750-5000
5000-5250
5250-5500
5500-5750
5750-6000
6000-6250
6250-6500
6500-6750
6750-7000
7000-7250
7250-7500
7500-7750
7750-8000
8000-8250
8250-8500
8500-8750
Fibre cross-sectional area (μm²)
C
Muscle weight/ body weight (%)
0.35
0.3
0.25
0.2
0.15
0.1
0.05
0
*
WT
PPARβ/δ-null
D
WT
PPAR β/δ-null
Percentage of myofibres with centrally formed nuclei
80
70
60
50
40
30
20
10
0
***
***
**
1
2
≥ 3
Number of central myonuclei

3.1.4 Loss of PPARβ/δ results in reduced centrally placed myonuclei in regenerated muscle

Histological analysis was performed to quantitatively examine muscle regeneration 28-days post notexin-induced injury (Figure 3.3A). Morphological analysis indicated an observable reduction in myofibre size in regenerated TA muscle from *PPARβ/*δ-null, when compared to WT controls (Figure 3.3A). Further analysis of myofibre CSA indicated reduced myofibre size in regenerated TA muscle from *PPARβ/*δ-null mice (Figure 3.3B) in comparison to WT, which was consistent with the atrophy phenotype noted in *PPARβ/*δ-null mice prior to injury (Figure 3.1D). Consistent with this, *PPARβ/δ*-null mice also showed significantly reduced TA muscle weight upon regeneration when compared to WT controls (Figure 3.3C). Regenerated myofibres are also characterized by the presence of centrally located myonuclei (Pinter *et al.*, 2003). Hence, we next assessed the number of central myonuclei per myofibre in regenerated TA muscle from WT and *PPARβ/*δ-null mice. As shown in Figure 3.3D, regenerated myofibres in *PPARβ/*δ-null mice had a significant increase in myofibres with 1 centrally placed nuclei, associated with a significant reduction in the percentage of myofibres with 2 and ≥3 centrally placed nuclei, when compared to WT controls (Figure 3.3D). In particular, the regenerated myofibres from WT mice had 52.99 ± 2.01% of 1 centrally placed nuclei and 66.76 ± 1.78% was observed in *PPARβ/δ*-null mice. Whereas the number of myofibres with 2 centrally placed nuclei were found to be 33.07 ± 0.7% in WT and 26.03 ± 1% in *PPARβ/δ*-null, and greater than 3 centrally placed nuclei was found to be 13.9 ± 1.53% in WT and 7.2 ± 0.87% in *PPARβ/δ*-null mice (Figure 3.3D).

3.1.5 Loss of PPARβ/δ does not significantly alter scar tissue formation or metabolic properties of regenerated muscle

Earlier studies have shown that, the final phase of skeletal muscle regeneration is usually characterized by fibrotic tissue formation, which contributes to incomplete functional recovery (Kaariainen *et al.,* 2000). Van Gieson's stain was used to examine and quantify the extent of fibrotic tissue formation in regenerated TA muscle of WT and *PPARβ/δ*-null mice. Quantification of fibrotic tissue formation revealed no significant difference in the area of fibrotic tissue in regenerated TA muscle sections between WT and *PPARβ/δ*-null mice (Figure 3.4A).

Skeletal muscle regeneration has been shown to increase the number of oxidative muscle fibres (Ciciliot *et al.,* 2010). Hence, through assessing Succinate dehydrogenase (SDH) activity (Masuda *et al.,* 2009), we further assessed the proportion of oxidative muscle fibres in regenerated (day 28-post notexin injection) TA muscles. Upon regeneration, TA muscles from both WT and *PPARβ/δ*-null mice showed an increase in SDH activity, as measured through increased SDH staining, when compared to respective uninjured controls. However, it is noteworthy to mention that SDH staining, and thus activity, was comparable between uninjured TA muscle from WT and *PPARβ/δ*-null mice and between regenerated TA muscle from WT and *PPARβ/δ*-null mice (Figure 3.4B, C). These results specify that loss of *PPARβ/δ* does not lead to a change in oxidative capacity in injured skeletal muscle tissue.

Figure 3.4 Scar tissue and muscle oxidative capacity remained unaltered between WT and *PPARβ/δ*-null during regeneration.
(A) Quantification of interstitial fibrotic tissue in TA muscle cross sections at day 28-post notexin injection, as assessed through Van Geison's staining. The percentage of fibrosis in each sample was calculated as the ratio of the fibrotic area to cross sectional area (CSA) (%) of the images. (B) Representative images of succinate dehydrogenase (SDH) staining of WT and *PPARβ/δ*- null TA muscle cross sections at day 28-post notexin injection. Black boxes in the lower panels indicate the regions in the magnified image in the upper panel; Scale bars in the upper panel represent 100 μm in higher-magnification image. (C) Quantitative analysis of SDH activity in uninjured and regenerated (day 28-post notexin-induced injury) TA muscles cross sections harvested from WT and *PPARβ/δ*-null mice. Error bars represent mean ± s.e.m, n=3 in each group. Statistical differences are indicated in relevant panels, $P<0.05$ (*).

A

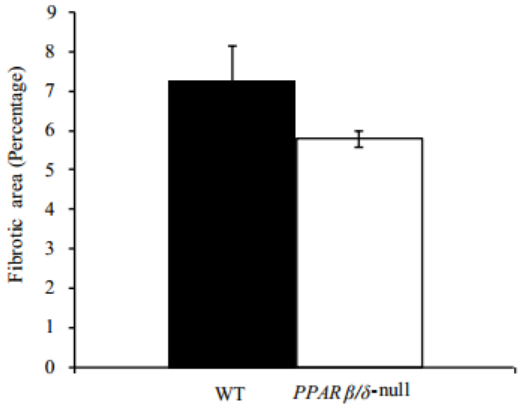
Fibrotic area (Percentage)
9
8
7
6
5
4
3
2
1
0
WT
PPARβ/δ-null

B

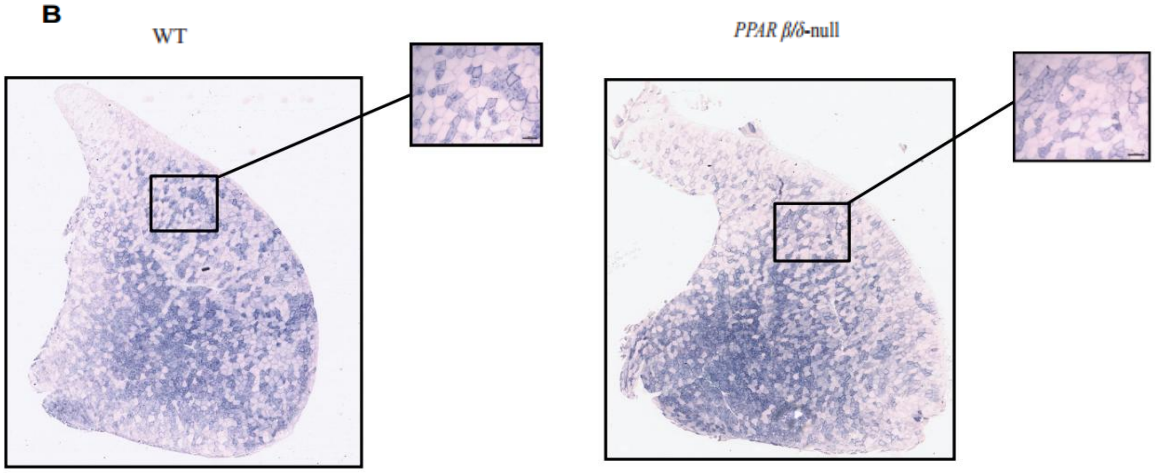
WT
PPARβ/δ-null

C

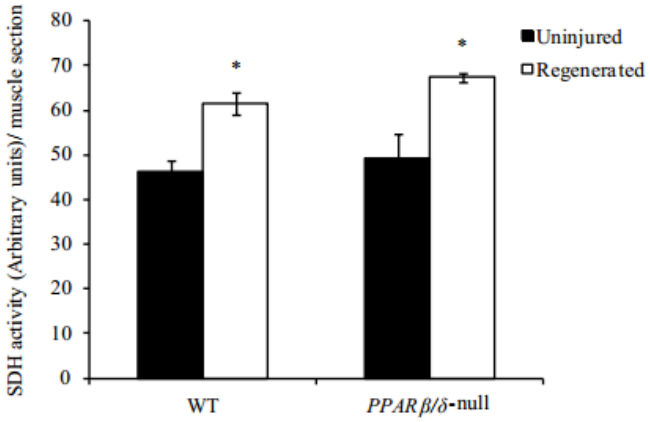
SDH activity (Arbitrary units)/ muscle section
80
70
60
50
40
30
20
10
0
*
*
Uninjured
Regenerated
WT
PPARβ/δ-null

Figure 3.5 Functional antagonism of Myostatin results in skeletal muscle hypertrophy pre and post notexin-induced injury.
(**A**) Increase in body weight (g) of *PPARβ/δ*-null mice injected with either vehicle control (Dialysis buffer; DB) or sActRIIB (4μg/g body weight) Myostatin antagonist for a period of 4 weeks. (**B**) Graph showing TA, Gas and Quad muscle weights from the right hindlimb, normalized to total body weight, of *PPARβ/δ*-null mice 4 weeks post-injection of either DB or sActRIIB (4μg/g body weight) Myostatin antagonist. (**C**) Graph showing EDL and Sol muscle weights from the right hindlimb, normalized to total body weight of *PPAR β/δ*-null mice 4 weeks post-injection of either DB or sActRIIB (4μg/g body weight) Myostatin antagonist. (**D)** Frequency distribution of TA muscle fibre cross-sectional area (CSA; μm^2) in *PPARβ/δ*-null mice 4 weeks post-injection of either DB or sActRIIB (4μg/g body weight) Myostatin antagonist. (**E**) Frequency distribution of muscle fibre cross-sectional area (CSA; μm^2) in regenerated (day 28-post notexin-induced injury) TA muscle from *PPAR β/δ*-null mice injected with either DB (day 28-DB) or sActRIIB (4μg/g body weight) Myostatin antagonist (day 28-sActRIIB). (**F**) Quantification of centrally formed myonuclei within regenerated (day 28-post notexin-induced injury) TA myofibres from *PPARβ/δ*-null mice injected with either DB (day 28-DB) or sActRIIB (4μg/g body weight) Myostatin antagonist (day 28-sActRIIB). Error bars represent mean ± s.e.m, n=3 in each group. Statistical differences are indicated in relevant panels, $P<0.05$ (*), $P<0.01$ (**).

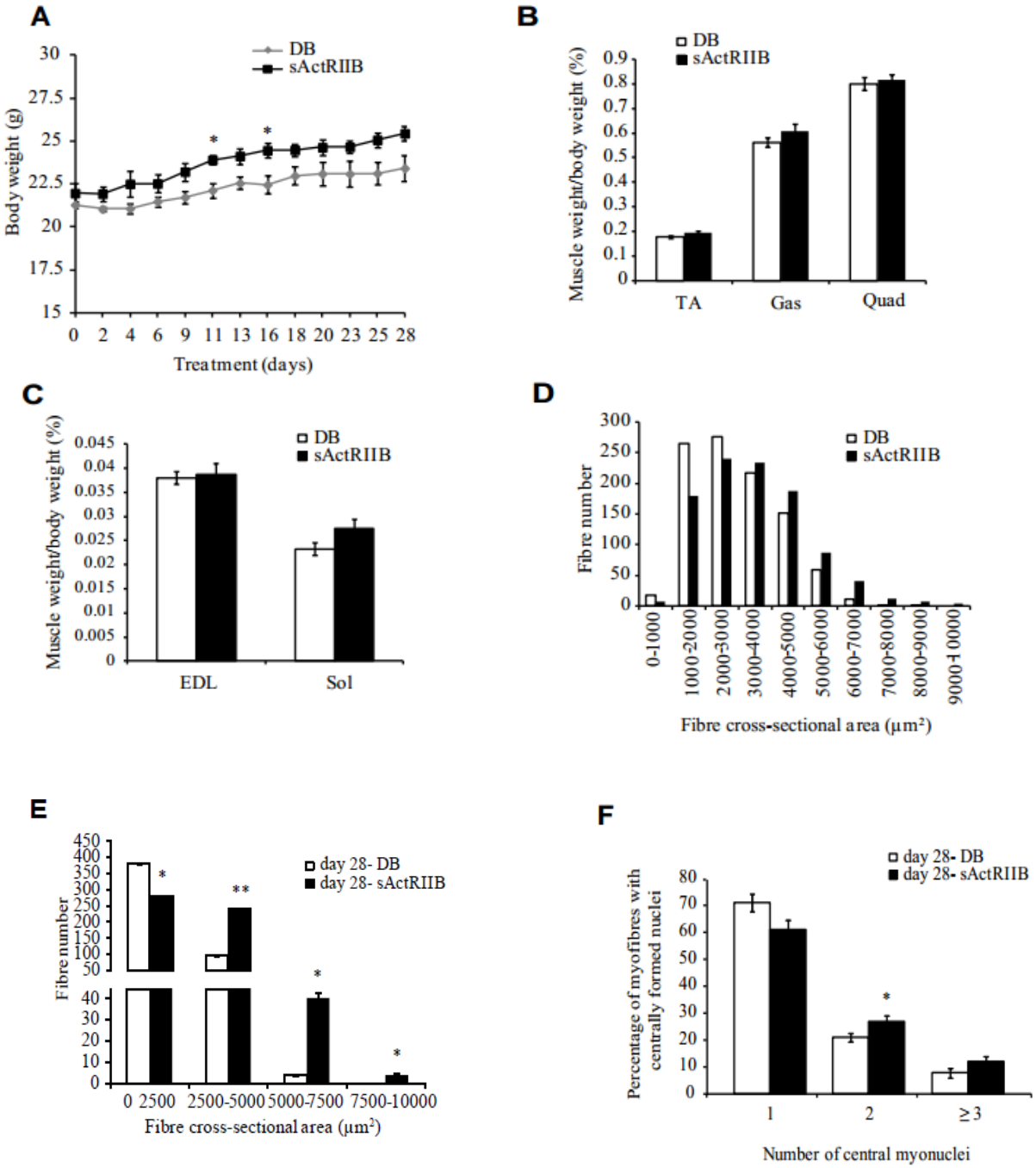
A
DB
sActRIIB
Body weight (g)
Treatment (days)
B
DB
sActRIIB
Muscle weight/body weight (%)
TA
Gas
Quad
C
DB
sActRIIB
Muscle weight/body weight (%)
EDL
Sol
D
DB
sActRIIB
Fibre number
Fibre cross-sectional area (µm²)
E
day 28- DB
day 28- sActRIIB
Fibre number
Fibre cross-sectional area (µm²)
F
day 28- DB
day 28- sActRIIB
Percentage of myofibres with centrally formed nuclei
Number of central myonuclei

3.1.6 Blockade of Myostatin leads to skeletal muscle hypertrophy in PPARβ/δ-null mice pre- and post-injury

Myostatin has been established to bind with high affinity to sActRIIB (Lee *et al.*, 2001), inhibiting myostatin signaling and contributing to increased musculature. Hence, we tested the effect of antagonism of myostatin in *PPARβ/δ*-null mice using sActRIIB. Upon administration of sActRIIB (4μg/g body weight), increased body weight was observed in *PPARβ/δ*-null mice compared to dialysis buffer (DB) injected control mice (Figure 3.5A). In addition, we also observed a slight increase in muscle weights of *PPARβ/δ*-null mice treated with sActRIIB, compared to control treated mice, although this increase was not statistically significant (Figure 3.5B, 3.5C). Histological analysis revealed an increase in muscle fibre CSA in sActRIIB treated *PPARβ/δ*-null mice (Figure 3.5D) when compared to control treated mice, which is consistent with skeletal muscle hypertrophy and loss of Myostatin activity. These data suggest that enhanced activity of Myostatin might be contributing to reduced body weight, muscle weights and muscle CSA observed in *PPARβ/δ*-null mice.

We further tested the effect of sActRIIB injection on skeletal muscle regeneration in *PPAR β/δ*-null mice. We observed no significant change in the muscle weights of regenerated (day 28-post notexin-induced injury) *PPARβ/δ*-null mice treated with sActRIIB, when compared to respective DB treated control (*data not shown*). However, we did find a significant increase in muscle fibre CSA, indicating hypertrophy, in regenerated TA muscle sections of sActRIIB treated *PPARβ/δ*-null mice, when compared to respective DB treated control (Figure 3.5E). However, a significant increase in the number of centrally formed nuclei was observed in regenerated TA muscle sections (day 28-post notexin-induced injury) from *PPARβ/δ*-null mice treated with sActRIIB, when compared to respective DB treated control (Figure 3.5F).

Collectively, these data suggest that sActRIIB-mediated blockade of Myostatin is able to improve skeletal muscle regeneration in *PPARβ/δ*-null mice in response to injury.

3.2 Discussion

Activation of *PPARβ/δ* isoform in mouse skeletal muscle promotes muscle development and enhances myogenesis by increasing both myoblast proliferation and differentiation in C2C12 myoblasts (Bonala *et al.,* 2012; Giordano *et al.,* 2009; Wang *et al.,* 2004). In this study, to understand the role of *PPARβ/δ* in postnatal myogenesis and skeletal muscle regeneration, we have used notexin-induced muscle injury model .

During postnatal myogenesis reduced body weight, reduced Tibialis anterior, Gastrocnemius, Extensor digitorum Longus and Soleus muscle weight (Figure 3.1A, 3.1B and 3.1C) was observed in *PPARβ/δ*-null mice. In contrast to the results presented here, Angione *et al.* have shown no significant change in body weight and muscle weights in skeletal muscle-specific *PPARβ/δ* knock-out mice (*PPAR δ*-cKO) (Angione *et al.,* 2011). The differences observed in body and muscle weights between Angione *et al*., and the current study could be due to the different transgenic mouse models used. Specifically, Angione *et al*., study made use of muscle-specific *PPARβ/δ* knock-out mice, whereas we have used germ line deleted *PPARβ/δ*-null mouse model. An important thing to note here is that Angione *et al*., assessed for differences in body weight between female WT and *PPARδ*-cKO mice, whereas we have assessed differences in body and muscle weights between male WT and *PPARβ/δ*-null mice. It is quite possible that the variation in body weights and muscle weights observed between the study by Angione *et al*., and our current study could be due to sexual dimorphism as previously reports indicate that hormones such as estrogen influence muscle growth (Enns *et al.,* 2008; McCormick *et al.,* 2004). However, further research will need to be performed to ascertain whether *PPAR β/δ* influences estrogen levels and thereby affects muscle mass. *PPARβ/δ*-null mice also showed decreased muscle fibre size (atrophy) , when compared to WT mice (Figure 3.1 D), with no appreciable change in fibre number (*data not shown*). This atrophy phenotype could be due to reduced satellite cell number and impaired satellite cell function. Previous work from our lab has also demonstrated that Myostatin is a potent negative regulator of satellite cell activation and function (McCroskery *et al.,* 2003) and excess Myostatin levels have been shown to promote muscle wasting (McFarlane *et al.,* 2006). As recent work from our lab has shown *PPARβ/δ*-null mice have increased

Myostatin activity (Bonala *et al.*, 2012), it is quite possible that the observed atrophy may be due to increased Myostatin activity. In agreement with this, Pax7 immunostaining on muscle sections confirmed there was a significant reduction in satellite cell number in TA muscles of 10-week-old *PPARβ/δ*-null mice. These data agree with Angione *et al*. study that reported a reduction of 40 % in the number of Pax7 positive satellite cells in *PPARδ-cKO* mice. As the number of $Pax7^{+}/MyoD^{-}$ quiescent Satellite cells (SCs) between resting muscle and regenerated muscle (day 28-post notexin injection) in *PPARβ/δ*-null mice are comparable, we suggest that SCs from *PPARβ/δ*-null mice are able to self-renew their population normally during postnatal growth (Figure 3.2E). As SC self-renewal may not be impaired in *PPARβ/δ*-null mice, we predict that the reduction in SCs is due to alterations in the specification of SCs during embryonic/foetal development (Motohashi *et al.,* 2014) in *PPARβ/δ*-null mice. Earlier studies have shown that a subset of Pax3/Pax7 expressing myoblasts in dermomyotome of embryonic day E16.5 to E18.5 mature into satellite cells (Relaix *et al.,* 2005). Perhaps lack of *PPARβ/δ* is responsible for either specification of these myoblasts in the dermomyotome or for their replication. Much more extensive investigations are required to investigate the precise mechanism of *PPARβ/δ* in regulating satellite cell specification during fetal growth. It has been shown previously that, in Xenopus development, *PPARβ/δ* is essential for muscle and neural differentiation as early as gastrulation when *PPARβ/δ* governs a massive wave of transcriptional modifications affecting the later differentiation of muscle and brain (Rotman *et al.,* 2013).

SCs are muscle precursor cells that give rise to new muscle fibres during skeletal muscle regeneration (Pannerec *et al.,* 2012). Therefore, the myogenic function of *PPARβ/δ*-null SCs was assessed by studying skeletal muscle regeneration. During the early phase of muscle regeneration, significantly increased macrophage infiltration was observed in *PPARβ/δ*-null injured muscle after 3 days of notexin-induced injury (Figure 3.2A, B). Consistent with the data presented here, reduced macrophage infiltration has been reported in diabetic nephropathy mice treated with PPARβ/δ agonist and activation of PPARβ/δ has been further shown to inhibit macrophage recruitment and vascular inflammatory gene expression (Matsushita *et al.,* 2011; Takata *et al.,* 2008). In addition, the regenerating TA skeletal muscle from *PPARβ/δ*-null

mice also showed reduced numbers of MyoD positive activated SCs after day 3 of notexin-induced injury (Figure 3.2D). Since *PPARβ/δ*-null mice have reduced SCs to begin with, and reduced proliferation rate which have previously been shown (Bonala *et al.,* 2012), we speculate that both these factors contribute to the reduced number of MyoD positive myoblasts observed at day 3 of regeneration. In addition, earlier results from our lab have revealed increased Myostatin activity in *PPARβ/δ*-null mice, which leads to reduced proliferation and differentiation of primary myoblasts (Bonala *et al.,* 2012). Thus, it is quite possible that the increased expression/activity of myostatin observed in these mice could be contributing to reduced numbers of MyoD positive myoblasts in *PPARβ/δ*-null mice during regeneration. Furthermore, despite increased macrophage infiltration and impaired SC activation in *PPARβ/δ*-null mice, no difference was observed in fibrotic tissue formation in regenerated muscle (day 28-post notexin injection) between WT and *PPAR β/δ*-null mice (Figure 3.4A).

In agreement with Angione *et al.,* histology of *PPARβ/δ*-null regenerated skeletal muscle at day 28 confirmed severely atrophied regenerated muscle fibres with lower number of centrally formed nuclei (Figure 3.3B, D) which could be a result of reduced differentiation potential of myoblasts. The lower percentage of 2 or more centrally formed nuclei and increased percentage of single centrally placed nuclei in *PPARβ/δ*-null regenerated skeletal muscle at day 28 signifies the reduced fusion of mononucleated myoblasts. Several factors have been shown to contribute to satellite cell activation, proliferation and differentiation (Angione *et al.,* 2011; Motohashi *et al.,* 2012). It has been well established that myostatin is a potent negative regulator of satellite cell activation and myoblast proliferation (McCroskery *et al.,* 2003). Therefore, absence of myostatin improved muscle healing by increasing both myoblast proliferation and differentiation. Since the *PPARβ/δ*-null mice used in this study have increased myostatin activity as shown earlier (Bonala *et al.,* 2012), it is quite possible that the impaired SCs function and reduced myogenesis observed in these mice could be due to increased Myostatin.

Clinically PPAR δ agonists have been shown to improve muscle function and rescue muscle wasting in *mdx* mice model (Jahnke *et al.,* 2012). In humans, PPAR δ have demonstrated an anti-apoptotic role and have shown the ability of survival and differentiation of epithelial cells (Sertznig *et al.,* 2008). In addition, activation of PPAR δ in moderately obese men has resulted in reversal of several metabolic abnormalities, decreased oxidative stress and increased fatty acid oxidation (Riserus *et al.,* 2008). Studies have also shown anti-inflammatory effects of PPAR δ in human model of dermal wound healing by secretion of IL-1 receptor antagonist in dermal fibroblasts (Chong *et al.,* 2009). Also, recent reports have indicated that PPAR δ activation in human myoblasts by L165041 results in increased hGASP-1 protein secretion and myostatin has been shown to be a downstream target of GASP-1 (Bonala *et al.,* 2012). PPAR δ agonists might also play a role in rescue of atrophy phenotype during young and old age (sarcopenia). As we observed, atrophy phenotype in *PPARβ/δ*-null mice which could be due to reduced satellite cell number (Figure 3.1E), it is quite possible that PPAR δ agonists might improve the satellite cell number and help in rescuing muscle wasting during young and old age.

Specifically, to confirm the role of myostatin in *PPARβ/δ*-null mice during regeneration, muscle injury was induced via notexin injection and excess myostatin signaling was blocked via treatment with a dominant negative soluble receptor decoy (sActRIIB) (Zhang *et al.,* 2011). The results suggest that blockade of excess myostatin signaling in *PPARβ/δ*-null mice resulted in increased muscle hypertrophy of not only resting muscle but also regenerated (day 28-post notexin injection) muscle. Therefore we propose that increased myostatin activity is at least in part responsible for the atrophy phenotype observed in *PPARβ/δ*-null mice. It is noteworthy that inactivation of Myostatin in Wild-type (C57Bl6) mice also leads to hypertrophy. Hence, transient inactivation of Myostatin in *PPARβ/δ*-null mice does not unequivocally rule out other mechanism. Hence, the contribution of Myostatin in atrophy of *PPARβ/δ*-null mice needs further investigation. For example, *PPARβ/δ*-null mice can be crossed to floxed myostatin null mice in order to delete myostatin postnatally in *PPARβ/δ*-null mice. In such double knockout mice evaluation of muscle fibre cross-sectional area and satellite cell biology would shed light on the role of

Myostatin in atrophy of *PPARβ/δ*-null mice. Similarly, double knockout mice studies also would be helpful in delineating the role of Smad2/Smad3 in muscle atrophy. Finally, notexin mediated muscle regeneration studies in double knockout mice will undoubtedly help us understand the role of Myostatin and the effectiveness of inactivating Myostatin in overcoming atrophy in *PPARβ/δ*-null mice.

In general myostatin antagonists overcome muscle wasting. For example, short-term inhibition of myostatin function through sActRIIB enhances skeletal muscle regeneration after injury in aged mice and during sarcopenia (Siriett *et al.,* 2007). These results agree with earlier results from aged myostatin-null mice skeletal muscles which continue to regenerate upon both chronic and acute injury (Wagner *et al.,* 2002; Siriett *et al.,* 2006). The effect of sActRIIB use in the regulation of muscle mass has also shown positive results, in the inhibition of muscle wasting with reversal of muscle loss, atrophy and enhancement of life by suppressing growth of human tumors in mice (Zhou *et al.,* 2010). Other studies have also shown rescue of muscular atrophy in caveolin-3 deficient mice upon inhibition of myostatin through sActRIIB (Ohsawa *et al.,* 2006). A large number of studies have also shown clinical perspective of sActRIIB, wherein inhibition of myostatin in *mdx* mice model of muscular dystrophy resulted in improvement of skeletal muscle mass and strength (Pistilli *et al.,* 2011). Therefore, clinically sActRIIB would help in reducing the atrophy of skeletal muscle.

In summary, *PPARβ/δ* plays a critical role in muscle regeneration from early inflammatory response, primary myogenesis and formation of completely regenerated myofibres. Based on the results from this study, we propose that *PPARβ/δ* regulates SC number, function and myoblast differentiation via regulation of myostatin.

CHAPTER 4

PPARβ/δ$^{-/-}$ MICE DISPLAY PREMATURE AGING OF SKELETAL MUSCLE

4.1 Results

4.1.1 Loss of PPARβ/δ results in reduced body weight and muscle weights

Previous results from this thesis (see Chapter 3; Figure 3.1A) revealed a significant reduction in body weight of 10-week-old *PPARβ/δ*-null mice when compared to age-matched wild type (WT) mice. As aging results in loss of muscle mass (sarcopenia), we further analyzed body weights and muscle weights of both WT and *PPARβ/δ*-null mice at different ages. There was a significant decrease in body weight of *PPARβ/δ*-null mice at 3 and 24 months of age when compared to WT mice (Figure 4.1A). However, we did not observe any significant difference in body weights between WT and *PPARβ/δ*-null mice at other time points analyzed (6, 12 and 18 months) (Figure 4.1A). Despite this we did observe a significant reduction in *M. tibialis anterior* (TA), *M. gastrocnemius* muscle (Gas), *M. extensor digitorum longus* (EDL), *M. soleus* (Sol), *M. quadriceps* muscle (Quad) and *M. biceps femoris* (BF) muscle weights in *PPARβ/δ*-null mice when compared to WT mice at all age groups assessed (3, 6, 12, 18 and 24 months) (Figure 4.1B-4.1C).

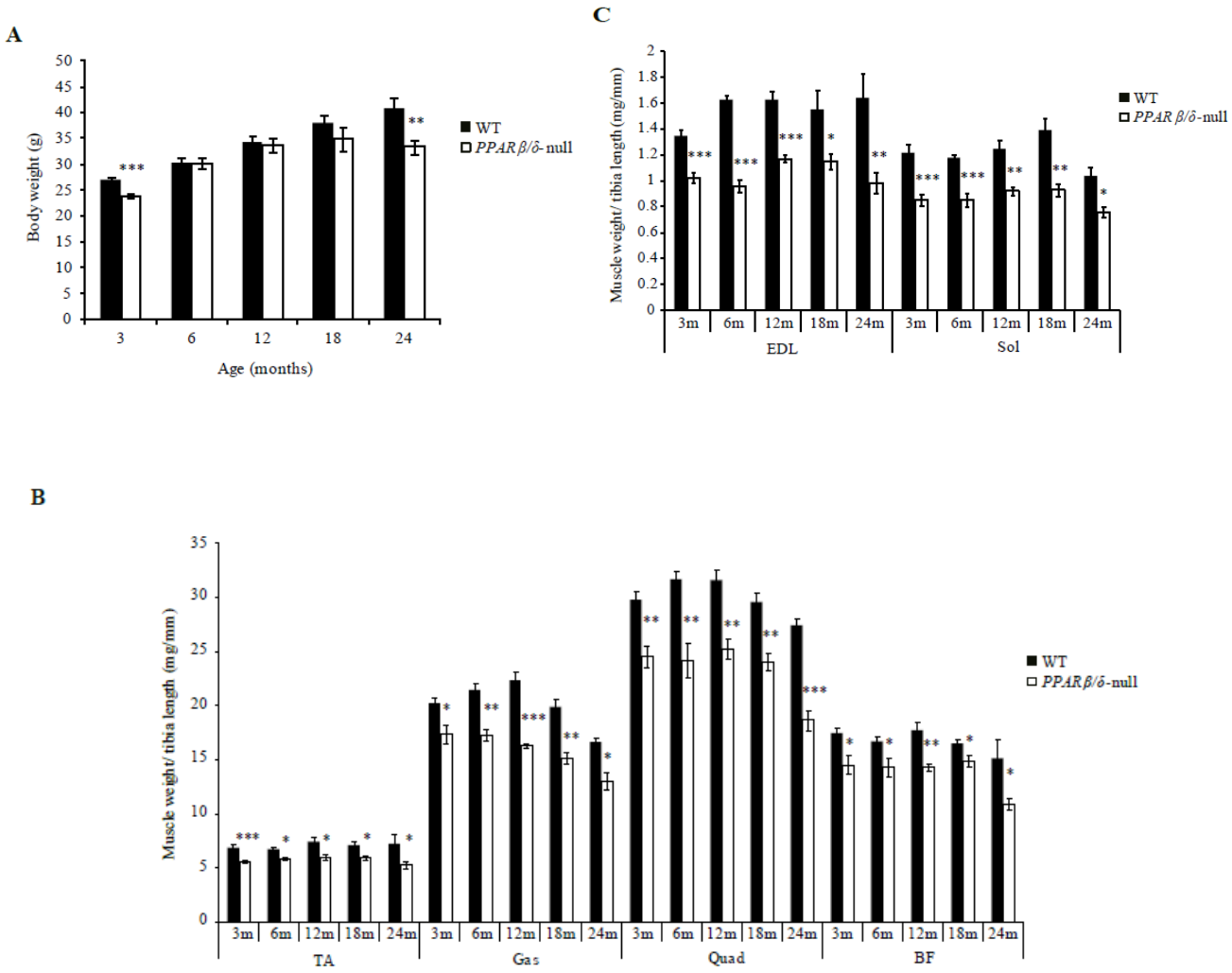

Figure 4.1 Reduced body and muscle weights in *PPARβ/δ*-null mice during aging.

(**A**) Body weight (g) of Wild type (WT) and *PPARβ/δ*-null mice at 3, 6, 12, 18 and 24 months of age. Bars represent mean ± s.e.m, n= 9-10 for *PPARβ/δ*-null mice and n=7-10 for WT mice in the different age groups. (**B**) Graph showing combined weight of left and right TA, Gas, Quad and BF muscles normalized to tibia length, of WT and *PPARβ/δ*-null mice at 3, 6, 12, 18 and 24 months of age. Bars represent mean ± s.e.m, n= 4-6 for *PPARβ/δ*-null mice and n= 3-6 for WT mice. (**C**) Graph showing combined weight of left and right EDL and Sol muscles normalized to tibia length, of WT and *PPARβ/δ*-null mice at 3, 6, 12, 18 and 24 months of age. Bars represent mean ± s.e.m, n= 4-6 for *PPARβ/δ*-null mice and n= 3-6 for WT mice. Statistical differences are indicated in relevant panels, P<0.05 (*), P<0.01 (**) and P<0.001 (***).

Figure 4.2 *PPARβ/δ* deficiency leads to enhanced skeletal muscle atrophy during aging

(**A**) Frequency distribution of TA muscle fibre cross-sectional area (CSA; μm^2) in resting muscle from WT and *PPARβ/δ*-null mice at 3 months of age. (**B**) Frequency distribution of TA muscle fibre cross-sectional area (CSA; μm^2) in resting muscle from WT and *PPARβ/δ*-null mice at 12 months of age. (**C**) Frequency distribution of TA muscle fibre cross-sectional area (CSA; μm^2) in resting muscle from WT and *PPARβ/δ*-null mice at 24 months of age. (**D**) Graph showing total myofibre number in TA muscle from 3- and 24-month-old WT and *PPAR β/δ*-null mice. Bars represent mean ± s.e.m, n=3 per group. (**E**) Graph showing grip strength in WT and *PPAR β/δ*-null mice at 3-, 18- and 24 months of age. Grip strength (peak force) was measured in Newtons (N) and normalized to total body weight. Bars represent mean ± s.e.m, n=3-6 per group. (**F**) Graph showing the number of quiescent SCs ($Pax7^+/MyoD^-$) per 100 myofibre, in resting TA muscle from 6- and 24-month-old WT and *PPARβ/δ*-null mice. Bars represent mean ± s.e.m, n=3 per group. Statistical differences are indicated in relevant panels, $P<0.05$ (*), $P<0.01$ (**) and $P<0.001$ (***).

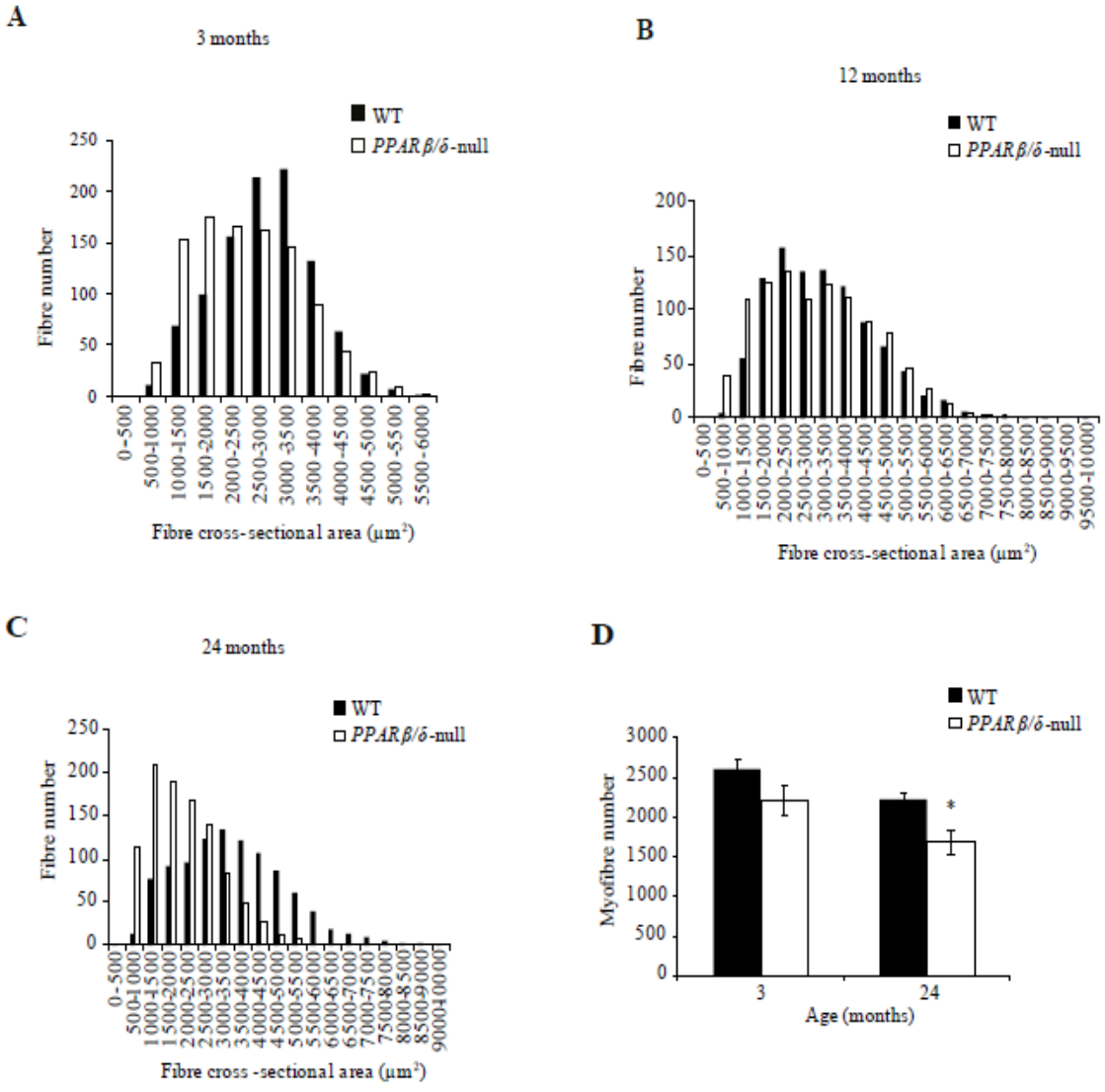
A
3 months
WT
PPARβ/δ-null
Fibre number
Fibre cross-sectional area (µm²)
B
12 months
C
24 months
Fibre cross -sectional area (µm²)
D
Myofibre number
Age (months)
E
Grip strength (normalised to body weight) (N)
F
Pax7+/Myod- cells/ 100 myofibre

4.1.2 PPARβ/δ-null mice display more pronounced skeletal muscle atrophy during aging

In order to elucidate if aging influences the muscle fibre size in the absence of *PPARβ/δ*, histological analysis and subsequent assessment of muscle fibre cross-sectional area (CSA) was performed using TA muscle from *PPARβ/δ*-null and WT mice. There was a significant reduction in TA muscle fibre CSA, consistent with enhanced muscle atrophy, in *PPARβ/δ*-null mice at 3, 12 and 24 months of age, when compared to age-matched WT mice (Figure 4.2A-4.2C). Furthermore, a reduction in total myofibre number was also seen in TA muscles of 24-month-old *PPARβ/δ*-null mice, when compared to WT mice (Figure 4.2D).

To determine whether or not reduced muscle fibre size leads to changes in muscle strength, we next assessed grip strength in *PPARβ/δ*-null mice and WT mice at 3, 18 and 24 months of age. Our results indicated reduced muscle strength in *PPARβ/δ*-null mice at all times points tested, however the reduced grip strength was only found to be significant at 18 months of age in *PPARβ/δ*-null mice, when compared to WT mice (Figure 4.2E). Together these data suggest that the pronounced muscle fibre atrophy noted in *PPARβ/δ*-null mice leads to impaired grip strength.

4.1.3 PPARβ/δ-null mice have reduced SC number during aging

SCs play a vital role during postnatal muscle growth (Carlson and Faulkner 1989; Bockhold *et al.*, 1998; Conboy and Rando 2002) and it has been well established that reduced pool of SCs is responsible for age-related muscle atrophy (Schmalbruch 2006). Since we observed a decline in muscle weights in *PPARβ/δ*-null mice, we next quantified the number of $Pax7^{+}$/$MyoD^{-}$ SCs in TA muscle fibres through immunohistochemical analysis from 6- and 24-month-old WT and *PPARβ/δ*-null mice. In agreement with previous results from this thesis (see Chapter 3; Fig.3.1E), 34 % and 77 % reduction in $Pax7^{+}$/$MyoD^{-}$ SCs was observed in TA muscle from *PPARβ/δ*-null mice, when compared to WT mice, at 6 and 24 months of age (Figure 4.2F).

4.1.4 Loss of PPARβ/δ results in reduced oxidative capacity and mitochondrial copy number in skeletal muscle

During aging a decline in glycolytic muscle fibre number and size, together with increased oxidative muscle fibres is observed (Coggan AR *et al.,* 1990; Lexell *et al.,* 1988). Therefore, we next determined the proportion of oxidative muscle fibres in TA muscles from 3-, 12- and 24-month-old WT and *PPARβ/δ*-null mice via assessing Succinate dehydrogenase (SDH) activity. Our results reveal a decline in oxidative capacity in *PPARβ/δ*-null mice at 3, 12 and 24 months with a statistically significant reduction noted at 12 months of age, when compared to WT mice controls (Figure 4.3A). Reduced SDH activity is often associated with mitochondrial DNA defects (Chen *et al.,* 2012), therefore, we next assessed mitochondrial DNA (mtDNA) copy number between WT and *PPARβ/δ*-null mice. A significant reduction in mtDNA copy number was observed in 12 month old *PPARβ/δ*-null mice, when compared to WT mice (Figure 4.3B). These results indicate that loss of *PPARβ/δ* leads to reduced oxidative capacity, which is associated with reduced mtDNA: nuDNA copy number, in skeletal muscle during aging.

4.1.5 Absence of PPARβ/δ results in impaired mitochondrial function

As loss of *PPARβ/δ* resulted in reduced mitochondrial copy number and skeletal muscle oxidative capacity, we next analysed mitochondrial function of *PPARβ/δ*-null myotubes by measuring Oxygen Consumption Rate (OCR). No significant difference was observed in basal mitochondrial respiration, ATP-linked OCR, maximal and spare respiratory capacity between primary myotube cultures isolated from 7-week-old WT and *PPARβ/δ*-null mice (Figure 4.3C, 4.3D). However, we observed a significant reduction in maximal respiratory capacity and spare respiratory capacity in primary myotubes cultures isolated from 24-month-old *PPARβ/δ*-null mice, when compared to age-matched WT mice controls (Figure 4.3E, 4.3F), although no significant difference was noted in ATP-linked OCR and basal mitochondrial respiration (Figure 4.3E, 4.3F). Collectively these data suggest that *PPARβ/δ*-null mice have reduced mitochondrial function during aging.

Figure 4.3 Absence of *PPARβ/δ* results in reduced mitochondrial content and impaired mitochondrial function in primary myotubes

(**A**) Quantitative analysis of SDH (Succinate dehydrogenase) activity in TA muscle cross sections from WT and *PPARβ/δ*-null mice at 3-, 12- and 24 months of age. Bars represent mean ± s.e.m, n=3 in each group. (**B**) Quantitative analysis of the ratio of mtDNA copy number to nuDNA copy number (mtDNA: nuDNA) from Gas muscle of 12 month old WT and *PPARβ/δ*-null mice. Bars represent mean ± s.e.m, n=3 in each group. **(C**) OCR (Oxygen consumption rate) in 72h differentiated primary myoblasts isolated from 7-week-old WT and *PPAR β/δ*-null mice at basal and after sequential injection of Oligomycin, FCCP and Antimycin+Rotenone (Ant/Rot). **(D)** Graph showing basal OCR, OCR due to ATP production, maximal OCR and spare respiratory capacity in 72h differentiated primary myoblasts isolated from 7-week-old WT and *PPARβ/δ*-null mice. All OCR data was normalized against total protein concentration. Bars represent mean ± s.e.m for 6 wells per group. (**E**) OCR in 72h differentiated primary myoblasts isolated from 24-month-old WT and *PPARβ/δ*-null mice at basal and after sequential injection of Oligomycin, FCCP and Antimycin+Rotenone (Ant/Rot). **(F)** Graph showing basal OCR, OCR due to ATP production, maximal OCR and spare respiratory capacity in 72h differentiated primary myoblasts isolated from 24-month-old WT and *PPARβ/δ*-null mice. All OCR data was normalized against total protein concentration. Bars represent mean ± s.e.m for 4 wells per group. Statistical differences are indicated in relevant panels, $P<0.05$ (*), $P<0.01$ (**).

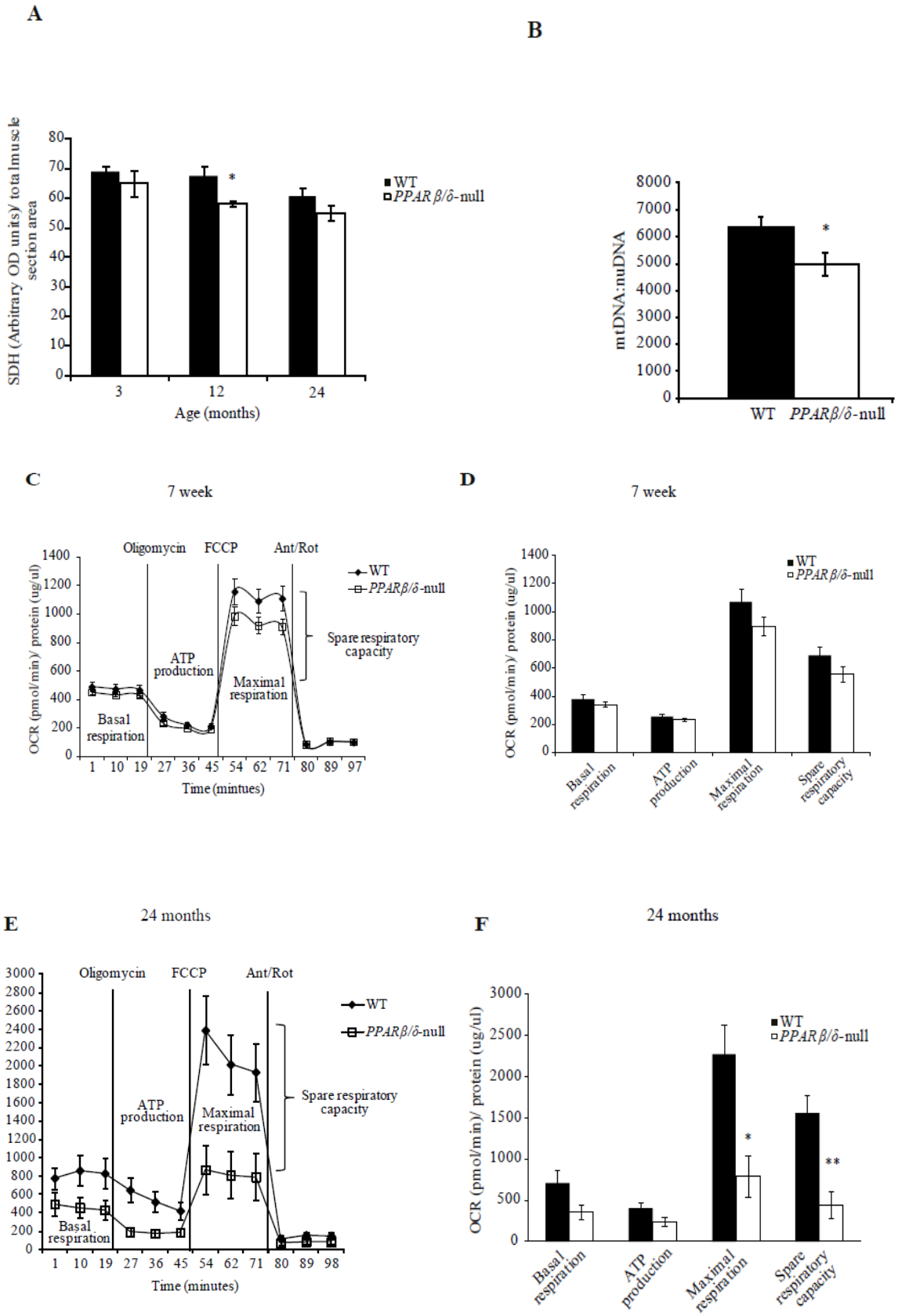
A
SDH (Arbitrary OD units)/ total muscle section area
Age (months)
WT
PPARβ/δ-null
B
mtDNA:nuDNA
WT
PPARβ/δ-null
C
7 week
OCR (pmol/min)/ protein (ug/ul)
Oligomycin
FCCP
Ant/Rot
Basal respiration
ATP production
Maximal respiration
Spare respiratory capacity
Time (mintues)
D
7 week
Basal respiration
ATP production
Maximal respiration
Spare respiratory capacity
E
24 months
Time (minutes)
F
24 months

Figure 4.4 Absence of *PPARβ/δ* leads to increased expression of the mitophagy markers Parkin, Mul1 and LC3 during aging

(**A**) qPCR analysis of *Parkin* expression in Quad muscle isolated from 3 month old WT and *PPARβ/δ*-null mice. Bars represent fold change (relative to WT control) ± s.e.m normalized to *Gapdh*, n=3 per group. (**B**) Immunoblot (IB) analysis of Parkin, Mul1, Mfn2 and p62 protein levels in Gas muscle from 3-month-old WT and *PPARβ/δ*-null mice. The levels of GAPDH were assessed for individual blots to ensure equal loading of samples (n=3). (**C**) Graph showing densitometric analysis of Parkin, Mul1, Mfn2, and p62 protein levels in Gas muscle from 3-month-old WT and *PPARβ/δ*-null mice. Bars represent average band intensity in arbitrary units (A.U.) ± s.e.m, n=3 in each group normalized to GAPDH levels. (**D**) IB analysis of Parkin, Mul1, Mfn2, p62 and LC3 protein levels in Gas muscle from 12-month-old WT and *PPARβ/δ*-null mice. The levels of GAPDH were assessed for individual blots to ensure equal loading of samples (n=3). Irrelevant lanes were removed for Mul1 and its corresponding GAPDH western blots. (**E**) Graph showing densitometric analysis of Parkin, Mul1, Mfn2, p62 and LC3 protein levels in Gas muscle from 12-month-old WT and *PPARβ/δ*-null mice. Bars represent average band intensity in arbitrary units (A.U.) ± s.e.m, n=3 in each group normalized to GAPDH levels. (**F**) IB analysis of Parkin protein levels in 120 hr differentiated primary myotubes isolated from WT and *PPARβ/δ*-null mice. The levels of GAPDH were assessed to ensure equal loading of samples (n=3). (**G**) Graph showing densitometric analysis of Parkin protein levels in 120 hr differentiated primary myotubes isolated from WT and *PPARβ/δ*-null mice. Bars represent average band intensity in arbitrary units (A.U.) ± s.e.m, n=3 in each group normalized to GAPDH levels. Some of the scanned IB images are resized to fit on the page. Statistical significance are indicated in relevant panels, $P<0.05$ (*), $P<0.01$ (**) and $P<0.001$ (***).

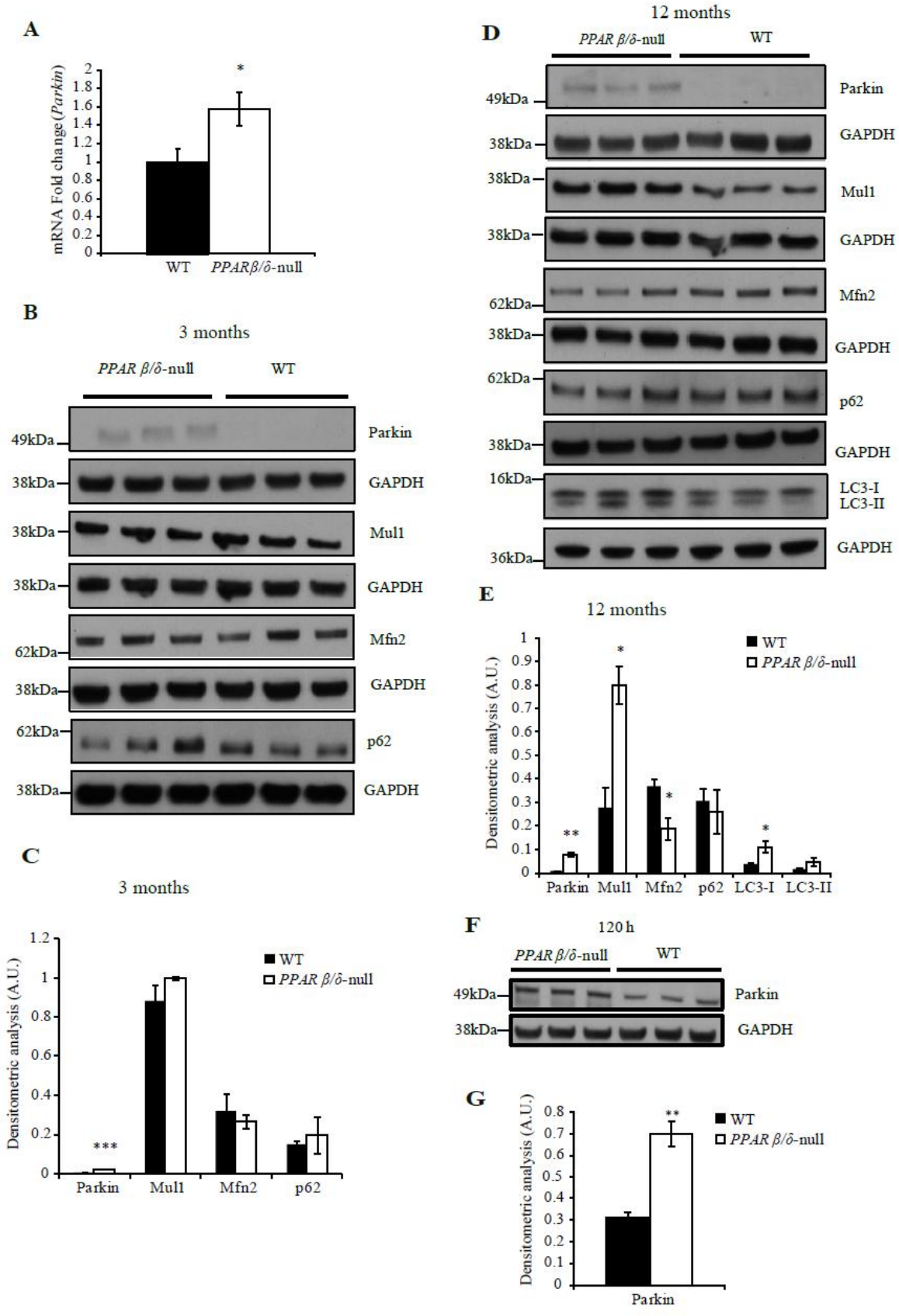
A
mRNA Fold change (Parkin)
WT
PPARβ/δ-null
B
3 months
PPAR β/δ-null
WT
49kDa
Parkin
38kDa
GAPDH
Mul1
Mfn2
62kDa
p62
C
3 months
Densitometric analysis (A.U.)
Parkin
Mul1
Mfn2
p62
D
12 months
16kDa
LC3-I
LC3-II
36kDa
E
12 months
LC3-I
LC3-II
F
120 h
G

4.1.6 Absence of PPARβ/δ induces mitophagy in skeletal muscle

The selective degradation and removal of mitochondria takes place through a specialized autophagy-mediated process termed mitophagy (Ashrafi G and Schwarz TL, 2013). To analyze if increased mitophagy is responsible for the reduction in mitochondrial number observed in *PPARβ/δ*-null mice during aging, we next assessed the levels of various mitophagy markers. qPCR results revealed significantly increased expression of the mitochondrial-specific ubiquitin E3 ligase Parkin in *PPARβ/δ*-null mice when compared to WT controls (Figure 4.4A). In addition, we also observed significantly increased levels of Parkin in Gas muscle from 3- and 12-month-old *PPARβ/δ*-null mice, when compared to aged-matched WT controls (Figure 4.4B-4.4E). Increased expression of Parkin was also observed in 120 hr differentiated primary myotubes cultures from *PPARβ/δ*-null mice, when compared to WT controls (Figure 4.4F, 4.4G). In addition to altered Parkin expression, elevated levels of the E3 ligase Mul1 (mitochondrial E3 ubiquitin protein ligase 1) was also observed; however a significant increase in Mul1 was only noted in Gas muscle isolated from 12-month-old *PPARβ/δ*-null mice, when compared to WT mice, with no significant difference in Mul1 levels noted between 3-month-old WT and *PPARβ/δ*-null mice (Figure 4.4B-4.4E). In addition, at 12 months of age, we also observed increased levels of the autophagy marker LC3 (both LC3-I and LC3-II) (light chain 3 subunit) in *PPARβ/δ*-null mice when compared to age-matched WT mice controls, although the increase in LC3-II was not statistically significant (Figure 4.4D, 4.4E). However, in contrast, additional autophagy/mitophagy markers, including PINK1 (PTEN-induced putative kinase 1) (data not shown) and p62, remained unaltered between WT and *PPAR β/δ*-null mice at both 3 months and 12 months of age (Figure 4.4B-4.4E). To further assess mitophagy *in vivo*, we also analyzed the levels of the Mul1 target protein Mfn2 (mitofusin-2). Consistent with increased Mul1, we observed a significant reduction in Mfn2 levels in *PPARβ/δ*-null mice Gas muscle at 12 months of age, when compared to WT controls (Figure 4.4D, 4.4E). Taken together these data suggest that *PPARβ/δ*-null mice have enhanced autophagy/mitophagy in skeletal muscle during aging.

4.2 Discussion

Previous work from our lab (Chapter 3) and others (Angione *et al.,* 2011) have revealed that either conditional skeletal muscle-specific knock out (*PPAR δ*-cKO) or germ-line deletion of *PPARβ/δ* in mice leads to impaired skeletal muscle regeneration following injury due to impaired satellite cell function, suggesting that PPARβ/δ has important functions during postnatal myogenesis. In this study we have utilized *PPARβ/δ*-null mice and have assessed the potential role of PPARβ/δ during aging and subsequent aging-related muscle loss, or sarcopenia.

During aging *PPARβ/δ*-null mice displayed reduced body and skeletal muscle weights. Although reduced skeletal muscle weights were observed in all muscles examined at all ages studied, we only noted a significant reduction in body weight at 3 months and 24 months of age in *PPARβ/δ*-null mice (Figure 4.1A-4.1C). In contrast to the results presented here, Angione *et al.,* have reported an increase in body weight in 9-month-old skeletal muscle-specific *PPARβ/δ* knock-out mice (*PPARδ*-cKO), when compared to WT controls (Angione *et al.,* 2011), which was attributed to development of metabolic syndrome. However, it is important to note that Angione *et al*., did not assess muscle weights and importantly Angione *et al*., measured differences in body weights between female WT and muscle-specific *PPARβ/δ* knock-out mice (*PPAR δ*-cKO); whereas we have performed our studies comparing male WT and germ-line deleted *PPARβ/δ*-null mice (Figure 4.1A-4.1C). Nevertheless, in agreement with the reduced muscle weights, we found observable skeletal muscle atrophy in 3-, 12- and 24-month old *PPARβ/δ*-null mice, when compared to age-matched controls (Figure 4.2A-4.2C). In addition, despite no significant difference in myofibre number between WT and *PPARβ/δ*-null mice at 3 months of age, a significant reduction in myofibre number was noted in 24-month-old *PPARβ/δ*-null mice, when compared to WT controls (Figure 4.2D). Loss of muscle mass also results in decreased muscle strength (Evans 2010). In agreement with this, *PPARβ/δ*-null mice have significantly reduced grip strength at 18 months of age with an observable decrease also noted at 3- and 24 months of age, albeit not statistically significant (Figure 4.2E). Consistent

with this a recent report by Fu *et al.,* have also reported reduced grip strength in *PPARβ/δ*-null mice at 1, 4, 12 and 18 months of age (Fu *et al.,* 2014).

Previously published data from our lab has revealed a significant reduction in SCs number in *PPARβ/δ*-null mice at 10 weeks of age (Chandrashekar *et al.,* 2015). Similarly, we also observed reduced satellite cell number in *PPARβ/δ*-null mice at both 6- and 24-months of age, when compared to age-matched controls (Figure 4.2F). As skeletal muscle atrophy during sarcopenia has also been attributed, at least in part, to reduced satellite cell number (Narici *et al.,* 2010) it is possible that the pronounced skeletal muscle atrophy observed in *PPARβ/δ*-null mice during aging may be due to impaired satellite cell number and/or function.

Aging is also thought to negatively influence the mitochondrial content in skeletal muscle, leading to increased mitochondrial DNA mutations, reduced total mitochondrial content and altered maximal respiration rates that in turn contribute to atrophy of muscle fibres (Peterson *et al.,* 2012). It has also been established that damaged mitochondrial DNA promotes muscle wasting through reducing SC number (Wang *et al.,* 2013). Therefore we next assessed changes in mitochondrial content between WT and *PPARβ/δ*-null mice during aging. Our analysis revealed a greater reduction in mitochondrial DNA content at 12 months of age, as assessed through quantification of mtDNA: nuDNA ratio, in *PPARβ/δ*-null mice when compared to respective WT controls (Figure 4.3B). In agreement with reduced mitochondrial content, we further noted reduced SDH staining in TA muscle of *PPARβ/δ*-null mice, suggesting reduced oxidative potential of *PPARβ/*δ-null muscle (Figure 4.3A). These data are quite consistent with previous work, which shows that PPARβ/δ can promote mitochondrial biogenesis leading to increased mitochondrial DNA content (Wang *et al.,* 2004) and that muscle-specific over expression of PPARβ/δ leads to an increase in oxidative muscle fibres (Luquet *et al.,* 2003). Reduced mitochondrial content was also associated with increased expression of autophagy/mitophagy markers in skeletal muscle from aged (12 months) *PPARβ/*δ-null mice, when compared to age-matched controls. Specifically, we noted increased expression of the mitochondrial ubiquitn E3 ligases Parkin and Mul1, the autophagosome associated protein LC3 and reduced levels of the Mul1-target protein Mfn2 during aging (Figure 4.4D, 4.4E). It is interesting to

surmise that the increased levels of Mul1 may be responsible, at least in part, for the skeletal muscle atrophy observed in *PPARβ/δ*-null mice during aging; indeed previously published results from our lab have revealed that Mul1 induced loss of Mfn2 and subsequent mitochondrial dysfunction contributes significantly to skeletal muscle wasting (Lokireddy *et al.,* 2012). However, more extensive studies should be undertaken to confirm the role of Mul1 and for that matter Parkin in the loss of mitochondria and skeletal muscle wasting observed in *PPARβ/δ*-null mice during aging.

Although no significant difference in mitochondrial function was noted in differentiated myotubes isolated from 7-week-old WT and *PPARβ/δ*-null mice, impaired mitochondrial function (significantly reduced maximal respiratory output and spare respiratory capacity) was observed in differentiated myotubes isolated from 24-month-old *PPARβ/δ*-null mice, when compared to age-matched WT controls (Figure 4.3E, 4.3F). This data suggests that PPARβ/δ is required for maintaining proper mitochondrial function. Consistent with this hypothesis, Hancock *et al.,* demonstrated that overexpression of PPARβ/δ leads to increased PGC1α protein content along with increased mitochondrial content (Wang *et al.,* 2004, Hancock *et al.,* 2008).

A gradual decrease in muscle mass and strength is seen naturally during aging (sarcopenia), not only in experimental animals but also in humans. The sarcopenia phenotype has been typified by loss of muscle fibre number, atrophy of muscle fibres and reduced satellite cell function and the onset of the sarcopenic phenotype in mice has been observed at around 18 months (Esposito *et al.,* 2013). The salient observation we find here is that the sarcopenia phenotype develops prematurely in *PPARβ/δ*-null mice, in fact changes in muscle mass are noted as early as 3 months of age (Figure 4.1B, C). The muscles of 3-month-old WT mice are quite robust in terms of growth, anabolism and metabolism. The fact that *PPARβ/δ*-null muscle displays such a drastic sarcopenic phenotype at such a young age, underscores the importance of maintaining PPARβ/δ expression for proper muscle function and metabolism during postnatal growth. However, given the fact that there are no gross abnormalities noted in skeletal muscles during early neonatal stages in *PPARβ/δ*-null mice, reveals that PPARβ/δ function is dispensable for embryonic growth of muscle. Taken together these data highlight the need for

further research to be conducted with PPARβ/δ agonists to generate proof of concept of their utility in overcoming sarcopenia.

The mitochondrial based theory of aging is quite well established (Bratic *et al.*, 2013). A gradual loss of mitochondria, which results in increased oxidative stress and eventual development of sarcopenia, has been previously described during aging (Cui *et al.*, 2012). Our current molecular analysis reveals that there is a significant increase in the expression of mitophagy markers in *PPARβ/δ*-null skeletal muscle. This premature increase in mitophagy observed in skeletal muscles could be partially responsible for the sarcopenic phenotype noted in *PPARβ/δ*-null mice. However, what is not clear here is the molecular basis for the increased mitophagy in *PPARβ/δ*-null muscles. Mitophagy is a normal phenomenon that is required to preserve functional mitochondria and remove and discard dysfunctional mitochondria (Ding *et al.*, 2012). At a simplistic level, the results presented here indicate that loss of *PPARβ/δ* expression results in mitochondrial dysfunction, which further leads to increased mitophagy and perhaps development of the premature sarcopenic phenotype. Both in this study and previously, it has been clearly proven that loss of *PPARβ/δ* results in reduced oxidative potential of skeletal muscles (Luquet *et al.*, 2005, Luquet *et al.*, 2003, Schuler *et al.*, 2006), which could lead to increased oxidative stress. It is also possible that in *PPARβ/δ*-null mice there may also be a loss of mitochondrial membrane potential (since we observed increased Parkin), which would in turn trigger the mitophagy cascade and increase the autophagic flux of mitochondria. However, further extensive research is required to identify the molecular basis for the increased mitophagy in *PPARβ/δ*-null postnatal muscle and the consequences that this imparts on muscle metabolism.

In summary, PPARβ/δ plays an important role in skeletal muscle during aging. Based on the current data we suggest PPARβ/δ helps to prevent sarcopenia, or aging-related loss of skeletal muscle mass and has a positive role in maintaining mitochondrial number and function during aging, perhaps through preventing mitophagy-mediated loss of mitochondria.

CHAPTER 5
CONCLUSION AND PERSPECTIVES

PPARs are ligand-activated transcription factors belonging to the nuclear hormone receptor superfamily (Tyagi *et al.,* 2011). Since the discovery of PPARs a significant amount of work has been undertaken to study the role of PPARβ/δ isotype in the control of fatty acid catabolism in tissues such as skeletal muscle and adipose tissue. Initially, much of the research focused on understanding PPARβ/δ activation and its role in muscle development, β-oxidation of fatty acids, fibre type switch and control of satellite cell function (Galuppo *et al.,* 2010, Giordano *et al.,* 2009). Collectively, these studies supported the fact that PPARβ/δ plays an important role in skeletal muscle development. Recent work from our laboratory has further highlighted a role for PPARβ/δ in the regulation of skeletal muscle postnatal myogenesis (Bonala *et al.,* 2012). Specifically, our results revealed that activation of PPARβ/δ led to increased interaction of Gasp-1 (downstream target of PPARβ/δ) with myostatin, which resulted in inhibition of myostatin activity (Bonala *et al.,* 2012). Since PPARβ/δ modulates myostatin activity, we hypothesized that PPARβ/δ may play an essential role in postnatal muscle growth and development. Therefore, the overall aim of this thesis was to examine this hypothesis in detail and define the role of PPARβ/δ in skeletal muscle regeneration and sarcopenia.

To investigate the role of PPARβ/δ during postnatal muscle growth and regeneration, we utilized *PPARβ/δ*-null mice and a notexin-induced-injury model of skeletal muscle regeneration. Initially, we observed significant skeletal muscle atrophy in *PPARβ/δ*-null mice as young as 10 weeks of age (Figure 3.1D), which appeared to be due to reduced satellite cell number and function (Figure 3.1E). Since *PPARβ/δ*-null mice have increased myostatin activity (Bonala *et al.,* 2012), it is quite possible that myostatin contributes to the impaired SC function and reduced myogenesis observed in *PPARβ/δ*-null mice. Additionally, our study reports that myoblasts from regenerated *PPARβ/δ*-null mice show impaired myoblast proliferation (Figure 3.2D) and that injury and subsequent regeneration of skeletal muscle in *PPARβ/δ*-null

mice results in reduced numbers of muscle fibres with multiple centrally placed nuclei (Figure 3.3D). Collectively, the various skeletal muscle regeneration parameters studied here highlight the fact that *PPARβ/δ*-null mice display impaired postnatal myogenesis and skeletal muscle regeneration, thus strongly supporting the role of PPAR*β/δ* in these functions.

Muscle satellite cell function is critical for postnatal skeletal muscle maintenance and, consistent with reduced skeletal muscle mass a gradual loss of satellite cell function in *PPARβ/δ*-null muscles is noted during aging (Figure 4.2F). Since *PPARβ/δ*-null muscles showed reduced satellite cell function, we next analyzed if *PPARβ/δ*-null muscles age prematurely. We observed that 3-month-old *PPARβ/δ*-null mice muscle showed decreased weight and reduced myofibre number and CSA (Figure. 4.1B-C, Figure. 4.2A-D). Sarcopenia is mainly characterized by loss of skeletal muscle mass, quality and strength associated with the normal progression of aging (Doherty 2003, Evans 1995). Consistent with this we observed that *PPARβ/δ*-null mice have reduced muscle grip strength by 3 months of age with significantly reduced skeletal muscle strength noted in *PPARβ/δ*-null mice at 18 months of age (Figure 4.2E). In addition, our results also revealed that *PPARβ/δ*-null mice displayed reduced mitochondrial DNA content and up-regulated mitophagy markers in skeletal muscle (Figure 4.3B, Figure 4.4B-E), suggesting that reduced mitochondrial number due to mitophagy could be partially responsible for the observed premature development of sarcopenia.

Characterization of the role of PPARβ/δ in improving skeletal muscle regeneration through the use of specific PPARβ/δ agonists is worth further investigation. In particular, activators of PPARβ/δ such as L165041 or GW0742 could be administered to notexin injured WT mice to determine whether the muscle regeneration could be rescued by activation of PPARβ/δ. In addition, it will be interesting to know if by administration of PPARβ/δ agonists we can rescue sarcopenia and muscle wasting caused due to mitophagy. The sarcopenic animal trial using PPARβ/δ agonist might help in the development of therapeutics, which could improve skeletal muscle wasting.

Therefore, the results presented here collectively suggest that lack of PPARβ/δ is quite detrimental for postnatal muscle growth and can lead to

premature aging. To provide more genetic evidence, several experiments can be contemplated; for example it would be useful to determine whether or not over expression of PPARβ/δ (either through the rAAV vector system or via generation of transgenic mice) alleviates sarcopenia. In addition, it will be interesting to know if through administration of PPARβ/δ agonists we could rescue sarcopenia and muscle wasting caused due to mitophagy. As such, an animal trial studying the development of sarcopenia and the effect of PPARβ/δ agonist treatment might help in determining the therapeutic potential of PPARβ/δ agonists in improving skeletal muscle wasting.

In Chapter 4, we showed that absence of *PPARβ/δ* led to mitophagy-induced skeletal muscle wasting. Specifically, we showed that absence of PPARβ/δ expression leads to increased expression of mitophagy/autophagy markers, such as Parkin, Mul1 and LC3 (Figure 4.4B-E), suggesting that PPARβ/δ may block mitophagy during normal postnatal muscle growth. However, the molecular mechanism responsible for the increased Parkin expression and how this contributes to mitophagy in *PPARβ/δ*-null mice has not yet been understood. Earlier reports suggest that Pink1 recruits Parkin to promote ubiquitination of outer membrane proteins, further resulting in mitophagy (Zheng *et al.,* 2013). It is well known that Parkin recruitment to mitochondria is increased during oxidative stress or during loss of mitochondrial membrane potential. So the next challenge will be to delineate which of these two mechanisms are activated in the absence of *PPARβ/δ*. In addition, earlier reports from our lab (Lokireddy *et al.*, 2012) and others (Webb *et al.*, 2014, Attaix *et al.*, 2012) have established that overexpression of another mitochondrial specific E3 ligase Mul1 leads to mitophagy. Since Mul1 expression is increased in *PPARβ/δ*-null mice, one of the future experiments would be to delineate the specific contribution of Mul1 in inducing mitophagy in *PPARβ/δ*-null mice.

Overall the outcomes of this thesis confirm that PPARβ/δ plays a major role during postnatal muscle growth and maintenance and has provided proof-of-concept that PPARβ/δ agonists may have benefits in overcoming sarcopenia.

REFERENCES

1. Agarkova, I., Perriard, J.C. (2005) The M-band: an elastic link that crosslinks thick filaments in the centre of the sarcomere. *Trends in Cell Biol*. **15**, 477-485.
2. Aiken, J., Bua, E., Cao, Z., Lopez, M., Wanagat, J., McKenzie, D., McKiernan, S. (2002) Mitochondrial DNA deletion mutations and sarcopenia. *Ann New York Acad Sci*. **959**, 412-423.
3. Allen, D.L., Cleary, A.S., Speaker, K.J., Lindsay, S.F., Uvenishi, J., Reed, J.M., Madden, M.C., Mehan, R.S. (2008) Myostatin activin receptor IIb, and follistatin-like 3 gene expression are altered in adipose tissue and skeletal muscle of obese mice. *Am J Physiol Endocrinol Metab.* **294(5)**, E918-27.
4. Alnaqeeb, M.A and Goldspink, G. (1987) Changes in fibre type, number and diameter in developing and ageing skeletal muscle. *J Anat.* **153**, 31-45.
5. Always, S.E., Myers, M.J., and Mohamed, J.S. (2014) Regulation of satellite cell function in sarcopenia. *FNAGI.* **6**, 1-15.
6. Always, S.E., and Siu, P.M. (2009) Nuclear apoptosis contributes to Sarcopenia. *Exerc Sport Sci Rev*. **36(2)**, 51-57.
7. Andersen, J.L. (2003) Muscle fibre type adaptation in the elderly human muscle. *Scand J Med Sci Sports* **13**, 40-7.
8. Angelis, M.H., Chambon, P., Brown, S. (2006) Standards of mouse model phenotyping.
9. Angione, A.R., Jiang, C., Pan, D., Wang, Y.X. and Kuang, S. (2011) PPARdelta regulates satellite cell proliferation and skeletal muscle regeneration. *Skeletal mus*. 1, 33.
10. Argiles, J.M., Busquets, S., Stemmler, B., Lopez-Soriano, F.J. (2014) Cancer cachexia: understanding the molecular basis. *Nature*. **14**, 754-762.
11. Ashrafi, G., and Schwarz, T.L. (2013) The pathways of mitophagy for quality control and clearance of mitochondria. *Cell Death Diff*. **20**, 31-42.

12. Attaix, D., Taillandier, D. (2012) The missing link: Mul1 signals mitophagy and muscle wasting. *Cell Metab*. **16**, 551-552.
13. Baoge, L., Van Den Steen, E., Rimbaut, S., Philips, N., Witvrouw, E., Almqvist, K.F,, Vanderstraeten, G., Vanden Bossche, L. C. (2012) Treatment of skeletal muscle injury: A review, *ISRN Orthopedics*.
14. Barazzoni, R., Short, K.R., Nair, K.S. (2000) Effects of aging on mitochondrial DNA copy number and cytochrome c oxidase gene expression in rat skeletal muscle, liver, and heart. *JBC*. **275**, 3343-3347.
15. Barberi, L., Scicchitano, B.M., De Rossi, M., Bigot, A., Duguez, S., Wielgosik, A., Stewart, C., McPhee, J., Conte, M., Narici, M., Franceschi, C., Mouly, V., Butler-Browne, G., Musaro, A. (2013) Age-dependent alteration in muscle regeneration: the critical role of tissue niche. *Biogerontology* **14**, 273–29210.
16. Bartali, B., Frongillo, E.A., Bandinelli, S., Lauretani, F., Semba, R.D., Fried, L.P., and Ferrucci, L. (2006) Low nutrient intake is an essential component of frailty in older persons. *J Gerontol A Biol Sci Med Sci* **61(6)**, 589-593.
17. Bartoli, M., and Richard, I. (2005) Calpains in muscle wasting. *Int J Biochem Cell Biol*. **37**, 2115-2133.
18. Baumeister, W., Walz, J., Zuhl, F., Seemuller, E. (1998) The proteasome: Paradigm of a self-compartmentalizing protease. *Cell*. **92**, 367-380.
19. Baumgartner, R.N., Koehler, K.M,, Gallagher, D., Romero, L., Heymsfield, S.B., Ross, R.R., Garry, P.J., Lindeman, R.D. (1998) Epidemiology of sarcopenia among the elderly in New Mexico. *Am J Epidemiol*. **147**, 755–63.
20. Beauchamp, J.R., Heslop, L., Yu, D.S.W., Tajbakhsh, S., Kelly, R.G., Wernig, A., Buckingham, M.E., Partridge, T.A., Zammit, P.S. (2000) Expression of Cd34 andMyf5 defines the majority of quiescent adult skeletal muscle satellite cells. *J Cell Biol*. **151(6),** 1221-1234.
21. Beccafico, A., Puglielli, C., Pietrangelo, T., Bellomo, R., Fano, G., Fulle, S. (2007) Age-dependent effects on functional aspects in human satellite cells. *Ann NY Acad Sci*. **1100**, 345-52.

22. Bechet, D., Tassa, A., Taillandier, D., Combaret, L., Attaix, D. (2005) Lysosomal proteolysis in skeletal muscle. *Int J Bioche Cell Biol*. **37**, 2098-2114.
23. Beck, F., Plummer, S., Senior, P.V., Byrne, S., Green, S., and Brammar, W.J. (1992) The ontogeny of peroxisome-proliferator-activated receptor gene expression in the mouse and rat. *Proc Royal Soc London Biol Sci.* **247**, 83-87.
24. Bischoff, R. (1994) The satellite cell and muscle regeneration. *Myology: Basic and Clinical*. McGraw Hill. **1**:97-112.
25. Bischoff, R. Chemotaxis of skeletal muscle satellite cells. (1997) *Dev Dynamics* **208(4)**, 505–515.
26. Bladt, F., Riethmacher, D., Isenmann, S., Aguzzi, A., Birchmeier, C. (1995) Essential role of the c-met receptor in the migration of myogenic precursor cells into the limb bud. *Nature*. **376**, 768-771.
27. Blaivas, M., and Carlson, B.M. (1991) Muscle fiber branching-difference between grafts in old and young rats. *Mech Ageing Dev*. **60(1)**, 43-53.
28. Blaveri, K.L., Heslop, D., Yu, J., Rosenblatt, J., Gross, J., Partridge, T., and Morgan, J. (1999) Patterns of repair of dystrophic mouse muscle: studies on isolated fibres. *Develop Dyn.* **216(3)**, 244-256.
29. Blumberg, B., Evans, R.M. (1998) Orphan nuclear receptors- new ligands and new possibilities. *Genes & Dev*. **12**, 3149-3155.
30. Bockhold, K.J., Rosenblatt, J.D., Partridge, T.A. (1998) Aging normal and dystrophic mouse muscle: analysis of myogenicity in cultures of living single fibers. *Mus Nerve*. **21**, 173-183.
31. Bodine, S.C., Latres, E., Baumhueter, S., Lai, V.K., Nunez, L., Clarke, B.A., Poueymirou, W.T., Panaro, F.J., Na, E., Dharmarajan, K., Pan, Z.Q., Valenzeula, D.M., DeChiara, T.M., Stitt, T.N., Yancopoulos, G.D., Glass, D.J. (2001) Identification of ubiquitin ligases required for skeletal muscle atrophy. *Science*. **294**, 1704-1708.
32. Bogdanovich, S., Krag, T.O., Barton, E.R., Morris, L.D., Whittemore, L.A., Ahima, R.S., and Khurana, T.S. (2002) Functional improvement of dystrophic muscle by myostatin blockade. *Nature.* **420**, 418-421.

33. Boitier, E., Gautier, J.C., and Roberts, R. (2003) Advances in understanding the regulation of apoptosis and mitosis by peroxisome-proliferator activated receptors in pre-clinical models: relevance for human health and disease. *Comp Hepat*. 1-15.
34. Bonala, S., Lokireddy, S., Arigela, H., Teng, S., Wahli, W., Sharma, M., McFarlane, C., Kambadur, R. (2012) Peroxisome Proliferator-activated Receptor β/δ induces myogenesis by modulating Myostatin activity. *J Biol Che* **16**, 12935-12951.
35. Borland, M.G., Foreman, J.E., Girroir, E.E., Zolfaghari, R., Sharma, A.K., Amin, S., Gonzalez, F.J., Ross, A.C., Peters, J.M. (2008) Ligand activation of peroxisome proliferator-activated receptor-beta/delta inhibits cell proliferation in human HaCaT keratinocytes. *Mol Pharmacol*. **74(5)**, 1429-42.
36. Bothe, G.W., Haspel, J.A., Smith, C.L., Wiener, H.H., Burden, S.J. (2000) Selective expression of Cre recombinase in skeletal muscle fibers. *Genesis*. **26**, 165-166.
37. Brack, A.S., Bildsoe, H., Hughes, S.M. (2005) Evidence that satellite cell decrement contributes to preferential decline in nuclear number from large fibres during murine age-related muscle atrophy. *J Cell Sci* **118**, 4813-21.
38. Bradford, M.M. (1976) A rapid and sensitive method for the quantitation of microgram quantities of protein utilizing the principle of protein-dye binding. *Anal Bioche*. **72,** 248-254.
39. Braissant, O., Foufelle, F., Scotto, C., Dauca, M., Wahli, W. (1996) Differential expression of peroxisome proliferator-activated receptors (PPARs): tissue distribution of PPAR-alpha, -beta, and -gamma in the adult rat. *Endo*. **137(1)**, 354-66.
40. Braissant, O. and Wahli, W. (1998) Differential expression of Peroxisome Proliferator Activated Receptor- α, -β, and -γ during rat embryonic development. *Endo*. **139(6)**, 2748-54.
41. Bratic, A., and Larrson, N.G. (2013) The role of mitochondria in aging. *JCI*, **123**, 951-957.

42. Breitbart, A., Auger-Messier, M., Molkentin, J.D., Heineke, J. (2011) Myostatin from the heart : local and systemic actions in cardiac failure and muscle wasting. *Am J Physiol Heart Circ Physiol*. H1973-82.
43. Brocca, L., Cannavino, J., Coletto, L., Biolo, G., Sandri, M., Bottinelli, R. (2012) The time course of the adaptations of human muscle proteome to bed rest and the underlying mechanisms. *J Physiol*. **590**, 5211-5230.
44. Brookes, P.S., Yoon, Y., Robotham, J.L., Anders, M.W., Sheu, S.S. (2004) Calcium, ATP, and ROS: a mitochondrial love-hate triangle. *Am J Physiol Cell Physiol*. **287**, C817-C833.
45. Brown, M. (1987) Change in fibre size, not number, in ageing skeletal muscle. *Age Ageing*. **16(4)**, 244-8.
46. Bua, E.A., McKiernan, S.H., Wanagat, J., McKenzie, D., and Aiken, J.M. (2002) Mitochondrial abnormalities are more frequent in muscles undergoing sarcopenia. *J. Appl. Physiol*. **92**, 2617–2624.
47. Buckingham, M., Bajard, L., Chang, T., Daubas, P., Hadchouel, J., Meilhac, S., Montarras, D., Rocan court, D., Relaix, F. (2003) The formation of skeletal muscle: from somite to limb. *J Anat.* **202**, 59-68.
48. Buford, T.W., Anton, S.D., Judge, A.R., Marzetti, E., Wohlgemuth, S.E., Carter, C.S., Leeuwenburgh, C., Pahor, M., Manini, T.M. (2010) Models of accelerated sarcopenia: critical pieces for solving the puzzle of age-related muscle atrophy. *Ageing Res. Rev*. **9**, 369–383.
49. Cadenas, E., Davies, K.J. (2000) Mitochondrial free radical generation, oxidative stress, and aging. *Free Rad Biol Med*. **29**, 222–230.
50. Campbell, M.J., McComas, A.J., Petito, F. (1973) Physiological changes in ageing muscles. *J Neurol Neurosurg Psych.* **36**, 174-82.
51. Carlson, M.E., Suetta, C., Conboy, M.J., Aagaard, P., Mackey, A., Kjaer, M., Conboy, I. (2009) Molecular aging and rejuvenation of human muscle stem cells. *EMBO Mol Med.* **1(8-9)**, 381-91.
52. Carlson, B.M., Faulkner, J.A. (1989) Muscle transplantation between young and old rats:age of host determines recovery. *Am J Physiol*. **256**, C1262-C1266.
53. Carnac, G., Vernus, B., Bonnieu, A. (2007) Myostatin in the pathophysiology of skeletal muscle. *Curr Gen*. **8(7)**, 415-422.

54. Chabi, B., Ljubicic, V., Menzies, K.J., Huang, J.H., Saleem, A., Hood, D.A. (2008) Mitochondrial function and apoptotic susceptibility in aging skeletal muscle. *Aging Cell.* **7(1),** 2-12.
55. Chandrashekar, P., Manickam, R., Ge, X., Bonala, S., McFarlane, C., Sharma, M., Wahli, W., Kambadur, R. (2015) Inactivation of PPAR β/δ adversely affects satellite cells and reduced postnatal myogenesis. *Am J Physiol Endo Metab.* **309(2)**, E122-31.
56. Charge, S.B., and Rudnicki, M.A. (2004) Cellular and Molecular Regulation of Muscle Regeneration. *Physiol Rev.* 209-238.
57. Chen, H., Vermulst, M., Wang, Y.E., Chomyn, A., Prolla, T.A., McCaffery, J.M., Chan, D.C. (2010) Mitochondrial fusion is required for mtDNA stability in skeletal muscle and tolerance of mtDNA mutations. *Cell*. **141**, 280-289.
58. Chen, Y., Ye, J., Cao, L., Zhang, Y., Xia, W., Zhu, D. (2010) Myostatin regulates glucose metabolism via the AMP-activated protein kinase pathway in skeletal muscle cells. *Int J Biochem Cell Biol.* **42(12)**, 2072-81.
59. Chen, L., Liu, T., Tran, A., Lu, X., Tomilv, A.A., Davies, V., Cortopassi, G., Chiamimonvat, N., Bers, D.M., Votruba, M., Knowlton, A.A. (2012) OPA1 mutation and late onset cardiomyopathy: mitochondrial dysfunction and mtDNA instability. *J Am Heart Assoc*.
60. Chinnery, P.F. (2014) Mitochondrial Disorders Overview. *Gene Rev.*
61. Chinnery, P.F., DiMauro, S., Shanske, S., Schon, E.A., Mariotti, C., Carrara, F., Lombe,s A., Laforet, P., Ogier, H., Jaksch, M., Lochmuller, H., Horvath, R., Deschauer, M., Thorburn, D.R., Bindoff, L.A., Poulton, J., Taylor, R.W., Matthews, J.N., and Turnbull, D.M. (2004) Risk of developing a mitochondrial DNA deletion disorder. *Lancet* . **364**, 592-596.
62. Chinnery, P.F., and Schon, E.A. (2003) Mitochondria. *J Neurol Neurosurg Psychiatry*. **74**, 1188-1199.
63. Chinnery, P.F., and Turnbull, D.M. (1999) Mitochondrial DNA and disease. *Lancet* . SI17-21.

64. Chinnery, P.F., and Turnbull, D.M. (2000) Mitochondrial DNA mutations in the pathogenesis of human disease. *Mol Med Today*. **6**, 425-432.
65. Choi, S.J. (2014) Differential susceptibility on myosin heavy chain isoform following eccentric-induced muscle damage. *J. Exerc Rehabil.* **10(6)**, 344-348.
66. Chong, H.C., Tan, M.J., Philippe, V., Tan, S.H., Tan, C.K., Ku, C.W., Goh, Y.Y., Wahli, W., Michalik, L., Tan, N.S. (2009) Regulation of epithelial-mesenchymal IL-1 signaling by PPARβ/δ is essential for skin homeostasis and wound healing. *J Cell Biol*. **184(6)**, 817-831.
67. Ciciliot, S., and Schiaffino, S. (2010) Regeneration of mammalian skeletal muscle. Basic mechanisms and clinical implications. *Curr Pharma Design*. **16**, 906-914.
68. Chu, C.T. (2010) A pivotal role for PINK1 and autophagy in mitochondrial quality control: implications for Parkinson disease. *Hum Mol Genet*. **19**, R28-R37.
69. Coggan, A.R., Spina, R.J., Rogers, M.A., King, D.S., Brown, M., Nemeth, P.M., Holloszy, J.O. (1990) Histochemical and enzymatic characteristics of skeletal muscle in master athletes. *J Appl Physiol*. **68**, 1896-1901.
70. Conboy, I.M., Rando, T.A. (2005) Aging, stem cells and tissue regeneration:lesions from muscle. *Cell cycle* **4**, 407-410.
71. Conboy, I.M., Rando, T.A. (2002) The regulation of Notch signaling controls satellite cell activation and cell fate determination in postnatal myogenesis. *Dev Cell*. **3**, 397-409.
72. Costelli, P., Muscaritoli, M., Bonetto, A., Penna, F., Reffo, P., Bossola, M., Bonelli, G., Doqlietto, G.B., Baccino, F.M., Rossi Fanelli, F. (2008) Muscle myostatin signalling is enhanced in experimental cancer cachexia. *Eur J Clin Invest*. **38**, 531-538.
73. Croall, D.E., and Ersfeld, K. (2007) The calpains: modular designs and functional diversity. *Genome Biol*. **8(6)**, 218.

74. Cuervo, A.M., Bergamini, E., Brunk, U.T., Droge, W., Ffrench, M., Terman, A. (2005) Autophagy and aging: the importance of maintaining "clean" cells. *Autophagy*. **1**, 131–40.
75. Cuervo, A.M., Dice, J.F. (2000) Age-related decline in chaperone-mediated autophagy. *J Biol Chem*. **275**, 31505–13.
76. Cui, H., Kong, Y., Zhang, H. (2012) Oxidative stress, Mitochondrial dysfunction, and Aging. *J Signal Trans*. 13
77. Degens, H., Always, S.E. (2006) Control of muscle size during disuse, disease, and aging. *Int. J. Sports Med*. **27**, 94–99.
78. Demontis, F., Piccirillo, R., Goldberg, A.L., Perrimon, N. (2013) Mechanisms of skeletal muscle aging: insights from Drosophila and mammalian models. *Dis Model Mech* **6,** 1339-1352.
79. Deschenes, M.R. (2004) Effects of aging on muscle fibre type and size. *Sports Med* **34(12)**, 809-24.
80. Desvergne, B., Wahli, W. (1999) Peroxisome proliferator- activated receptors: Nuclear control of metabolism. *Endocrine Rev*. **20**, 649-688.
81. Deval, C., Mordier, S., Obled, C., Bechet, D., Combaret, L., Attaix, D. (2001) Identification of cathepsin L as a differentially expressed message associated with skeletal muscle wasting. *Bioche J*. **360**, 143-150.
82. Dhawan, J., Rando, T.A. (2005) Stem cells in postnatal myogenesis:molecular mechanisms of satellite cell quiescence, activation and replenishment. *Trends in Cell Biol*. **15**, 666-673.
83. Dimmer, K.S., Scorrano, L. (2006) (De)constructing mitochondria:what for? *Physiol*. **21**, 233-241.
84. Ding, W.X., Yin, X.M. (2012) Mitophagy: mechanisms, pathophysiological roles, and analysis. *Biol chem*. **393(7),** 547-564.
85. Dirks, A.J., Hofer, T., Marzetti, E., Pahor, M., Leeuwenburgh, C. (2006) Mitochondrial DNA mutations, energy metabolism and apoptosis in aging muscle. *Ageing Res Rev* **5(2)**, 179-95.
86. Dirks, A.J., Leeuwenburgh, C. (2004) Aging and lifelong calorie restriction result in adaptations of skeletal muscle apoptosis repressor,

apoptosis-inducing factor, X-linked inhibitor of apoptosis, caspase-3, and caspase-12. *Free Radic Biol Med*. **36**, 27-39.

87. DiRenzo, J., Soderstrom, M., Kurokawa, R., Ogliastro, M.H., Ricote, M., Ingrey, S., Horlein, A., Rosenfeld, M.G., and Glass, C.K. (1997) Peroxisome proliferator-activated receptors and retinoic acid receptors differentially control the interactions of retinoid X receptor heterodimers with ligands, coactivators, and corepressors. *Mol and Cell Biol.* **17**, 2166-2176.

88. Doherty, T.J. (2003) Invited review: Aging and Sarcopenia. *J Appl Physiol*. **95(4)**, 1717-27.

89. Drew, B., Phaneuf, S., Dirks, A., Selman, C., Gredilla, R., Lezza, A., Barja, G., Leeuwenburgh, C. (2003) Effects of aging and caloric restriction on mitochondrial energy production in gastrocnemius muscle and heart. *Am. J. Physiol. Regul. Integr. Comp. Physiol*. **284**, R474–R480.

90. Dreyer, C., Krey, G., Keller, H., Givel, F., Helftenbein, G., Wahli, W. (1992) Control of the peroxisomal beta-oxidation pathway by a novel family of nuclear hormone receptors. *Cell*. **68**, 879-887.
91. Dreyer, C., Keller, H., Mahfoudi, A., Laudet, V., Krey, G., Wahli, W. (1993) Positive regulation of the peroxisomal beta-oxidation pathway by fatty acids through activation of peroxisome proliferator-activated receptors (PPAR). *Biol Cell*. **77**, 67-76.

92. Durieux, A.C., Amirouche, A., Banzet, S., Koulmann, N., Bonnefor, R., Pasdeloup, M., Mouret, C., Bigard, X., Peinnequin, A., and Freyssenet, D. (2007) Ectopic expression of myostatin induces atrophy of adult skeletal muscle by decreasing muscle gene expression. *Endo*. **148**, 3140-3147.

93. Edstrom, E., Altun, M., Bergman, E., Johnson, H., Kullberg, S., Ramirez-Leon, V., Ulfhake, B. (2007) Factors contributing to neuromuscular impairment and sarcopenia during aging. *Physiol Behav*. **92(1-2)**, 129-35.

94. Enns, D.L., and Tidus, P.M. (2008) Estrogen influences satellite cell activation and proliferation following downhill running in rats. *J App Physiol*. **104**, 347-353.
95. Epstein, J.A., Shapiro, D.N., Cheng, J., Lam, P.Y., Maas, R.L. (1996) Pax3 modulates expression of c-Met receptor during limb muscle development. *Proc Natl Acad Sci USA.* **93(9)**, 4213-4218.
96. Eskelinen, E.L. (2008) New insights into the mechanisms of macroautophagy in mammalian cells. *Int Rev Cell Mol Biol*. **266**, 207-247.
97. Esposito, A., Campana, L., Palmisano, A., Cobelli, F.D., Canu, T., Santarella, F., Colantoni, C., Monno, A., Vezzoli, M., Pezzetti, G., Manfredi, A.A., Rovere-Querini, P., Maschio, A.D. (2013) Magnetic resonance imaging at 7T reveals common events in age-related sarcopenia and in the homeostatic response to muscle sterile injury. *PLoS One*. **8(3)**.
98. Evans, R.M. (1988) The steroid and thyroid receptor superfamily. *Science*. **240**, 889-895.
99. Evans, W.J. (1995) What is sarcopenia? *J Gerontol A Biol Sci Med Sci.* **50**, 5-810.
100. Evans, W.J. (2010) Skeletal muscle loss: cachexia, sarcopenia, and inactivity. *Am J Clin Nutr*. **91**, 11235-11275.
101. Evans, R.M., Mangelsdorf, D.J. (2014) Nuclear receptors, RXR, and the Big Bang. *Cell* **157**, 255-266.
102. Faulkner, J.A., Brooks, S.V., Zerba, E. (1995) Muscle atrophy and weakness with aging: contraction-induced injury as an underlying mechanism. *J Gerontol A Biol Sci Med Sci*. **50**, 124-129.
103. Feige, J.N., Gelman, L., Tudor, C., Engelborghs, Y., Wahli, W., and Desvergne, B. (2005) Fluorescence imaging reveals the nuclear behavior of peroxisome proliferator activated receptor/retinoid X receptor heterodimers in the absence and presence of ligand. *J Biol Chem*. **280**, 17880–17890.

104. Ferre, P. (2004) The biology of peroxisome proliferator-activated receptors: relationship with lipid metabolism and insulin sensitivity. *Diabetes.* **53**, S43-S50.

105. Fluck, M., Hoppeler, H. (2003) Molecular basis of skeletal muscle plasticity-from gene to form and function. *Rev Physiol Biochem Pharmacol.* **146**, 159-216.

106. Frontera, W.R., Hughes, V.A., Fielding, R.A., Fiatarone, M.A,. Evans, W.J., Roubenoff, R. (2000) Aging of skeletal muscle: a 12-yr longitudinal study. *J Appl Physiol*. **88**, 1321-1326.

107. Fulle, S., Protasi, F., Di Tano, G., Pietrangelo, T., Beltramin, A., Boncompagni, S., Vecchiet, L., Fano, G. (2004) The contribution of reactive oxygen species to sarcopenia and muscle ageing. *Exp Gerontol*. **39(1)**, 17-24.

108. Fu, H., Desvergne, B., Ferrari, S., and Bonnet, D.N. (2014) Impaired musculoskeletal response to age and exercise in PPAR$^{-/-}$ diabetic mice. *Endo*. **155(12)**, 4686-4696.

109. Galler, S., Schmitt, T.L., Pette, D. (1994) Stretch activation, unloaded shortening velocity, and myosin heavy chain isoforms of rat skeletal muscle fibres. *J Physiol*. 513-521.

110. Galuppo, M., Di Paola, R., Mazzon, E., Genovese, T., Crisafulli, C., Paterniti, I., Cuzzocrea, E., Bramanti, P., Kapoor, A., Thiemermann, C., Cuzzocrea, S. (2010) Role of PPAR-delta in the development of zymosan-induced multiple organ failure: an experiment mice study. *J Inflamm*. **7**, 12.

111. Garcia, P.S., Cabbabe, A., Kambadur, R., Nicholas, G., Csete, M. (2010) Elevated Myostatin Levels in Patients with Liver Disease: A Potential Contributor to Skeletal Muscle Wasting. *Anesth Analg*. 707-709.

112. Gaudel, C., and Grimaldi, P.A. (2007) Metabolic functions of Peroxisome Proliferator-Activated Receptor β/δ in skeletal muscle. *PPAR Research*.

113. Gaudel, C., Schwartz, C., Giordano, C., Abumrad, N.A., Grimaldi, P.A. (2008) Pharmacological activation of PPAR beta promotes rapid and calcineurin-dependent fiber remodeling and angiogenesis in mouse skeletal muscle. *Am J Physiol Endocrinol Metab*. **295**, E297-304.

114. Gearing, K.L., Gottlicher, M., Teboul, M., Widmark, E., and Gustafsson, J.A. (1993) Interaction of the peroxisome-proliferator-activated receptor and retinoid X receptor. *Proc Natl Acad Sci USA*. **90**, 1440-1444.

115. Ge, X., Vajjala, A., McFarlane, C., Wahli, W., Sharma, M., Kambadur, R. (2012) Lack of Smad3 signaling leads to impaired skeletal muscle regeneration. *Am J Endo Physiol Metab*. **303**, E90-102.

116. Giguere, V., Yang, N., Segui, P., Evans, R.M. (1988) Identification of a new class of steroid hormone receptors. *Nat*. **331**, 91-94.

117. Gilson, H., Schakman, O., Combaret, L., Lause, P., Grobet, L., Attaix, D., Ketelslegers, J.M., and Thissen, J.P. (2007) Myostatin gene deletion prevents glucocorticoid-induced muscle atrophy. *Endocrinol*. **148(1)**, 452-460.

118. Giordano, C., Rousseau, A.S., Wagner, N., Gaudel, C., Murdaca, J., Jehl-Pietri, C., Sibille, B., Grimaldi, P.A., Lopez, P. (2009) Peroxisome proliferator-activated receptor β activation promotes myonuclear accretion in skeletal muscle of adult and aged mice. *Eur J Physiol*. 901-913.

119. Glickman, M.H., Ciechanover, A. (2002) The ubiquitin-proteasome proteolytic pathway: Destruction for the sake of construction. *Physiol Rev*. **82**, 373-428.

120. Goetsch, S.C., Hawke, T.J., Gallardo, T.D., Richardson, J.A., Garry, D.J. (2003) Transcriptional profiling and regulation of the extracellular matrix during muscle regeneration. *Physiol Genomics*. **14**, 261-271.

121. Gomes, M.D., Lecker, S.H., Jagoe, R.T., Navon, A., Goldberg, A.L. (2001) Atrogin-1, a muscle specific F-box protein highly expressed during muscle atrophy. *Proc Natl Acad Sci USA*. **98**, 14440-14445.

122. Gonzalez-Cadavid, N.F., Taylor, W.E., Yarasheski, K., Sinha-Hikim, I., Ma, K., Ezzat, S., Shen, R., Lalani, R., Asa, S., Mamita, M., Nair, G., Arver, S., Bhasin, S. (1998) Organization of the human myostatin gene and expression in healthy men and HIV-infected men with muscle wasting. *Proc Natl Acad Sci USA*. **95(25)**, 14938-43.

123. Gonzalez. E., Delbono, O. (2001) Age-dependent fatigue in single intact fast- and slow fibers from mouse EDL and soleus skeletal muscles. *Mech Ageing Dev*. **122**, 1019-1032.

124. Goodpaster, B.H., Park, S.W., Harris, T.B., Kritchevsky, S.B., Nevitt, M., Schwartz , A.V,, Simonsick, E.M., Tylavsky, F.A., Visser, M., Newman, A.B. (2006) The loss of skeletal muscle strength, mass, and quality in older adults: the health, aging and body composition study. *J Gerontol A Biol Sci Med Sci*. **61**, 1059-64.

125. Green, D.R., Reed, J.C. (1998) Mitochondria and apoptosis. *Science*. **281**, 1309–1312.

126. Grimby, G., Saltin, B. (1983) The ageing muscle. *Clin Physiol*. **3**, 209-18.

127. Grumati, P., Coletto, L., Sabatelli, P., Cescon, M., Angelin, A., Bertaggia, E. (2010) Autophagy is defective in collagen VI muscular dystrophies, and its reactivation rescues myofiber degeneration. *Nat Med*. **16**, 1313-1320.

128. Grumati, P., and Bonaldo, P. (2012) Autophagy in skeletal muscle homeostasis and in muscular dystrophies. *Cells*. **1**, 325-345.

129. Grygiel-Gornial, B. (2014) Peroxisome proliferator-activated receptors and their ligands: nutritional and clinical implications- a review. *Nut J*. **13**: 1-10.

130. Hancock, C.R., Han, D.H., Chen, M., Terada, S., Yasuda, T., Wright, D.C., Holloszy, J.O. (2008) High-fat diets cause insulin resistance despite an increase in muscle mitochondria. *Proc Natl Acad Sci U S A* .**105**: 7815–7820

131. Hara, T., Nakamura, K., Matsui, M., Yamamoto, A., Nakahara, Y., Suzuki-Migishima, R. (2006) Suppression of basal autophagy in neural cells causes neurodegenerative disease in mice. *Nature*. **441**, 885-889.

132. Harris, A.J., Duxson, M.J., Fitzsimons, R.B., Rieger, F. (1989) Myonuclear birthdates distinguish the origins of primary and secondary myotubes in embryonic mammalian skeletal muscles. *Develop.* **107**, 771-78.

133. Hasselgren, P.O., Fischer, J.E. (2001) Muscle cachexia: current concepts of intracellular mechanisms and molecular regulation. *Ann Surg*. **233**, 9-17.

134. Hasten, D.L., Pak-Loduca, J., Obert, K.A., Yarasheski, K.E. (2000) Resistance exercise acutely increases MHC and mixed muscle protein synthesis rates in 78-84 and 23-32 yr olds. *Am J Physiol*. **278**, E620-E626.

135. Hawke, T.J., Garry, D.J. (2001) Myogenic satellite cells:physiology to molecular biology. *J App Physiol.* **91**, 534-551.

136. Hepple, RT. (2014) Mitochondrial involvement and impact in aging skeletal muscle. *Front Aging Neurosci* 1-13.

137. Herbst, A., Pak, J.W., McKenzie, D., Bua, E., Bassiouni, M., Aiken, J.M. (2007) Accumulation of mitochondrial DNA deletion mutations in aged muscle fibers: evidence for a causal role in muscle fiber loss. *J. Gerontol. A Biol. Sci. Med. Sci*. **62**, 235–245.

138. Hooper, A.C.B. (1981) Length, diameter and number of ageing skeletal muscle fibers. *Gerontol*. **27**, 121-126.

139. Huang, J., Forsberg, N.E. (1998) Role of calpain in skeletal muscle protein degradation. *Proc Natl Acad Sci USA*. **95**, 12100-12105.

140. Huang, Z., Chen, D., Zhang, K., Yu, B., Chen, X., and Meng, J. (2007) Regulation of myostatin signaling by c-Jun N-terminal kinase in C2C12 cells. *Cell Sig*. **19**, 2286-2295.

141. Hughes, V.A., Frontera, W.R., Wood, M., Evans, W.J., Dallal, G.E., Roubenoff, R., Fiatarone Singh, M.A. (2001) Longitudinal muscle strength changes in older adults: influence of muscle mass, physical activity, and health. *J Gerontol A Biol Sci Med Sci*. **56**, B209-17.

142. Huin, C., Corriveau, L., Bianchi, A., Keller, J.M., Collet, P., Kremarik-Bouillad, P., Domenjoud, L., Becuwe, P., Schohn, H., Menard, D., Dauca, M. (2000) Differential expression of peroxisome proliferator-activated receptors (PPARs) in the developing human fetal digestive tract. *J Histo Cytoche.* **48(5)**, 603-611.

143. IJpenberg, A., Jeannin, E., Wahli, W., and Desvergne, B. (1997) Polarity and specific sequence requirements of peroxisome proliferator-activated receptor (PPAR)/retinoid X receptor heterodimer binding to DNA. A functional analysis of the malic enzyme gene PPAR response element. *J Biol Chem.* **272**, 20108-20117.

144. Issemann, I., Green, S. (1990) Activation of a member of the steroid hormone receptor superfamily by peroxisome proliferators. *Nature*. **347**, 645-650.

145. Jahnke, V.E., Meulen, J.H.V.D., Johnston, H.K., Ghimbovschi, S., Partridge, T., Hoffman, E.P., Nagaraju K. (2012) Metabolic remodeling agents show beneficial effects in the dystrophin-deficient *mdx* mouse model. *Skel Mus*. **2**, 16.

146. Janssen, I., Heymsfield, S.B., Wang, Z.M., Ross, R. (2000) Skeletal muscle mass and distribution in 468 men and women aged 18–88 yr. *J. Appl. Physiol*. **89**, 81–88.

147. Janssen, I., Heymsfield, S.B., and Ross, R. (2002) Low relative skeletal muscle mass (sarcopenia) in older persons is associated with functional impairment and physical disability. *J Am Geriatr Soc.* **50**, 889-896.

148. Jenkins, G.W., Kemnitz, C.P., Tortora, G.J. *Anat and Physiol: From Sci to Life*. (2006), New York: Wiley. 1152.

149. Jin, S.M., Youle, R.J. (2012) PINK1- and Parkin- mediated mitophagy at a glance. *J Cell Sci.* **125**, 795-799.

150. Johnston, A.P., De Lisio, M., Parise, G. (2008) Resistance training, sarcopenia, and the mitochondrial theory of aging. *Appl. Physiol. Nutr. Metab*. **33**, 191–199.

151. Joulia, D., Bernardi, H., Garandel, V., Rabenoelina, F., Vernus, B., Cabello, G. (2003) Mechanisms involved in the inhibition of myoblast proliferation and differentiation by myostatin. *Exp Cell Res.* 263-275.

152. Kablar, B., Krastel, K., Ying, C., Asakura, A., Tapscott, S.J., and Rudnicki, M.A. (1997) MyoD and Myf-5 differentially regulate the development of limb versus trunk skeletal muscle. *Develop*. **124**, 4729-4738.

153. Kambadur, R., Sharma, M., Smith, T P.L. (1997) Mutations in myostatin (GDF-8) in double-muscled belgian blue and peidmontese cattle. *Gen Res.* 910-915.

154. Karagounis, L.G., Hawley, J.A. (2010) Skeletal muscle: Increasing the size of the locomotor cell. *Int J Bio Cell Biol.* **42**, 1376-1379.

155. Karalaki, M., Fili, S., Philippou, A., Koutsilieris, M. (2009) Muscle Regeneration: Cellular and Molecular Events. *In Vivo*. **23**, 779-796.

156. Kaariainen, M., Jarvinen, T., Jarvinen, M., Rantanen, J., Kalimo, H. (2000) Relation between myofibers and connective tissue during muscle injury repair. *Scan J Med Sci Sports*. **10**, 332-337.

157. Kasper, C.E., and Xun, L. (1996) Cytoplasm-to-myonucleus ratios in plantaris and soleus muscle fibres following hindlimb suspension. *J Muscle Res Cell Moti.l* **17(5)**, 603-10.

158. Kasper, C.E., and Xun, L. (1996a) Cytoplasm-to-myonucleus ratios following microgravity. *J Muscle Res Cell Motil.* **17(5)**, 595-602.

159. Kassar-Duchossoy, L., Gayraud-Morel, B., Gom`es D., Rocancourt. D., Buckingham, M., Shinin, V., Tajbakhsh, S. (2004) Mrf4 determines skeletal muscle identity in Myf5: Myod double-mutant mice. *Nature*. **431**, 466–71.

160. Keller, H., Dreyer, C., Medin, J., Mahfoudi, A., Ozato, K., and Wahli, W. (1993) Fatty acids and retinoids control lipid metabolism through activation of peroxisome-proliferator-activated receptor-retinoid X receptor heterodimers. *Proc Natl Acad Sci USA.* **90**, 2160-2164.

161. Kim. H.I., and Ahn, Y.H. (2004) Role of peroxisome proliferator-activated receptor gamma in the glucose-sensing apparatus of liver and beta-cells. *Diabetes* **53 (Suppl 1)**, S60–S65.

162. Kliewer. S.A., Umesono. K., Noonan, D.J., Heyman, R.A., and Evans, R.M. (1992) Convergence of 9-cis retinoic acid and peroxisome proliferator signalling pathways through heterodimer formation of their receptors. *Nature.* **358**, 771–774.

163. Klitgaard. H., Bergman, O., Betto, R., Salviati, G., Schiaffino, S., Clausen, T., Saltin, B. (1990a) Co-existence of myosin heavy chain I and IIa isoforms in the human skeletal muscle fibres with endurance training. *Pflugers Arch.* **416**, 470-2.

164. Klitgaard, H., Zhou, M., Schiaffino, S., Betto, R., Salviati, G., Saltin, B. (1990) Ageing alters the myosin heavy chain composition of single fibres from human skeletal muscle. *Acta Physiol Scand*. **140**, 55-62.

165. Jornayvaz, F.R., Shulman, G.I. (2010) Regulation of mitochondrial biogenesis. *Essays Biochem*. **47**, 1-15.

166. Kim, I., Rodriguez-Enriquez, S., Lemasters, JJ. (2007) Selective degradation of mitochondria by mitophagy. *Arch Biochem Biophys.* **462(2)**, 245-253.

167. Kowaltowski, A.J., De Souza-Pinto, N.C., Castilho, R.F., Vercesi, A,E. (2009). Mitochondria and reactive oxygen species. *Free Radic Biol Med*. **47**, 333-343.

168. Krey, G., Braissant, O., L'Horset, F., Kalkhoven, E., Perroud, M., Parker, M.G., and Wahli, W. (1997) Fatty acids, eicosanoids, and hypolipidemic agents identified as ligands of peroxisome proliferator-activated receptors by coactivator-dependent receptor ligand assay. *Mol Endo.* **11**, 779-791.

169. Kuang. S., Kuroda, K., Le Grand, F., & Rudnicki, M.A. (2007) Asymmetric self-renewal and commitment of satellite stem cells in muscle. *Cell.* 129, 999–1010.

170. Kubli, D.A., Gustafsson, A.B. (2012) Mitochondria and mitophagy: The Yin and Yang of cell death control. *Circ Res*. **111**, 1198-1207.

171. Kundu, M., Thompson, C.B. (2008) Autophagy: basic principles and relevance to disease. *Annu Rev Pathol*. **3**, 427-455.

172. Lahiri, S., and Wahli, W. (2010) Peroxisome proliferator-activated receptor β/δ: a master regulator of metabolic pathways in skeletal muscle. *Horm Mol Biol Clin Invest*. **4(2)**, 565-573.

173. Langley, B., Thomas, M., Bishop, A., Sharma, M., Gilmour, S., Kambadur, R. (2002) Myostatin inhibits myoblast differentiation by down-regulating MyoD expression. *J Biol Chem*. **277**, 49831-49840.

174. Larsson, L., Sjodin, B., Karlsson, J. (1978) Histochemical and biochemical changes in human skeletal muscle with age in sedentary males, age 22–65 years. *Acta Physiol Scand.* **103**, 31–9.

175. Larsson, L (1983) Histochemical characteristics of human skeletal muscle during aging. *Acta Physiol Scand.* **117**, 469-471.

176. Larsson, L., Biral, D., Campione, M., and Schiaffino, S. (1993) An age-related type IIB to IIX myosin heavy chain switching in rat skeletal muscle. *Acta Physiol Scand* **147(2)**, 227-34.

177. Laudet, V., Auwerx, J., Gustafsson, J., and Wahli, W. (1999) A unified nomenclature system for the nuclear receptor superfamily. *Cell*. **97**, 161-163.

178. Lee, S.J., McPherron, A.C. (2001) Regulation of myostatin activity and muscle growth. *Proc Natl Acad Sci USA.* 9306-9311.

179. Lee, C.H., Olson, P., Hevener, A., Mehl, I., Chong, L.W., Olefsky, J.M., Gonzalez, F.J., Ham, J., Kang, H., Peters, J.M., and Evans, R.M. (2006) PPAR delta regulates glucose metabolism and insulin sensitivity. *Proc Natl Acad Sci USA*. **103**, 3444-3449.

180. Lee, W.S., Cheung, W.H., Qin, L., Tang, N., Leung, K.S. (2006) Age-associated decrease of type IIA/B human skeletal muscle fibers. *Clin Orthop Relat Res*. **450**, 231-7.

181. Lenk, K., Schur, R., Linke, A., Erbs, S., Matsumoto, Y., Adams, V., and Schuler, G. (2009) Impact of exercise training on myostatin expression in the myocardium and skeletal muscle in a chronic heart failure model. *Eur J Heart Fail*. **11**, 342-348.

182. Leeuwenburgh, C. (2003) Role of apoptosis in Sarcopenia. *J Gerontol*. 999-1001.

183. Levine, B., Klionsky, D.J. (2004) Development by self-digestion: molecular mechanisms and biological functions of autophagy. *Dev Cell*. **6**, 463-477.

184. Lexell, J., Henriksson-Larsen, K., Winblad, B., Slostrom, M. (1983) Distribution of different fiber types in human skeletal muscles: effects of aging studied in whole muscle cross sections. *Mus Ner* **6**, 588–95.

185. Lexell, J., Taylor, C.C., Sjostrom, M. (1988) What is the cause of the ageing atrophy? Total number, size and proportion of different fiber types studied in whole vastus lateralis muscle from 15-to 83-year-old men. *J Neurol* Sci **84**, 275–94.

186. Lexell, J. (1995) Human aging, muscle mass, and fibre type composition. *J Gerontol A Biol Sci Med Sci.* **50**, 11-6.

187. Liu, Y., Schlumberger, A., Wirth, K., Schmidtbleicher, D., Steinacker, J.M. (2003) Different effects on human skeletal myosin heavy chain isoform expression: strength vs combination training. *J Appl Physiol.* **94**, 2282-8.

188. Lokireddy, S., Mouly, V., Butler-Browne, G., Gluckman, PD., Sharma, M., and Kambadur, R. (2011) Myostatin promotes the wasting of human myoblast cultures through promoting ubiquitin-proteasome pathway-mediated loss of sarcomeric proteins. *Am J Physiol Cell Physiol.* **301,** C1316-C1324.

189. Lokireddy, S., McFarlane, C., Ge, X., Zhang, H., Sze, S.K., Sharma, M., and Kambaur, R. (2011a) Myostatin Induces Degradation of Sarcomeric Proteins through a Smad3 Signaling Mechanism During Skeletal Muscle Wasting. *Mol. Endocrinol.* **25**, 1936-1949.

190. Lokireddy, S., Wijesoma, I,W., Teng, S., Bonala, S., Gluckman, P,D., McFarlane, C., Sharma, M., Kambadur, R. (2012) The ubiquitin ligase Mul1 induces mitophagy in skeletal muscle in responce to muscle-wasting stimuli. *Cell Metab*. **16(5)**, 613-624.

191. Lokireddy, S., Wijesoma, I,W., Bonala, S., Wei, M., Sze, S,K., McFarlane, C., Kambadur, R., and Sharma, M. (2012a) Myostatin is a

novel tumoral factor that induces cancer cachexia. *Biochem J.* **446**, 23-36.

192. Lunde, I.G., Ekmark, M., Rana, Z.A., Buonanno, A., Gundersen, K. (2007) PPAR δ expression is influenced by muscle activity and induces slow muscle properties in adult rat muscles after somatic gene transfer. *J Physiol.* 1277-1287.

193. Luquet, S., Lopez-Soriano, J., Holst, D., Fredenrich, A., Melki, J., Rassoulzadegan, M., Grimaldi, P.A. (2003) Peroxisome proliferator-activated receptor delta controls muscle development and oxidative capability. *FASEB J.* **17**, 2299-2301.

194. Luquet, S., Gaudel, C., Holst, D., Lopez-Soriano, J., Jehl-Pietri, C., Fredenrich, A., Grimaldi, P.A. (2005) Roles of PPAR delta in lipid absorption and metabolism: a new target for the treatment of type 2 diabetes. *Biochim Biophys Acta*. **1740**, 313-317.

195. Luz, M.A, Marques, M.J, Santo Neto, H. (2002) Impaired regeneration of dystrophin-deficient muscle fibers is caused by exhaustion of myogenic cells. *Braz J Med Bio Res*. **35**, 691-5.

196. MacIntosh, B.R., Gardiner, P.F., McComas, A.J. (2006) Skeletal muscle: Form and function. 2nd ed., 191.

197. Maltzahn, Jv., Chang, N.C., Bentzinger, C.F., Rudnicki, M.A. (2012) Wnt signaling in myogenesis. *Trends Cell Bio*. **22(11)**, 602-609.

198. Mammucari, C., Milan, G., Romanello, V., Masiero, E., Rudolf, R., Del Picollo, P., Burden, S.J., Di Lisi, R., Sandri, C., Zhao, J., Goldberg, A.L, Schiaffino, S., Sandri, M. (2007) FoxO3 controls autophagy in skeletal muscle in vivo. *Cell Metab*. 458-471.

199. Mammucari, C., Schiaffino, S., Sandri, M. (2008) Downstream of Akt: FoxO3 and mTOR in the regulation of autophagy in skeletal muscle. *Autophagy*. 524-526.

200. Mangelsdorf, D.J., Thummel, C., Beato, M., Herrlich, P., Schütz, G., Umesono, K., Blumberg, B., Kastner, P., Mark, M., Chambon, P., Evans, R.M. (1995) The nuclear receptor superfamily: the second decade. *Cell*. **83**, 835–839.

201. Mann, C.J., Perdiquero, E., Kharraz, Y., Aqilar, S., Pessina, P., Serrano, A.L., Munoz-Canoves, P. (2011) Aberrant repair and fibrosis development in skeletal muscle. *Skeletal mus.*1-21.

202. Mansouri, A., Muller, F.L., Liu, Y., Ng, R., Faulkner, J., Hamilton, M., Richardson, A., Huang, T.T., Epstein, C.J., Van Remmen, H. (2006) Alterations in mitochondrial function, hydrogen peroxide release and oxidative damage in mouse hind-limb skeletal muscle during aging. *Mech. Ageing Dev*. **127**, 298–306.

203. Martinez, F.O., Gordon, S. (2014) The M1 and M2 paradigm of macrophage activation: time for reassessment. *F1000Prime Reports*. 6-13.

204. Martini, Frederic, H. (2007). Anatomy and Physiology.

205. Marzetti, E., Calvani, R., Bernabei, R., Leeuwenburgh, C. (2012) Apoptosis in skeletal myocytes: a potential target for interventions against sarcopenia and physical frailty — a mini-review. *Gerontology*. **58**, 99–106.

206. Marzetti, E., Hwang, J.C., Lees, H.A., Wohlgemuth, S.E., Dupont-Versteegden, E.E., Carter, C.S., Bernabi. R., Leeuwenburgh, C. (2010) Mitochondrial death effectors: relevance to sarcopenia and disuse muscle atrophy. *Biochim Biophys Acta* **1800**, 235-244.

207. Masuda. S., Hayashi, T., Hashimoto, T., Taguchi, S. (2009) Correlation of dystrophin-glycoprotein complex and focal-adhesioncomplex with myosin heavy chain isoforms in rat skeletal muscle. *Acta Physiol*. **195**, 483-494.

208. Matsakas. A., Patel, K. (2009) Skeletal muscle fibre plasticity in response to selected environmental and physiological stimuli. *Histol Histopathol.* **24**, 611-629.

209. Matsushita. Y., Ogawa, D., Wada, J., Yamamoto, N., Shikata, K., Sato, C., Tachibana, H., Toyota, N., Makino, H. (2011) Activation of peroxisome proliferator activated receptor delta inhibits streptozotocin-induced diabetic nephropathy through anti-inflammatory mechanisms in mice. *Diabetes*. **60**, 960-968.

210. McBride, H.M., Neuspiel, M., Wasiak. S. (2006) Mitochondria: more than just a powerhouse. *Curr. Biol*. **16(14)**, R551-60.

211. McCormick. K.M., Burns. K.L., Piccone. C.M., Gosselin. L.E., and Brazeau. G.A. (2004) Effects of ovariectomy and estrogen on skeletal muscle function in growing rats. *J Mus Res & Cell Mot*. **25**, 21-27.

212. McCroskery, S., Thomas, M., Maxwell, L., Sharma, M., and Kambadur, R. (2003) Myostatin negatively regulates satellite cell activation and self-renewal. *J Cell Biol*. **162**, 1135-1147.

213. McCroskery, S., Thomas, M., Platt, L., Hennebry, A., Nishimura, T., McLeay, L., Sharma, M., and Kambadur, R. (2005) Improved muscle healing through enhanced regeneration and reduced fibrosis in myostatin-null mice. *J Cell Sci*. **118**, 3531-3541.

214. McFarlane, C., Plummer, E., Thomas, M., Hennebry, A., Ashby, M., Ling, N., Smith, H., Sharma, M., and Kambadur, R. (2006) Myostatin induces cachexia by activating the ubiquitin proteolytic system through an NF-κB-independent, FoxO1-dependent mechanism. *J Cell Physiol*. **209**, 501-514.

215. McFarlane, C., Hennebry, A., Thomas, M., Plummer, E., Ling, N., Sharma, M., Kambadur, R. (2008) Myostatin signals through pax7 to regulate satellite cell self-renewal. *Exp Cell Res*. **314**, 317-329.

216. McFarlane, C., Hui, G.Z., Amanda, W.Z.W., Lau, H.Y., Lokireddy, S., Xiaojia, G., Mouly, V., Butler-Browne, G., Gluckman, P.D., Sharma, M., Kambadur, R. (2011) Human myostatin negatively regulates human myoblast growth and differentiation. *Am J Physiol Cell Physiol*. **301(1)**, C195-C203.

217. McPherron, A.C., Lawler, A.M., Lee, S.J. (1997) Regulation of skeletal muscle mass in mice by a new TGF-beta superfamily member. *Nature*. **387,** 83-90.

218. McPherron, A.C., and Lee, S.J. (1997) Double muscling in cattle due to mutations in the myostatin gene. *Proc. Natl. Acad. Sci. USA*. **94**: 12457-12461.

219. Megeney, L.A., Kablar, B., Garrett, K., Anderson, J.E., Rudnicki, M.A. (1996) MyoD is required for myogenic stem cell function in adult skeletal muscle. *Genes & Dev*. **10**, 1173-1183.

220. Meijer, A.J., Codogno, P. (2004) Regulation and role of autophagy in mammalian cells. *Int J Biochem Cell Biol*. **36**, 2445–62.

221. Menetrey, J., Kasemkijwattana, C., Fu, F.H., Moreland, M.S., and Huard, J. (1999) Suturing versus immobilization of a muscle laceration: a morphological and functional study in a mouse model. *Am. J Sports Med*. **27**, 222–229.

222. Messina, G., Cossu, G. (2009) The origin of embryonic and fetal myoblasts: a role of Pax3 and Pax7. *Genes and Development.* **23**, 902-905.

223. Metter, E.J., Lynch, N., Conwit, R., Lindle, R., Tobin, J., Hurley, B. (1999) Muscle quality and age: cross-sectional and longitudinal comparisons. *J Gerontol A Biol Sci Med Sci*. **54**, B207-B218.

224. Michalik, L., Desvergne, B., Dreyer, C., Gavillet, M., Laurini, R.N., and Wahli, W. (2002) PPAR expression and function during vertebrate development. *Int J Dev Biol.* **46**, 105-114.

225. Michalik, L., Desvergne, B., Wahli, W. (2004) Peroxisome-proliferator-activated receptors and cancers: complex stories. *Nat Rev Cancer*. 61-70.

226. Min, K., Smuder, A.J., Kwon, O.S., Kavazis, A.N., Szeto, H.H., Powers, S.K. (2011) Mitochondrial-targeted antioxidants protect skeletal muscle against immobilization-induced muscle atrophy. *J Appl.Physiol.* **111**, 1459-1466.

227. Mizushima, N. (2007) Autophagy: process and function. *Genes and Dev*. **21**, 2861-2873.

228. Mofarrahi, M., Sigala, I., Guo, Y., Godin, R., Davis, E.C., Petrof, B. (2012) Autophagy and skeletal muscles in sepsis. *PLoS ONE.* **7(10)**:e47285.

229. Mohan, R., Heyman, R.A. (2003) Orphan nuclear receptor modulators. *Curr Topic Med Chem*. **3,** 1637-1647.

230. Morley, J.E., Baumgartner, R.N., Roubenoff, R., Mayer, J., Nair, K.S. (2001) Sarcopenia. *J Lab Clin Med.* **137**, 231-43.

231. Motohashi, N., Asakura, A. (2012) Molecular regulation of muscle satellite cell self-renewal. *J Stem Cell Res and Therapy*, Suppl 11,e002.

232. Motohashi, N., and Asakura, A. (2014) Muscle satellite cell heterogeneity and self-renewal. *Front Cell Develop Biol*. **2**, 1.

233. Murphy, R.M. (2010) Calpains, skeletal muscle function and exercise. *Clin ExpPharmacol Physiol.* **37(3)**, 385-91.

234. Musaro, A., Cusella De Angelis, M.G., Germani, A., Ciccarelli, C., Molinaro, M., and Zani, B.M. (1995) Enhanced expression of myogenic regulatory genes in aging skeletal muscle. *Exp Cell Res.* **221(1)**, 241-8.

235. Nair, K.S. (2005) Aging muscle. *Am J Clin Nutr*. **81**, 953-963.

236. Nandi, D., Tahilani, P., Kumar, A., and Chandu, D. (2006) The ubiquitin-proteasome system. *J Biosci*. **31**, 137-155.

237. Narici, M.V., Maffulli. N. (2010) Sarcopenia: characteristics, mechanisms and functional significance. *Brit Med Bulletin*. **95**, 139-159.

238. Nilwik. R., Snijders, T., Leenders, M., Groen, B.B., van Kranenburg, J., Verdijk, L.B., van Loon, L.J. (2013) The decline in skeletal muscle mass with aging is mainly attributed to a reduction in type II muscle fibre size. *Exp Gerontol*. **48(5)**, 492-498.

239. Novac. N., Heinzel. T. (2004) Nuclear receptors: overview and classification. *Curr Drug Targ: Inflamm & Allerg.* **3**, 335-346.

240. Ohsawa, Y., Hagiwara, H., Nakatani, M., Yasue, A., Moriyama, K., Murakami, T., Tsuchida, K., Noji, S., Sunada, Y. (2006) Muscular atrophy of caveolin-3 defiicient mice is rescued by myostatin inhibition. *J Clin Invest*. **116**, 2924-2934.

241. O'Leary, M.F., Vainshtein, A., Carter, H.N., Zhang, Y., Hood, D.A. (2012) Denervation-induced mitochondrial dysfunction and autophagy in skeletal muscle of apoptosis-deficient animals. *Am J Physiol Cell Physiol*. **303**, C447-C454.

242. Osada, S., Tsukamoto, T., Takiguchi, M., Mori, M., and Osumi, T. (1997) Identification of an extended half-site motif required for the function of peroxisome proliferator-activated receptor alpha. *Genes Cells.* **2**, 315-327.

243. Ott, M.O., Bober, E., Lyons, G., Arnold, H., and Buckingham, M. (1991) Early expression of the myogenic regulatory gene, myf-5, in

precursor cells of skeletal muscle in the mouse embryo. *Develop*. **111**, 1097-107.

244. Palmer, C.N., Hsu, M.H., Griffin, H.J., Johnson, E.F. (1995) Novel sequence determinants in peroxisome proliferator signaling. *JBC*. **270**, 16114-16121.

245. Pandurangan, M., Hwang, I. (2012) The role of calpain in skeletal muscle. *Animal cell sys*. 431-437.

246. Pannerec, A., Marazzi, G., Sassoon, D. (2012) Stem cells in the hood: the skeletal muscle niche. *Trends in Mol Med.* **18**, 599-606.

247. Patel, A.S., Lin, L., Geyer, A., Haspel, J.A., An, C.H., Cao, J., Rosas, I.O., Mores, D. (2012) Autophagy in idiopathic pulmonary fibrosis. *PLoS ONE*. **7(7)**:e41394.

248. Paulsen, G., Crameri, R., Benestad, H.B., Field, J.G., Mokrid, L., Hallen, J., Raastad, T. (2010) Time course of leukocyte accumulation in human muscle after eccentric exercise. *Med Sci Sports Exerc.* **42**, 75-85.

249. Penna, F., Costamagna, D., Pin, F., Camperi, A., Fanzani, A., Chiarpotto, E.M. (2013) Autophagic degradation contributes to muscle wasting in cancer cachexia. *Am J Pathol*. **182**, 1367-1378.

250. Peters, J.M., Shah, Y.M., Gonzalez, F.J. (2012) The role of peroxisome proliferator-activated receptors in carcinogenesis and chemoprevention. *Nat Rev Cancer*. **12**, 181-195.

251. Peterson, C.M., Johannsen, D.L., and Ravussin, E. (2012) Skeletal Muscle Mitochondria and Aging: A Review. *J Aging Res*. 1-20.

252. Philip. B., Lu, Z., and Gao, Y. (2005) Regulation of GDF-8 signaling by the p38 MAPK. *Cell Sig*. **17**, 365-375.

253. Pickart, C.M. (2004) Back to the future with ubiquitin. *Cell*. **116**, 181-190.

254. Pinter, S., Mendler, L., Dux, L. (2003) Neural impacts on the regeneration of skeletal muscle. *Acta Biochimica Polonica*. **50**, 1229-1237.

255. Pistilli, E,E., Bogdanovich, S., Goncalves, M.D., Ahima, R.S., Lachey, J., Seehra, J., Khurana, T. (2011) Targeting the Activin type IIB receptor to improve muscle mass and function in the *mdx* mouse model of duchenne muscular dystrophy. *Am J Pathol*. **178(3)**, 1287-1297.

256. Powers, S.K., Wiggs, M.P., Duarte, J.A., Zergeroglu, A.M., Demirel, H.A. (2012) Mitochondrial signaling contributes to disuse muscle atrophy. *Am J Physiol Endocrinol Metab.* **303(1)**: E31-9.

257. Qian, B.Z., and Pollard, J.W. (2010) Macrophage diversity enhances tumor progression and metastasis. *Cell*. **141**, 39–51.

258. Rantanen, J., Ranne, J., Hurme, T., Lukka, R., Heino, J., Kalimo, H. (1995) Satellite cell proliferation and expression of myogenin and desmin in regenerating skeletal muscle: evidence for two different populations of satellite cells. *Lab Invest.* **72**, 341-347.

259. Ravnskjaer, K., Frigerio, F., Boergesen, M., Nielsen, T., Maechler, P., Mandrup, S. (2010) PPARδ is a fatty acid sensor that enhances mitochondrial oxidation in insulin-secreting cells and protects against fatty acid-induced dysfunction. *J Lipid Res.* **51(6),** 1370-1379.

260. Rebbapragada, A., Benchabane, H., Wrana, J.L., Celeste, A.J., Attisano, L. (2003) Myostatin signals through a Transforming growth factor β-like signaling pathway to block adipogenesis. *Mol Cell Biol.* **23(20)**, 7230-7242.

261. Relaix, F., Rocancourt, D., Mansouri, A., Buckingham, M.A. (2005) A Pax3/Pax7-dependent population of skeletal muscle progenitor cells. *Nature.* **435**, 948–53.

262. Reisz-Porszasz, S., Bhasin, S., Artaza, J.N., Shen, R., Sinha-Hikim, I., Hogue, A., Fielder, T.J., Gonzalez-Cadavid, N.F. (2003) Lower skeletal muscle mass in male transgenic mice with muscle-specific overexpression of myostatin. *Am J Physiol Endocrinol Metab.* **285(4)**, E876-88.

263. Rigamonti, E., Zordan, P., Sciorati, C., Rovere-Querini, P., and Brunelli, S. (2014) Macrophage plasticity in skeletal muscle repair. *Biomed Res Int*. 560629.

264. Ríos, R., Carneiro, I., Arce, V.M., Devesa, J. (2002) Myostatin is an inhibitor of myogenic differentiation. *Biochem and Biophy Res Comm.* **19**, 561-566.

265. Riserus, U., Sprecher, D., Johnson, T., Olson, E., Hirschberg, S., Liu, A., Fang, Z., Hegde, P., Richards, D., Sarov-Blat, L., Strum, J.C., Basu, S., Cheeseman, J., Fielding, B.A., Humphreys, S.M., Danoff, T., Moore, N.R., Murgatroyd,P., O'Rahilly, S., Sutton, P., Willson, T., Hassall, D., Frayn, K.N., Karpe, F. (2008) Activation of peroxisome proliferator0activated receptor (PPAR)δ promotes reversal of multiple metabolic abnormalities, reduces oxidative stress, and increases fatty acid oxidation in moderately obese men. *Diabetes*. **57**, 332-339.

266. Rodgers, J.T., King, K.Y., Brett, J.O., Cromie, M.J., Charville, G.W., Maguire, K.K., Brunson, C., Mastey, N., Liu, L., Tsai, C.R., Goodell, M.A., Rando, T.A. (2014) mTORC1 controls the adaptive transition of quiescent stem cells from G_0 to $G_{Alert.}$ *Nature*. **510**, 393-396.

267. Rogers, M.A., Evans, W.J. (1993) Changes in skeletal muscle with aging: effects of exercise training. *Exerc Sport Sci Rev*. **21**, 65-102.

268. Rooyackers, O.E., Adey, D.B., Ades, P.A., Nair, K.S. (1996) Effect of age on in vivo rates of mitochondrial protein synthesis in human skeletal muscle. *Proc Natl Acad Sci USA*. **93**, 15364-15369.

269. Rosen. E.D., Sarraf, P., Troy, A.E., Bradwin, G., Moore, K., Milstone, D.S., Spiegelman, B.M., Mortensen, R.M. (1999) PPARγ is required for the differentiation of adipose tissue *in vivo* and *in vitro*. *Mol Cell*. **4**, 611-617.

270. Rosenberg, I.H. (1997) "Sarcopenia: origins and clinical relevance". *J Nutr*. **127**, 990-991.

271. Rotman, N., Guex, N., Gouranton, E., and Wahli, W. (2013) PPARbeta interprets a chromatin signature of pluripotency to promote embryonic differentiation at gastrulation. *PLOS ONE*. **8**: e83300.

272. Rowan, S.L., Rygiel, K., Purves-Smith, F.M., Solbak, N.M., Turnbull, D.M., Hepple, R.T. (2012) Denervation causes fibre atrophy and myosin heavy chain co-expression in senescent skeletal muscle. *PLOS ONE*. **7(1)**, e29082.

273. Rudnicki, M.A., Schneglesberg, P.N.J., Stead, R.H., Braun, T., Arnold, H., Jaenisch, R. (1993) MyoD or myf-5 is required for the formation of skeletal muscle. *Cell*. **75**, 1351–9.

274. Sambasivan, R., Tajbakhsh, S. (2007) Skeletal muscle stem cell birth and properties. *Sem Cell Dev Biol*. **18**: 870-882.

275. Sandri, M., Sandri, C., Gilbert, A., Skurk, C., Calabria, E., Picard, A., Walsh, K., Schiaffino, S., Lecker, S.H., Goldberg. A.L. (2004) FOXO transcription factors induce the atrophy-related ubiquitin ligase Atrogin-1 and cause skeletal muscle atrophy. *Cell*. **117(3)**, 399-412.

276. Sandri, M. (2010) Autophagy in skeletal muscle. *FEBS Letters*. **584**, 1411-1416.

277. Sato. T., Akatsuka. H., Kito. K., Tokoro. Y., Tauchi. H., and Kato, K. (1984) Age changes in size and number of muscle fibers in human minor pectoral muscle. *Mech Ageing Dev*. **28(1)**, 99-109.

278. Scheibye-Knudsen, M., Fang, E.F., Croteau, D.L., Bohr, V.A. (2014) Conttribution of defective mitophagy to the neurodegeneration in DNA repair-deficient disorders. *Autophagy*. **10(8)**, 1468-9.

279. Schiaffino, S., Reggiani, C. (2011) Fiber types in mammalian skeletal muscles. *Phy Rev*. **91**, 1447-1531.

280. Schienda, J., Engleka, K.A., Jun, S., Hansen, M.S., Epstein, J.A., Tabin, C.J., Kunkel, L.M., Kardon, G. (2006) Somitic origin of limb muscle satellite and side population cells. *Proc Natl Acad Sci USA*. **103(4)**, 945-950.

281. Schmalbruch, H. (2006) The satellite cell of skeletal muscle fibres. *Braz. J. Morphol. Sci*. **23(2)**, 159-172.

282. Schuelke, M., Wagner, K.R., Stolz, L.E., Hubner, C., Riebel, T., Komen, W., Braun, T., Tobin, J.F., Lee, S.J. (2004) Myostatin mutation associated with gross muscle hypertrophy in a child. *New Engl J of Med*. **350**, 2682-2688.

283. Schuler, M., Ali, F., Chambon, C., Duteil, D., Bornert, J., Tardivel, A., Desvergne, B,, Wahli, W., Chambon, P., and Metzger, D. (2006) PGC1a expression is controlled in skeletal muscles by PPAR β, whose ablation

results in fiber-type switching, obesity and type 2 diabetes. *Cell Metab*. **4**: 407-414.

284. Schulte, J.N., and Yarasheski, K.E. (2001) Effects of resistance training on the rate of muscle protein synthesis in frail elderly people. *Int J Sport Nutr Exerc Metab.* Suppl:S111-118.

285. Schultz, E., McCormick, K.M. (1994) Skeletal muscle satellite cells. *Rev Physiol Biochem Pharmacol.* **123**, 213–257.

286. Scott, W., Stevens, J., and Binder-Macleod, S.A. (2001) Human skeletal muscle fibre type classifications. *Phy Ther*. **81**, 1810-1816.

287. Seale, P., Sabourin, L.A., Girgis-Gabardo, A., Mansouri, A., Gruss, P., and Rudnicki, M.A. (2000) Pax7 is required for the specification of myogenic satellite cells. *Cell* **102**, 777–786.

288. Sertznig, P., Seifert, M., Tilgen, W., Reichrath, J. (2008) Peroxisome proliferator-activated receptors (PPARs) and the human skin: importance of PPARs in skin physiology and dermatologic diseases. *Am J Clin Dermatol*. **9(1)**, 15-31.

289. Siriett, V., Salerno, M.S., Berry, C., Nicholas, G., Bower, R., Kambadur, R., Sharma, M. (2007) Antagonism of myostatin enhances muscle regeneration during sarcopenia. *Mol Therapy*. **15**, 1463-1470.

290. Siriett, V., Platt, L., Salerno, M.S., Ling, N., Kambadur, R., Sharma, M. (2006) Prolonged absence os myostatin reduces sarcopenia. *J Cell Physiol*. **209(3)**, 866-873.

291. Snijders, T., Verdijk, L.B., Van loon, L.J. (2009) The impact of sarcopenia and exercise training on skeletal muscle satellite cells. *Ageing Res Rev* **8**, 328-33810.

292. Sohal, R.S., Ku, H.H., Agarwal, S., Forster, M.J., Lal, H. (1994) Oxidative damage, mitochondrial oxidant generation and antioxidant defenses during aging and in response to food restriction in the mouse. *Mech Ageing Dev*. **74**, 121–133.

293. Solomon, V., Goldberg, A.L. (1996) Importance of the ATP-ubiquitin-proteasome pathway in the degradation of soluble and myofibrillar proteins in rabbit muscle extracts. *J Biol Chem*. **271**, 26690-26697.

294. Soukup, T., Zacharova, G., Smerdu,V. (2002) Fibre type composition of soleus and extensor digitorum longus muscles in normal female inbred Lewis rats. *Acta Histochem*. **104(4)**, 399-405.

295. Spencer, M.J., Croall, D.E., Tidball, J.G. (1995) Calpains are activated in necrotic fibers from mdx dystrophic mice. *J Biol Chem*. **270**, 10909-10914.

296. Sriram, S., Subramanian, S., Juvvuna, P.K., McFarlane, C., Salerno, M.S., Kambadur, R., and Sharma, M. (2014) Myostatin induced DNA damage in skeletal muscle of streptozotocin induced type1 diabetic mice. *J.Biol.Chem*. **289(9)**, 5784-98.

297. Storr, S.J., Carragher, N.O., Frame, M.C., Parr, T., Martin, S.G. (2011) The calpain system and cancer. *Nat Rev Cancer*. **11**, 364-374.

298. Szczesny, B., Tann, A.W., Mitra, S. (2010) Age- and tissue-specific changes in mitochondrial and nuclear DNA base excision repair activity in mice: Susceptibility of skeletal muscles to oxidative injury. *Mech Ageing Dev*. **131**, 330-337.

299. Takata, Y., Liu, J., Yin, F., Collins, A.R., Lyon, C.J., Lee, C.H., Atkins, A.R., Downes, M., Barish, G.D., Evans, R.M., Hsueh, W.A., Tangirala, R.K. (2008) PPARdelta-mediated antiinflammatory mechanisms inhibit angiotensin II-accelerated atherosclerosis. *Proc Natl Acad Sci USA*. **105**, 4277-4282.

300. Tajbakhsh, S., Rocancourt, D., Cossu, G., Buckingham, M. (1997). Redefining the genetic hierarchies controlling skeletal myogenesis: Pax-3 and myf-5 act upstream of MyoD. *Cell*. **89**, 127-138.

301. Tamilselvan, J., Jayaraman, G., Sivarajan, K., Panneerselvam, C. (2007) Age-dependent upregulation of p53 and cytochrome c release and susceptibility to apoptosis in skeletal muscle fiber of aged rats: role of carnitine and lipoic acid. *Free Radic Biol Med*. **43**, 1656-1669.

302. Taylor, W.E., Bhasin, S., Artaza, J., Byhower, F., Azam, M., Willard, D.H, Kull Jr, F.C., Gonsalez-Cadavid Jr, N. (2001) Myostatin inhibits

cell proliferation and protein synthesis in C2C12 muscle cells. *Am J Phy Endo and Metab.* **280**, E221-E228.

303. Teixeira, C.E., Duarte, J.A. (2011) Myonuclear domain in skeletal muscle fibres. A critical review. *Arch Exer Health Dis.* **2(2)**, 92-101.

304. Thomas, M., Langley. B., Berry. C., Sharma, M., Kirk, S., Bass, J., Kambadur, R. (2000) Myostatin, a negative regulator of muscle growth functions by inhibiting myoblast proliferation. *J Biol Chem*. **275**, 40235-40243.

305. Tidball, J.G. (2005) Inflammatory processes in muscle injury and repair. *Am J Pysiol Regul Integr Comp Physiol.* **288**, 345-353.

306. Tomanek, R.J., Lund, D.D. (1974) Degeneration of different types of skeletal muscle fibres. II. Immobilization. *J Anat.* **118**, 531-541.

307. Tugwood, J.D., Issemann, I., Anderson, R.G., Bundell, K.R., McPheat, W.L., Green, S. (1992) The mouse perxisome proliferator activated receptor recognizes a response element in the 5' flanking sequence of the rat acyl CoA oxidase gene. *EMBO J*. **11**, 433-439.

308. Turner, N.J., Badylak, S.F. (2012) Regeneration of skeletal muscle. *Cell Tissue Res* **347**, 759-774.

309. Tyagi, S., Gupta, P., Saini, A.S., Kaushal, C., and Sharma, S. (2011) The peroxisome proliferator-activated receptors: A family of nuclear receptors role in various diseases. *J Adv Pharm Technol Res*. **2(4)**, 236-240.

310. Ventadour, S., Attaix, D. (2006) Mechanisms of skeletal muscle atrophy. *Curr Opin Rheumatol*. **18(6)**, 631-5.

311. von Zglinicki, T., Martin-Ruiz, C.M. (2005) Telomeres as biomarkers for ageing and age-related diseases. *Curr Mol Med.* **5(2)**, 197-203.

312. Wada, K.I., Katsuta, S., Soya, H. (2003) Natural occurence of myofiber cytoplasmic enlargement accompanied by decrease in myonuclear number. *JPN Physiol.* **53(2)**, 145-50.

313. Wagner, K.R., McPherron, A.C., Winik, M., Lee, S.J. (2002) Loss of myostatin attenuates severity of muscular dystrophy in mdx mice. *Ann Neurol*. **52**, 832-836.

314. Wahli, W. (2002) Peroxisome proliferator-activated receptors (PPARs): from metabolic control to epidermal wound healing. *Swiss Med Week*. **132**, 83-91.

315. Wanagat, J., Cao, Z., Pathare, P., Aiken, J.M. (2001) Mitochondrial DNA deletion mutations colocalize with segmental electron transport system abnormalities, muscle fiber atrophy, fiber splitting, and oxidative damage in sarcopenia. *FASEB*. 322-332.

316. Wang, Y.X., Zhang, C.L., Yu, R.T., Cho, H.K., Nelson. M.C., Bavuga-Ocampo, C.R., Ham, J., Kang, H., Evans, R.M. (2004) Regulation of muscle fiber type and running endurance by PPAR delta. *PLoS Biol*. **2**, 1532-9.

317. Wang, X., Pickrell, A.M., Rossi, S.G., Pinto, M., Dillon, L.M., Hida, A., Rotundo, R.L., Moraes, C.T. (2013) Transient systemic mtDNA damage leads to muscle wasting by reducing the satellite cell pool. *Hum Mol Genet*. **22(19)**, 3976-3986.

318. Webb, A.E., and Brunet, A. (2014) FoxO transcription factors: key regulators of cellular quality control. *Trends Bioche Sci*. **39**, 159-169.

319. Wenz, T., Rossi, S.G., Rotundo, R.L., Spiegelman, B.M., Moraes, C.T. (2009) Increased muscle PGC-1alpha expression protects from sarcopenia and metabolic disease during aging. *Proc Natl Acad Sci USA*. **106**, 20405-20410.

320. Westerblad, H., Bruton. J.D., and Katz, A. (2010) Skeletal muscle: Energy metabolism, fiber types, fatigue and adaptibility. *Exp Cell Res*. **316**, 3093-3099.

321. Whalen, R.G., Harris, J.B., Butler-Browne, G.S., and Sesodia, S. (1990) Expression of Myosin lsoforms during Notexin-Induced Regeneration of Rat Soleus Muscles. *Dev Biol*. 24-40.

322. Williams, A.B., Decourten-Myers, G.M., Ficher, J.E., Luo, G., Sun, X., Hasselgren, P.O. (1999) Sepsis stimulates release of myofilaments in

skeletal muscle by a calcium-dependent mechanism. *FASEB J.* **13(11)**, 1435-1443.

323. Williams, G.N., Higgins, M.J., Lewek, M.D. (2002) Aging skeletal muscle: Physiologic changes and the effects of training. *Phys Ther*. **82**, 62-68.

324. Wohlgemuth, S.E., Seo, A.Y., Marzetti, E., Lees, H.A., Leeuwenburgh, C. (2010) Skeletal muscle autophagy and apoptosis during aging: effects of calorie restriction and life-long exercise. *Exp Gerontol*. **45(2)**, 138-148.

325. Wozniak, A.C., Kong, J., Bock, E., Pilipowicz, O., Anderson, J.E. (2005) Signaling satellite-cell activation in skeletal muscle: Markers, models, stretch, and potential alternate pathways. *Mus Nerve.* **31(3)**, 283–300.

326. Xie. Z., Klionsky. D.J. (2007) Autophagosome formation: core machinery and adaptations. *Nat Cell Biol*. **9**, 1102–9.

327. Yablonka-Reuveni, Z., Rivera, A.J. (1994) Temporal expression of regulatory and structural muscle proteins during myogenesis of satellite cells on isolated adult rat fibres. *Dev Biol.* **164(2)**, 588-603.

328. Yarasheski, K.E., Pak-Loduca, J., Hasten, D.L., Obert, K.A., Brown, M.B., Sinacore, D.R. (1999) Resistance exercise training increases mixed muscle protein synthesis rate in frail women and men ≥76yr old. *Am J Physiol*. **277**, E118-E125.

329. Yarasheski, K.E., Bhasin, S., Sinha-Hikim, I., Pak-Loduca, J., Gonzalez-Cadavid, N.F. (2002) Serum myostatin-immunoreactive protein is increased in 60–92 year old women and men with muscle wasting. *J Nutr Health Aging*. **6**, 343-348.

330. Yarovaya, N.O., Kramarova, L., Borg, J., Kovalenko, S.A., Caragounis, A., Linnane, A.W. (2002) Age-related atrophy of rat soleus muscle is accompanied by changes in fibre type composition, bioenergy decline and mtDNA rearrangements. *Biogerontol.* **3**, 25-27.

331. Youle RJ., Karbowski M. (2005) Mitochondrial fission in apoptosis. *Nat Rev Mol Cell Biol.* **6**, 657-663.

332. Zhang, C., McFarlane, C., Lokireddy, S., Bonala, S., Ge, X., Masuda, S., Glukman, P.D., Sharma, M., Kambadur, R. (2011) Myostatin-deficient mice exhibit reduced insulin resistance through activating the AMP-activated protein kinase signalling pathway. *Diabet.* **54(6)**, 1491-501.

333. Zhao, J., Brault, J.J., Schild, A., Cao, P., Snadri, M., Schiaffino, S. (2007) FoxO3 coordinately activates protein degradation by the autophagic/lysosomal and proteosomal pathways in atrophying muscle cells. *Cell Metab*. **6**, 472-483.

334. Zheng, X., Hunter, T. (2013) Parkin mitochondrial translocation is achieved through a novel catalytic activity coupled mechanism. *Cell Res.* **23**, 886-897.

335. Zhou, X., Wang, J.L., Lu, J., Song, Y., Kwak, K.S., Jiao, Q., Rosenfeld, R., Chen, Q., Boone, T., Simonet, W.S., Lacey, D.L., Goldgerg, A.L., Han, H.Q. (2010) Reversal of cancer cachexia and muscle wasting by ActRIIB antagonism leads to prolonged survival. *Cell*. **142**, 531-543.

336. Zhu, Y., Qi, C., Jain, S., Rao, M.S., and Reddy, J.K. (1997) Isolation and characterization of PBP, a protein that interacts with peroxisome proliferator- activated receptor. *J Biol Chem.* **272**, 25500-25506.

337. Zimmers, T.A., Davies, M.V., Koniaris, L.G., Haynes, P., Esquela, A.F., Tomkinson, K.N., McPherron, A.C., Wolfman, N.M., Lee, S.J. (2002) Induction of cachexia in mice by systemically administered myostatin. *Science.* **296**, 1486-1488.

PUBLICATIONS

Chandrashekar, P., Manickam, R., Ge, X., Bonala, S., McFarlane, C., Sharma, M., Wahli, W., Kambadur, R. (2015) Inactivation of PPAR β/δ adversely affects satellite cells and reduces postnatal myogenesis. *Am J Physiol Endo Metab.* **309(2)**, E122-31.

POSTERS

Regulation of postnatal skeletal muscle growth by PPAR β/δ. P.Chandrashekar, R.Manickam, S.Bonala, G.Xiaojia, C.McFarlane, M.Sharma, W.Wahli, R.Kambadur. Poster presented in "EMBO Workshop-Molecular Mechanisms of muscle growth and wasting in health and disease" held at Congressi Stefano Franscini, Monte Verita, Ascona, Switzerland, Sep 15-20, 2013.